A Search For Multiple Periodicities In Three Delta Scuti Stars

by

© Laureen G. Reed
June 1986

A thesis submitted as partial requirement for the degree of Master of Science (~~Astr~~onomy)

Saint Mary's University

Halifax, N.S.

ISBN 0-315-31053-7

Table of Contents

Signatures of the Examining Committee

Dr. Gary A. Welch, Supervisor

Dr. George F. Mitchell

Dr. David G. Turner

Dr. William P. Lonc

Acknowledgements

I would like to thank my supervisor, Dr. Gary Welch, for believing that, despite all obstacles (and there were many!), I would eventually sit down and write this thesis. Discussions with Drs. David Swingler and David DuPuy, and Gary Collins about period search techniques helped tremendously. I am grateful to Randall Brooks, who shared his expertise on the presentation of my results. Thanks go also to Dr. Art Hoag and the staff of Lowell Observatory for providing the observing time, and to Bill Allwright, who lent his ears over the years more times than I can remember. The comments of the examining committee were also very helpful. I am grateful also to my family for giving me lots of love, advice and moral support along the way, especially during those times (and there were a few!) when the light at the end of the tunnel seemed to disappear. Finally, a special thank-you to my husband, Dr. B. Cameron Reed, for encouragement, love, criticism, and just plain being there.

A Search for Multiple Periodicities in Three Delta Scuti Stars

by

Laureen G. Reed
June 1986

Abstract

New photoelectric photometry and period searches are presented for three northern delta Scuti variables: LT Vulpeculae, V1208 Aquilae, and 63 Herculis. In past work, two of these three stars were shown to exhibit single-period, high-frequency, low-amplitude variations, with V1208 Aql pulsating with at least two periods. Swingler's (1985) modification of the Jurkevich (1971) period search technique has been used to determine that the three program stars appear to be pulsating with at least four, three and three periods, respectively.

List of Figures

List of Tables

"A star looks down at me
And says: 'Here I and you
Stand, each in our degree:
What do you mean to do?'"

from Waiting Both, st. I
Thomas Hardy
(1840-1928)

Chapter 1: Introduction

1. The Delta Scuti Phenomenon

Delta Scuti stars are small-amplitude ($\Delta V = 0^m.003$ to $0^m.40$) short-period ($0^d.02$ to $0^d.40$) A to F-type pulsating variable stars residing on the low luminosity extension of the Cepheid instability strip. They range in luminosity from about 2.5 magnitudes above the Population I main sequence to just below it (Breger 1979). Figure I.1.1. shows their position on the HR diagram relative to other groups of intrinsic pulsators. Presently numbering around 300, known δ-Scuti stars comprise one of the largest groups of pulsators in the Galaxy, second in number only to known pulsating white dwarfs. Most of the large-amplitude δScuti stars belong to Population I, but a few have metallicities and space velocities more typical of Population II. The driving mechanism for δ-Scuti pulsation is believed to originate in the HeII and H ionization zones. Downwards helium diffusion in the surface layers leading to helium depleted outer zones may also be an important factor in the pulsation mechanisms for a significant fraction of these stars (Andreasen et al. 1983).

Main sequence δ-Scuti stars are somewhat different from their more luminous counterparts. On the main sequence, periods are generally about one hour and amplitudes are less than $0^m.02$ in V. The more luminous

Figure I.1.1. Location of intrinsic pulsating variables on the Hertzsprung-Russell Diagram

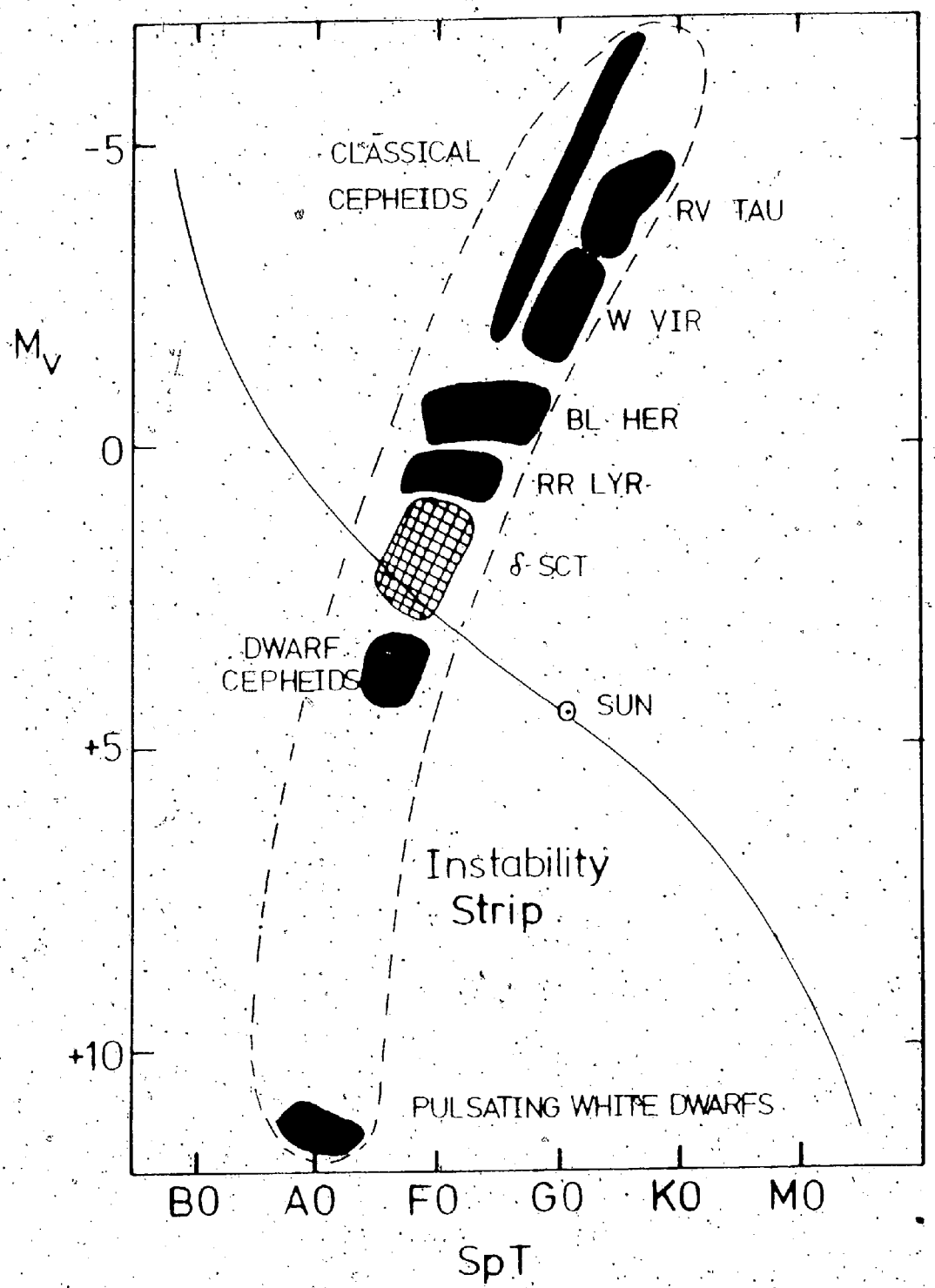
CLASSICAL
CEPHEIDS
RV TAU
W VIR
BL HER
RR LYR
δ-SCT
DWARF
CEPHEIDS
SUN
Instability
Strip
PULSATING WHITE DWARFS
M_V
-5
0
+5
+10
B0
A0
F0
G0
K0
M0
SpT

Figure I.1.2. Light curves of two sample δ-Scuti stars, BN Cancri and AD Canis Minoris. In each case, the length of the arrow indicates an amplitude of 0.01 magnitudes.

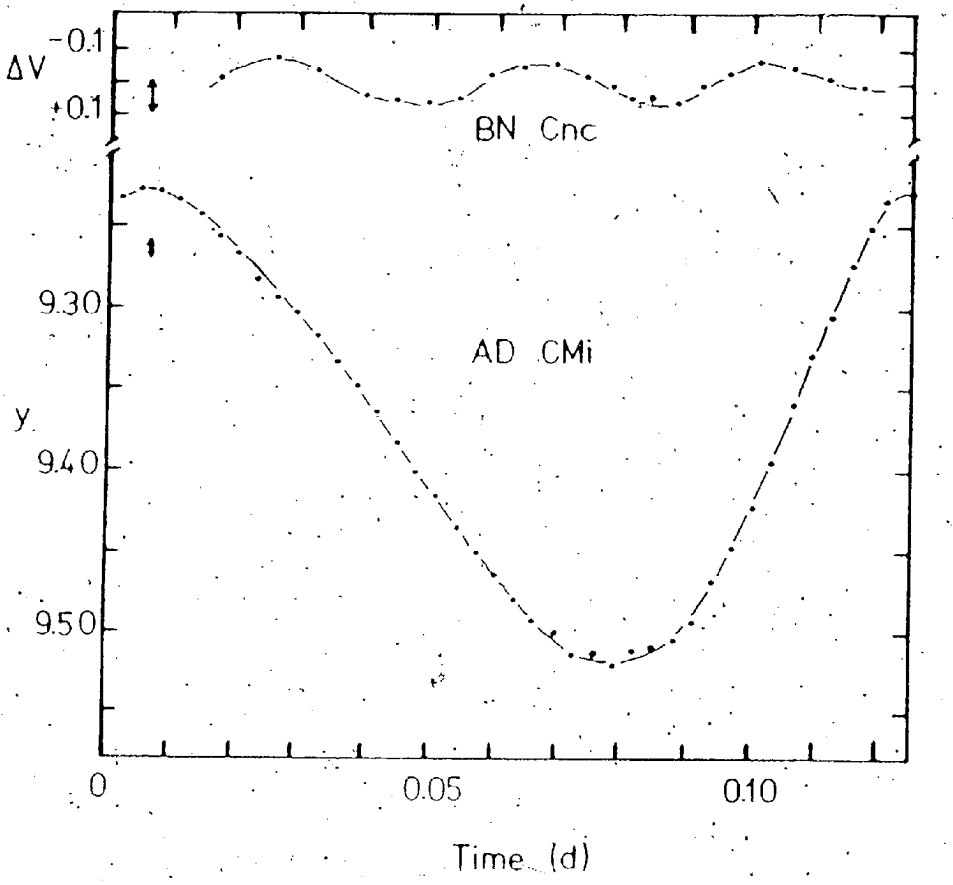
ΔV
-0.1
+0.1
BN Cnc
AD CMi
9.30
y
9.40
9.50
0
0.05
0.10
Time (d)

variables tend to have longer periods and larger amplitudes. Figure I.1.2. shows sample light curves of two δ-Scuti stars: BN Cancri, a small amplitude variable, and AD CMi, a larger amplitude star.

While many δ-Scuti variables exhibit only one observed pulsational period, the majority pulsate with more than one period. Identification of multiple periods must be made on a star-by-star basis, and considerable amounts of observing time are necessary to accurately determine a given star's pulsational parameters.

From fundamental (P_0) and overtone (P_1, P_2, ...) periods, information may be gleaned about the structure and composition of δ-Scuti stars. For example, the period ratio P_1/P_0 provides a dimensionless, reddening and distance-independent number which, if determined accurately enough, could be used in conjunction with stellar models to construct a period ratio versus mass relation. Thus, if accurate (to within one percent) period ratios could be determined photometrically, they could be indicators of stellar mass (Andreasen et al., 1983; Andreasen 1983). Unfortunately, insufficient data or data with large time gaps tend to yield misleading results for periods and, hence, period ratios no matter what period search technique is used. Therefore, a number of very accurately determined period ratios will be necessary before the appropriate stellar models can be selected. Mass-independent pulsation constants,

$$Q_n = P_n \sqrt{\bar{\rho}} \; , \qquad (1)$$

where P = period, $\bar{\rho}$ = mean stellar density relative to solar density, and n = periodicity order, can also be calculated for δ -Scuti stars given mean stellar densities previously determined from models; theoretical Q_n versus log P_n diagrams show reasonable agreement with empirical values.

2. Background on the Three Chosen Program Stars

All three stars in the present program were first observed by Breger (1969) as part of a two-year search for δ -Scuti variables in a sample of 300 A to F-type field and cluster stars; he reported 16 new suspected δ -Scuti variables. Three of these, LT Vul, 63 Her, and V1208 Aql, are the subject of this thesis. Breger's (1969) results are summarized in Table I.2.1.

Breger's (1969) data for LT Vul and 63 Her consist of only 26 and 50 V-band observations taken, respectively, over times of ~3.5 hours and 2 nights separated by 4 days. Since his observations are not extensive, his results for these two stars are best taken as starting points only. No further photometric work has been done on these stars to our knowledge, which makes them good candidate objects for a multi-period search.

V1208 Aql was the central object of a phase and amplitude study by Breger et al. (1976) because of its apparently uncomplicated nature and large amplitude. Pena

Table I.2.1.: The Program Stars

Name	R.A. (1983)	Dec. (1983)	⟨V⟩ (mag)	Spec Type	P (d)	Δ V (mag)
HR7222 HD177392 SAO086753 BD+21 3648 LT Vul	$19^h02^m.7$	$+21^\circ16'$	6.46	F2	0.096	0.040
HR7331 HD181333 SAO104722 BD+12 3879 28 Aql V1208 Aql	19 19 .0	+12 20	5.34	F0 III	0.157 --- 0.141 and 0.15 ⋆	0.050
HR6391 HD155514 SAO084896 BD+24 3140 V620 Her 63 Her	17 10 .2	+24 16	6.22	A3	0.077	0.025

⋆ Pena and Warman 1979

Figure I.2.1: Positions of the three program stars on the Hertzsprung-Russell Diagram. Dashed lines indicate the approximate borders of the instability strip. (Adapted from Petersen and Jorgensen 1972)

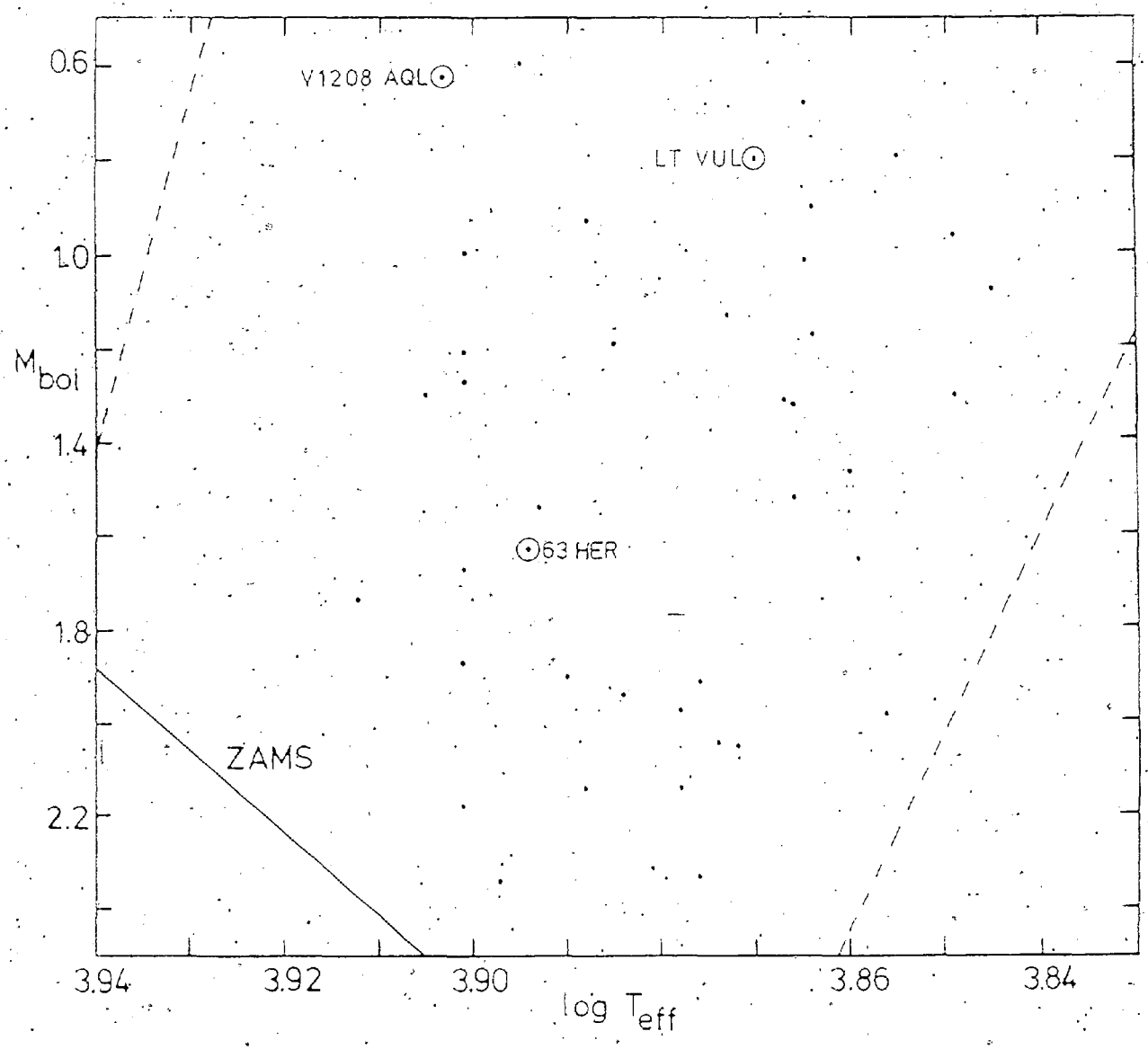
V1208 AQL
LT VUL
63 HER
ZAMS
0.6
1.0
1.4
1.8
2.2
M_{bol}
3.94
3.92
3.90
3.86
3.84
log T_{eff}

and Warman (1979) performed a multi-period analysis and found periods of $0^d.1406$ (7.112 cycles per day) and $0^d.1497$ (6.678 cy/d). To our knowledge, no further period-search work has been done for V1208 Aql.

Figure I.2.1., showing the positions of selected δ-Scuti stars on the HR diagram, was plotted from Table 3 of Petersen and Jorgensen (1972). Instability strip (IS) borders were calculated from Breger (1979) and are only approximate. Note the positions of the three program stars. V1208 Aql, the most massive of the three, resides farthest off the main sequence and is closest to the blue edge of the IS. LT Vul is closest to the red edge of the IS, and 63 Her, besides being intermediate in temperature, is also the least massive and hence the closest to the main sequence. Discussion of the HR diagram positions of the three program stars will continue in Chapter V.

Chapter II: Data Acquisition and Preliminary Reduction

1. Equipment Used

Three months of observing time on the 24-inch f/13.5 Ronnie Morgan Reflector at Lowell Observatory were granted in 1983 to obtain the photoelectric photometry for this thesis. An electrically cooled, pulse-counting, single-channel photometer equipped with a photomultiplier tube (EMI 6256s/a operated at -1000 volts d.c.) and Johnson UBV filters was used for the observations. The photomultiplier pulses passed through an amplifier/discriminator (PAR 1121) and were displayed, after integration times of 10 seconds, as a photon count which was recorded on both magnetic tape cassettes and paper tape by a microcomputer (HP 9815A).

2. Observations and Preliminary Reduction

Standard stars chosen from Iriarte et al. (1965) and Crawford et al. (1971) were observed in all three bandpasses during the nights of May 24/25 and 29/30, 1983. Johnson V-band photometry only was obtained for program objects and their comparison stars on the nights of June 3-5, 11, and 13-15 for 63 Her, June 17 and 20 for LT Vul and June 28-29 and July 4 for V1208 Aql. Only one program star was monitored on a given night. Each observation of star or sky through a given filter consisted of three 10-second integrations, and the computer displayed and recorded the

average signal and its standard deviation after the three integrations were complete.

The two nights of standard star photometry were reduced by hand using the methods of Hardie (1962). Extinction coefficients and typical (observed - standard) residuals for these two nights are given in Table II.2.1. The abnormally high extinction coefficients in all three colours seen here also appear in the reduction of the program star data, and are presumably due to particulate matter left in the Earth's atmosphere after eruptions of El Chichón in March and April, 1982. These values are consistent with those obtained by other observers at Lowell Observatory during the same time periods. This standard star photometry was performed only as a check of the equipment, the sky conditions, and the observing technique. No attempt was made to use the standard star data to transform the program star magnitudes to the Johnson system; it was deemed unnecessary since the technique of differential photometry (cf. Section II.3.) does not require magnitudes transformed to a standard photometric system.

Each program star was observed concurrently with two comparison stars designated "comparison" and "check". These were chosen to be positioned well within half a degree of the variable and to be similar to it in spectral type and V magnitude (cf. Table II.2.2.). Observations of LT Vul and 63 Her were made in the sequence (variable,

Table II.2.1.: Three Colour Extinction Coefficients and Residuals for the Standard Star Photometry

	May 24/25	May 29/30
k_v	0.293	0.334
k_{bv}	0.144	0.170
k_{ub}	0.316	0.287
k_{bv}	0.082	0.148
k_{bv}	-0.067	-0.029
ΔV	$\pm$0.027	$\pm$0.028
$\Delta B-V$	$\pm$0.021	$\pm$0.014
$\Delta U-B$	$\pm$0.020	$\pm$0.025

Table II.2.2.: The Comparison and Check Stars

	Name	R.A. (1983)	Dec. (1983)	V (mag)	Spec Type
LT Vul					
Comp Star	HR7250	19^h06^m	$+24^\circ 13'$	5.71	A3
Check Star	HR7207	19 01	+22 16	6.34	A3
V1208 Aql					
Comp Star	HR7332	19 19	+11 30	5.99	A3V
Check Star	HR7315	19 17	+11 34	5.06	A3
63 Her					
Comp Star	HR6480	17 23	+22 58	5.67	A4
Check Star	HD157087	17 19	+25 33	5.30	A3III

comparison, variable, check, variable, comparison). Data for V1208 Aql were obtained in a straightforward sequence between comparison and variable, with the check star being observed after every tenth observation of the variable.

The effects of atmospheric extinction are readily removed from the data, leaving shot noise associated with the random arrival of photons as a source of observational uncertainty. A series of measurements made in a fixed time interval resulting in a total of N photons (where N > 0) is expected to be uncertain by N according to Poisson statistics; the corresponding uncertainty in measured magnitude is then given by:

$$m = \pm \frac{1.0857}{N^{1/2}}$$

Table II.2.3. shows estimates of the uncertainty in magnitudes due to shot noise for single observations of the program stars and their comparison objects.

A FORTRAN routine REDUCE was written by the author for use on the Saint Mary's University VAX 11/780 computer to handle the program star data. This program (Appendix D-1) uses Hardie's (1962) method to reduce raw photon count/universal time data to extinction-corrected instrumental magnitudes using observations of the comparison star to calculate the extinction in V. The dead time for this particular discriminator/photometer combination, 1.0×10^{-7} seconds, as well as the appropriate equation for deadtime correction (shown below) were

Table II.2.3.: Uncertainty in Magnitudes Due to Shot Noise

Star	Typical Photon Counts Over 3 10-s Integ	Uncertainty (mag)
LT Vul	39402	±0.0055
Comp Star	85920	±0.0037
Check Star	46134	±0.0051
V1208 Aql	104292	±0.0034
Comp Star	65484	±0.0042
Check Star	130884	±0.0030
63 Her	57924	±0.0045
Comp Star	91146	±0.0036
Check Star	128061	±0.0030

obtained from a previous observer (Osborn, 1983)

$$\text{dead time corrected counts} = \text{counts} \times (1.0 + 10^{-7} \times \text{counts}).$$

A more realistic estimate of uncertainty, however, might be obtained using the comparison and check stars observed during each program night. The root-mean-square (RMS) deviation in (comparison (C) - check (CH)) values over the span of a night would be a good indicator of, for example, short-term atmospheric effects which would also influence observations of the variable. Table II.2.4. lists RMS deviations in C-CH values obtained during nights when 63 Her and LT Vul were being monitored, and RMS deviations in comparison star magnitudes only obtained during nights when V1208 Aql was observed. Average RMS deviations over the 7 nights (63 Her), 2 nights (LT Vul), and 3 nights (V1208 Aql), which are also listed in the table, were adopted as best estimates of observational uncertainty and are illustrated as error bars in all following magnitude versus time diagrams.

3. The Differential Photometry

The technique of differential photometry is to choose a comparison star close enough in position, apparent magnitude, and spectral type to the program star so that differences in atmospheric extinction between the two cancel out. Extinction values, however, were found to be larger than normal throughout the entire observing run. It was decided, therefore, to correct for average nightly

Table II.2.4.: Comparison (C) and Check (CH) Star RMS Deviations

Star	Night	RMS (mag)	⟨RMS⟩ (mag)
63 Her (C-Ch)	830603	±0.0076	
	830604	±0.0072	
	830605	±0.0052	
	830611	±0.0074	
	830613	±0.0058	
	830614	±0.0058	
	830615	±0.0070	
			±0.0066
LT Vul (C-Ch)	830617	±0.0076	
	830620	±0.0065	
			±0.0070
V1208 Aql (C only)	830628	±0.0095	
	830629	±0.0058	
	830704	±0.0058	
			±0.0070

extinction before calculating differential magnitudes, although this was probably unnecessary since air mass differences between program and comparison stars seldom corresponded to more than a few thousandths of a magnitude. Extinction in V remained close to 0.3 magnitudes per air mass for the entire observing run (cf. Table II.3.1.). Figure II.3.1. shows a typical extinction curve for the night of June 28/29, 1983 using the comparison star HR 7332. Figures II.3.2., II.3.3., and II.3.4. show the individual nights of differential photometry for LT Vul, V1208 Aql and 63 Her, respectively. Differential V magnitudes were calculated in the sense variable - comparison for LT Vul and V1208 Aql, and variable - check for 63 Her. All figures show raw, unsmoothed, extinction-corrected data, and the error bars denote observational uncertainties expected from RMS deviations in comparison - check (comparison only, for V1208 Aql) magnitudes (cf. Table II.2.4.).

Table II.3.1.: Extinction in V
From Each Night of
Program Star Photometry

Night	kv (mag/air mass)
June 3	0.275
4	0.215
5	0.268
11	0.326
13	0.350
14	0.245
15	0.226
17	0.324
20	0.215
28	0.262
29	0.265
July 4	0.240
mean kv	0.268
stand dev	0.045

Figure II.3.1. Atmospheric extinction in V for the night of June 28/29, 1983, using the comparison star HR 7332

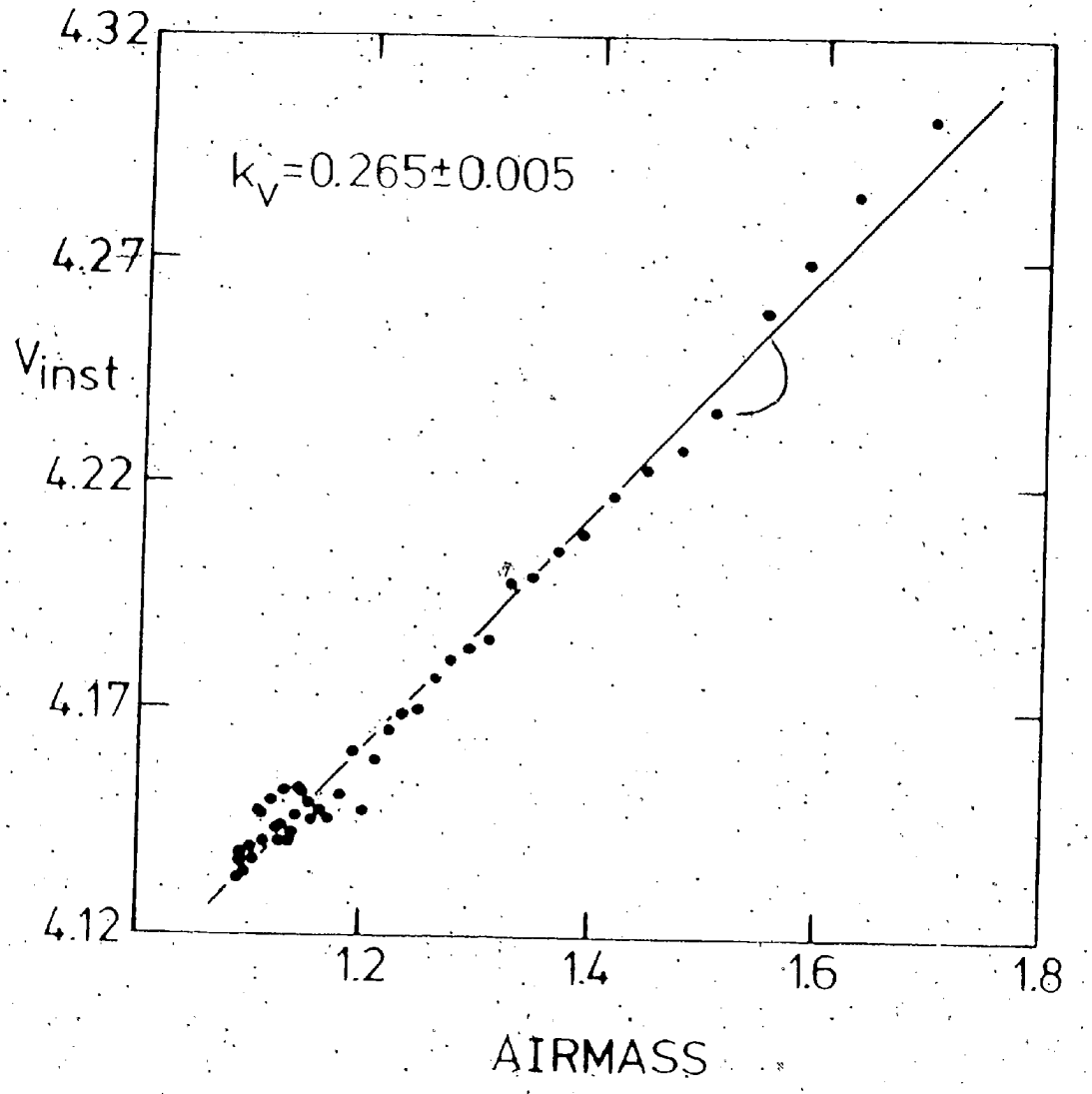
4.32
4.27
4.22
4.17
4.12
V_{inst}
$k_V = 0.265 \pm 0.005$
1.2
1.4
1.6
1.8
AIRMASS

Figure II.3.2. Differential V photometry of LT Vul for the nights of a) June 16/17, 1983 and b) June 19/20, 1983.
Julian Day (shown) = Julian Day - 244 5500

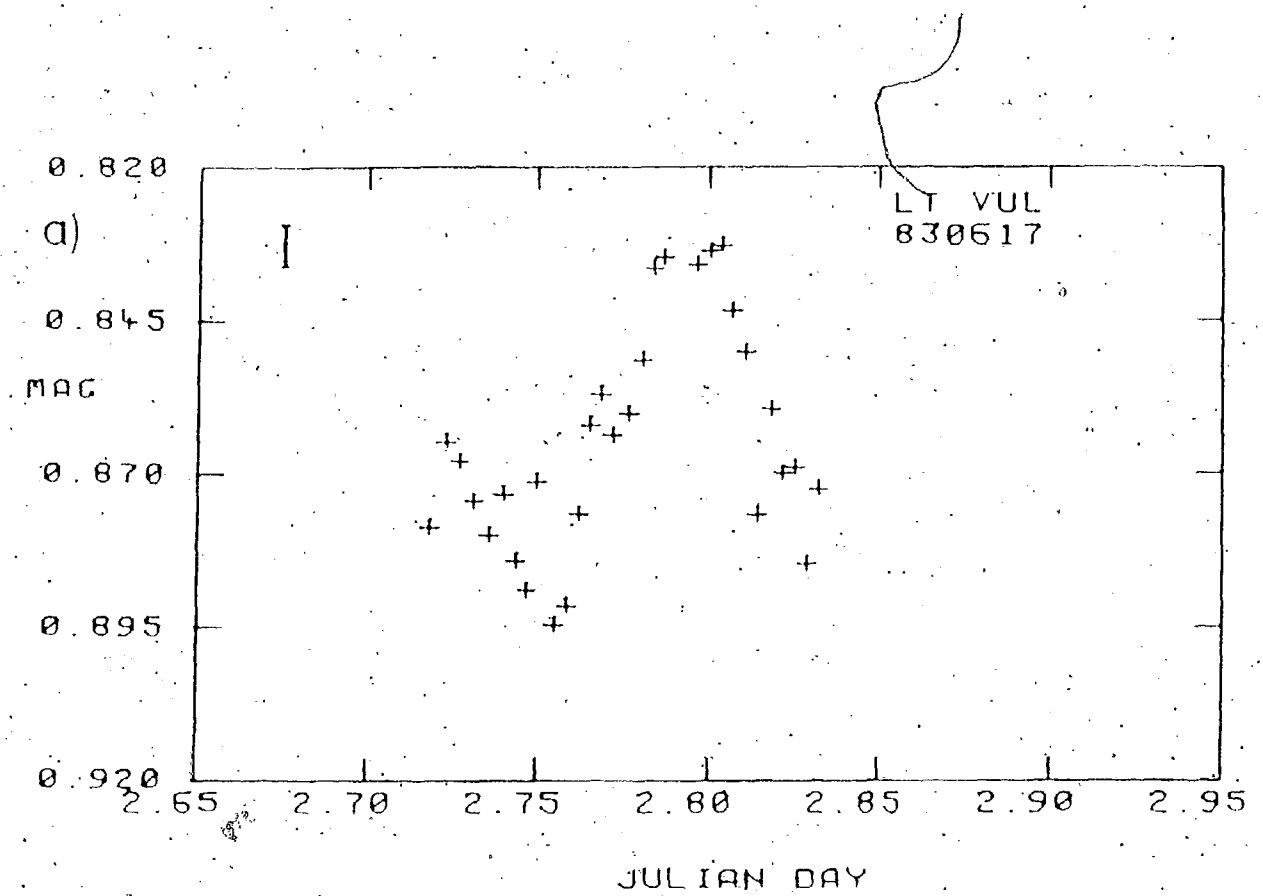
a)
LT VUL
830617
0.820
0.845
0.870
0.895
0.920
MAG
2.65
2.70
2.75
2.80
2.85
2.90
2.95
JULIAN DAY

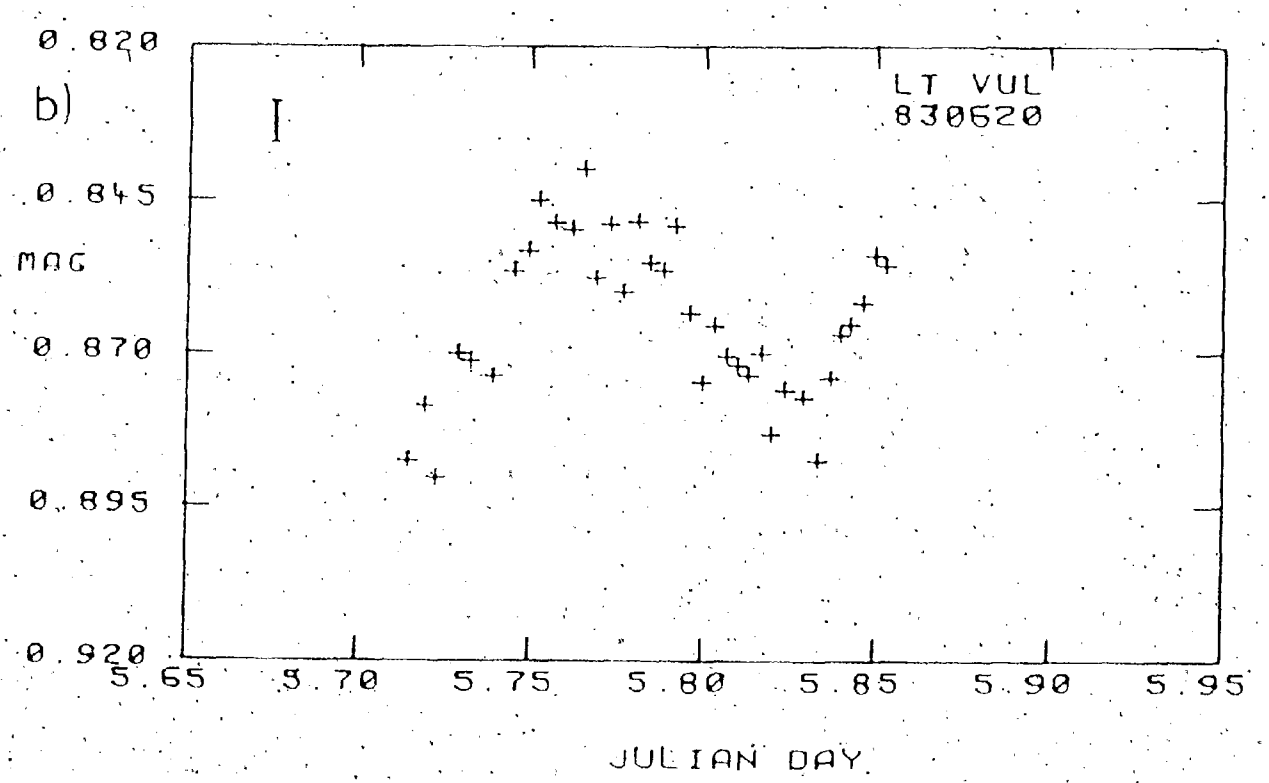
b)
LT VUL
830620
0.820
0.845
0.870
0.895
0.920
MAG
5.65
5.70
5.75
5.80
5.85
5.90
5.95
JULIAN DAY

Figure II.3.3. Differential V photometry of V1208 Aql for the nights of a) June 27/28; 1983, b) June 28/29, 1983 and c) July 4, 1983.
Julian Day (shown) = Julian Day - 244 5510

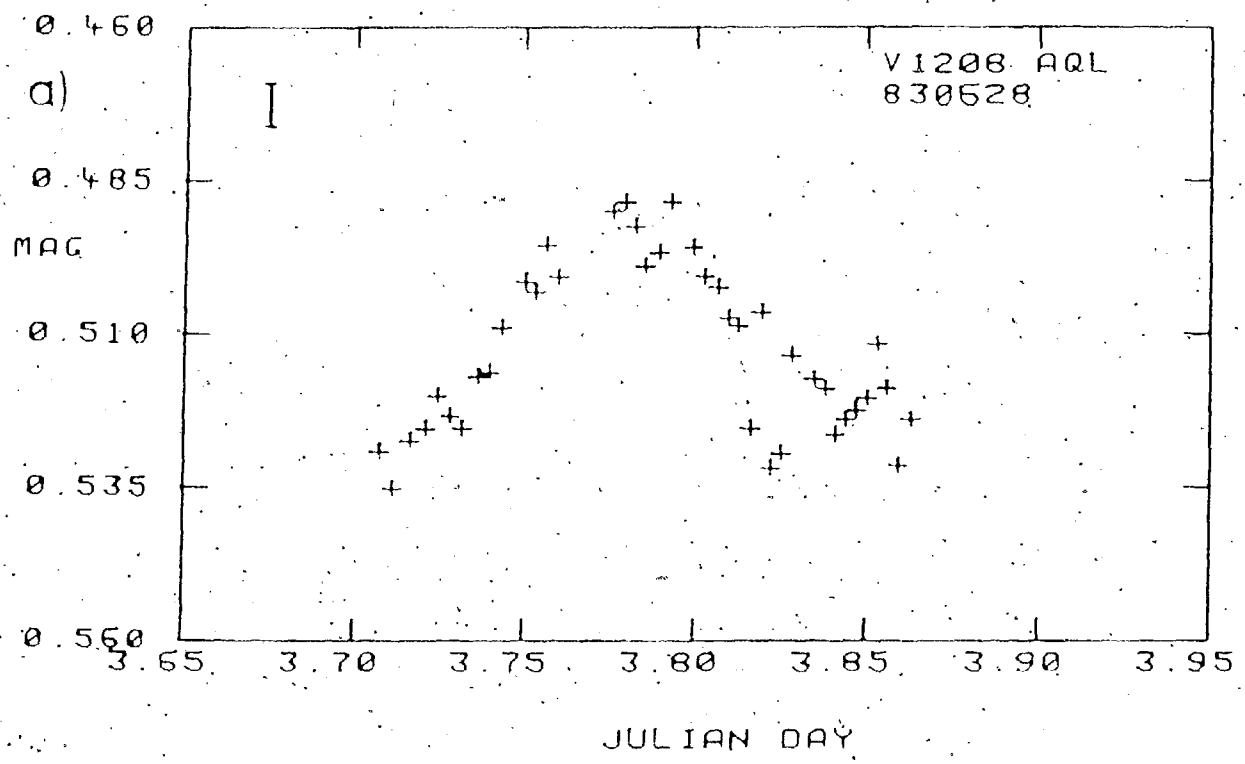
a)
I
V1208 AQL
830628
0.460
0.485
MAG
0.510
0.535
0.560
3.65
3.70
3.75
3.80
3.85
3.90
3.95
JULIAN DAY

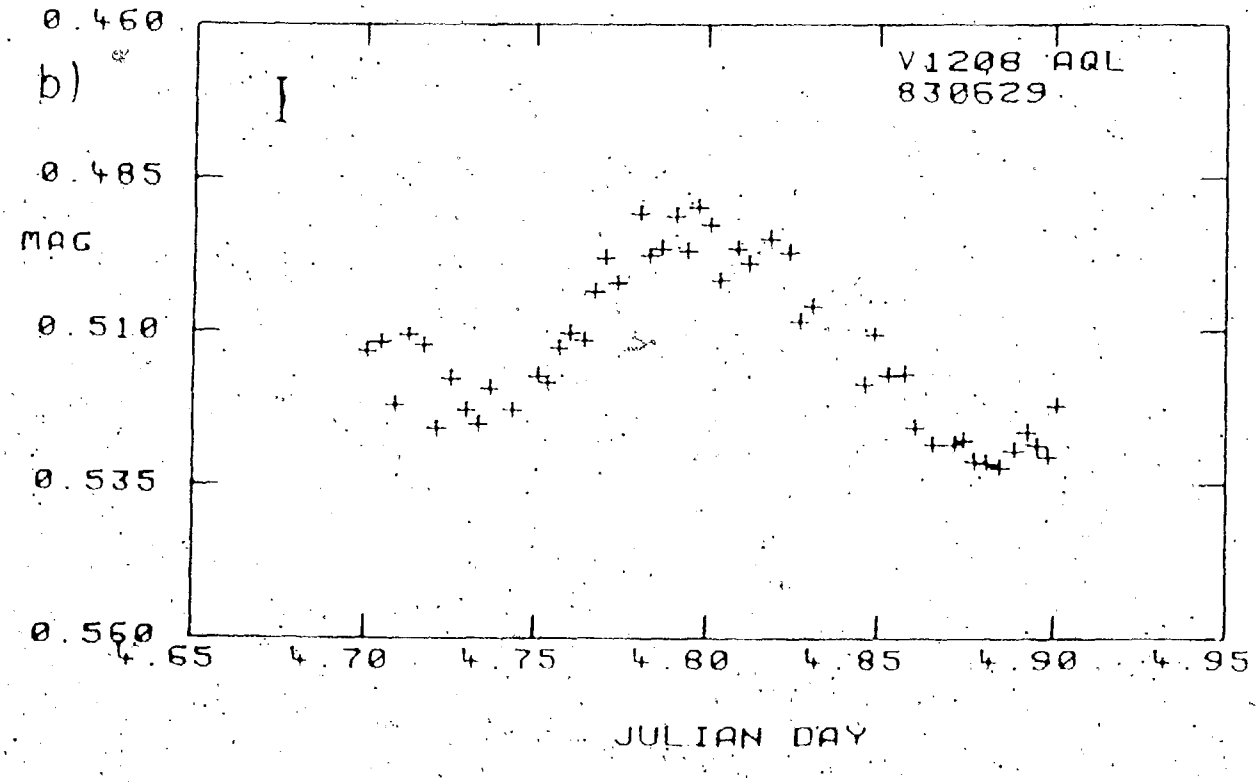
b)
I
V1208 AQL
830629
0.460
0.485
MAG
0.510
0.535
0.560
4.65
4.70
4.75
4.80
4.85
4.90
4.95
JULIAN DAY

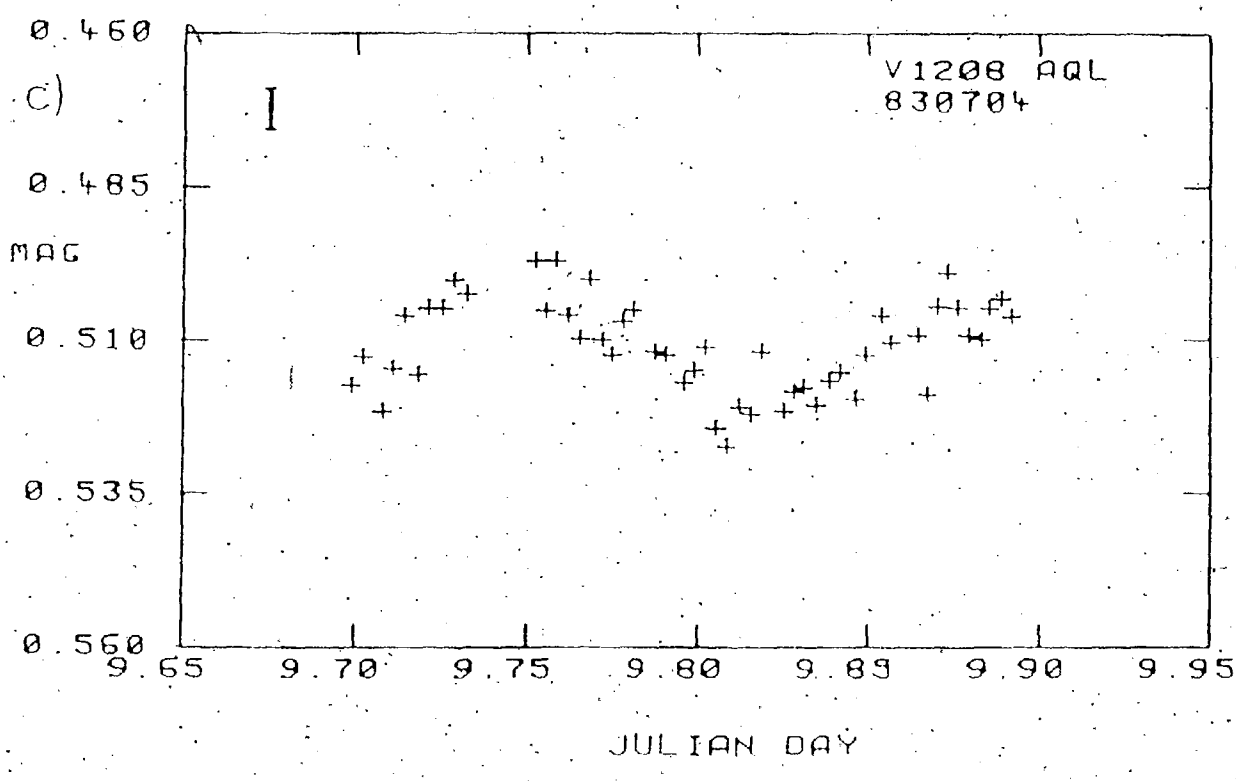
C)
V1208 AQL
830704
0.460
0.485
0.510
0.535
0.560
MAG
9.65
9.70
9.75
9.80
9.85
9.90
9.95
JULIAN DAY

Figure II.3.4. Differential V photometry of 63 Her for the nights of a) June 2/3, 1983, b) June 3/4, 1983, c) June 4/5, 1983, d) June 10/11, 1983, e) June 12/13, 1983, f) June 13/14, 1983 and g) June 14/15, 1983.
Julian Day (shown) = Julian Day - 244 5480

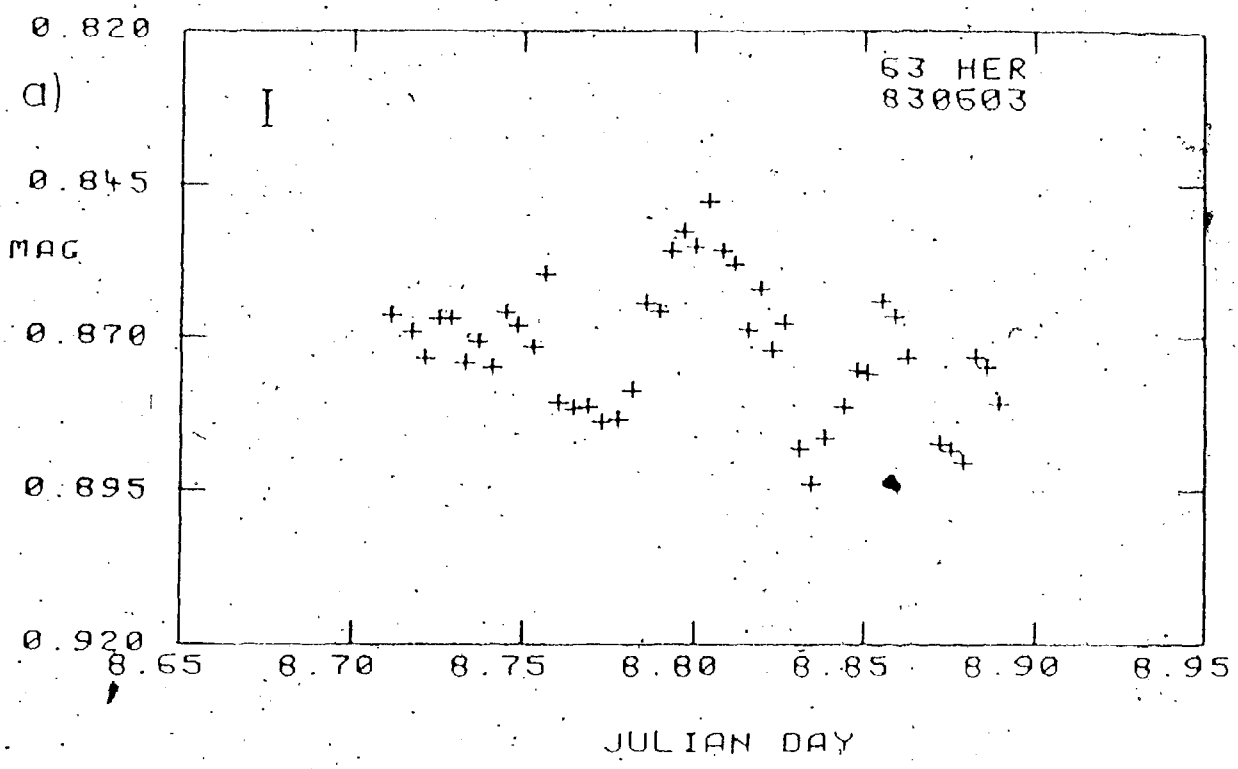
a)
I
63 HER
830603
0.820
0.845
MAG
0.870
0.895
0.920
8.65
8.70
8.75
8.80
8.85
8.90
8.95
JULIAN DAY

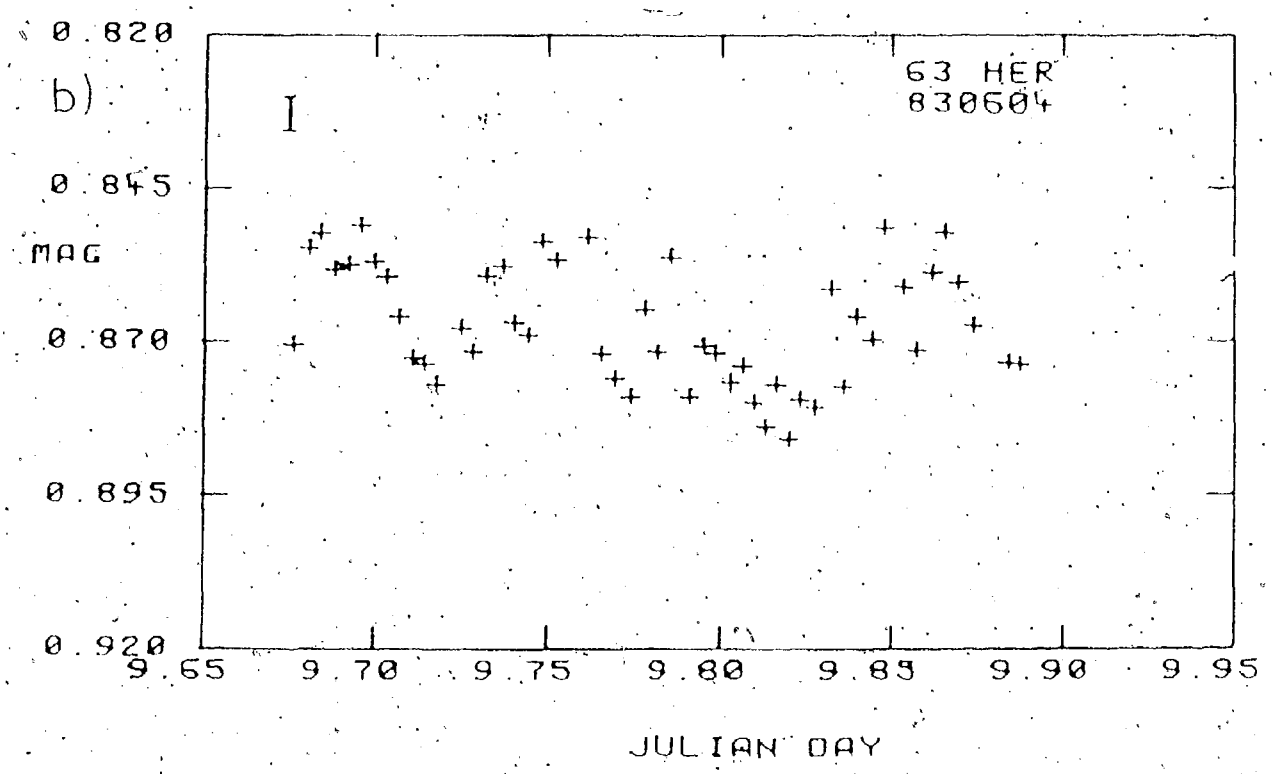
b)
I
63 HER
830604
0.820
0.845
MAG
0.870
0.895
0.920
9.65
9.70
9.75
9.80
9.85
9.90
9.95
JULIAN DAY

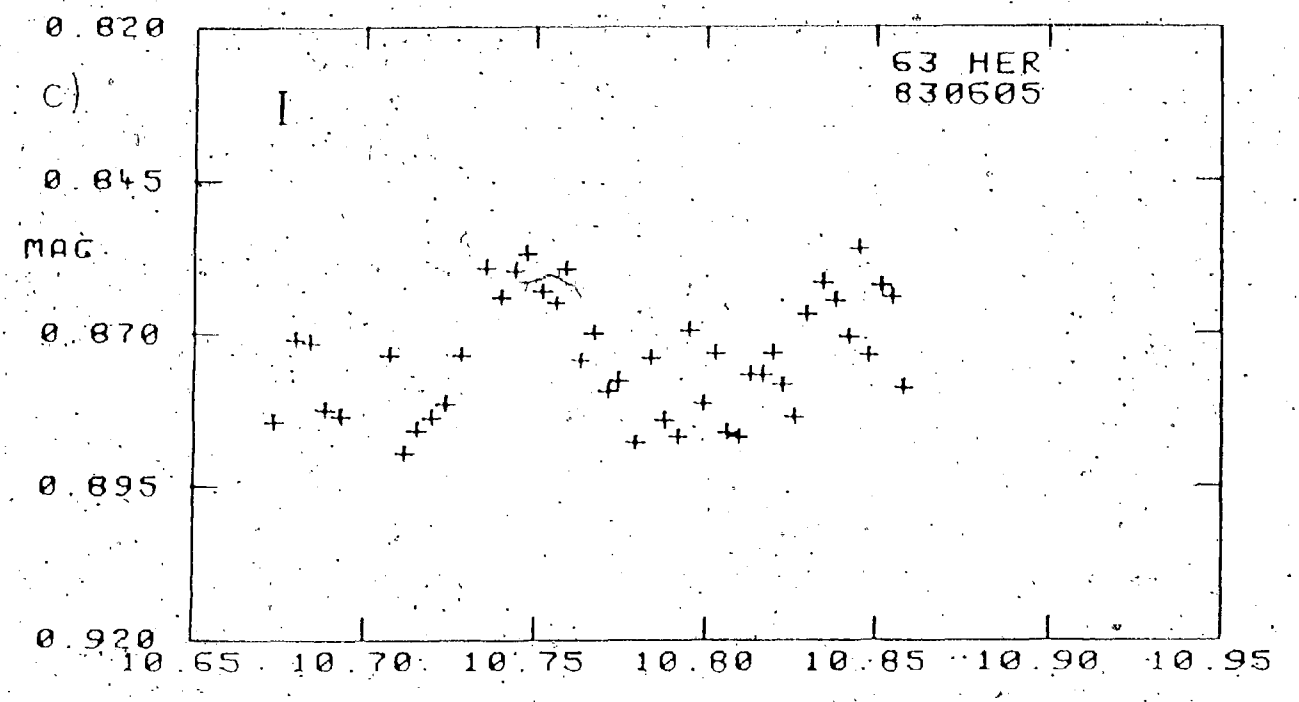
c)
I
63 HER
830605
0.820
0.845
MAG
0.870
0.895
0.920
10.65
10.70
10.75
10.80
10.85
10.90
10.95
JULIAN DAY

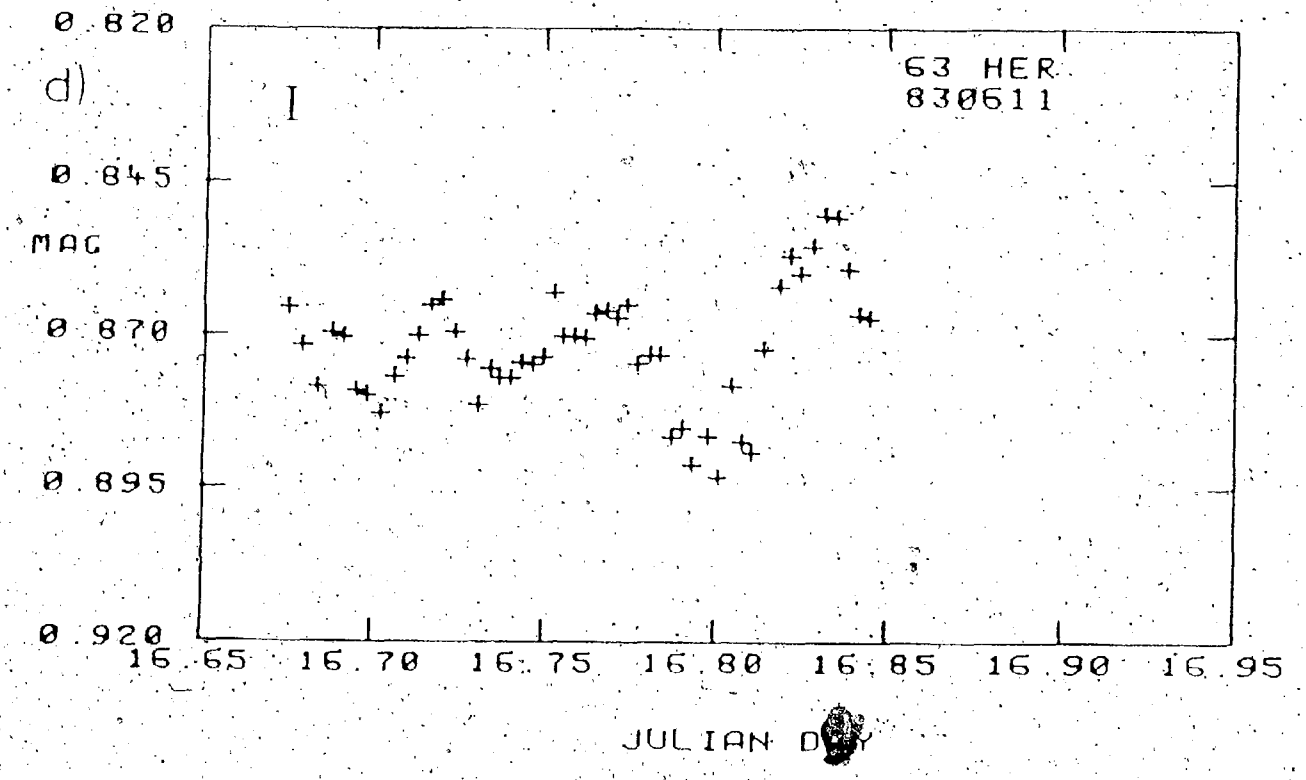
d)
I
63 HER
830611
0.820
0.845
MAG
0.870
0.895
0.920
16.65
16.70
16.75
16.80
16.85
16.90
16.95
JULIAN DAY

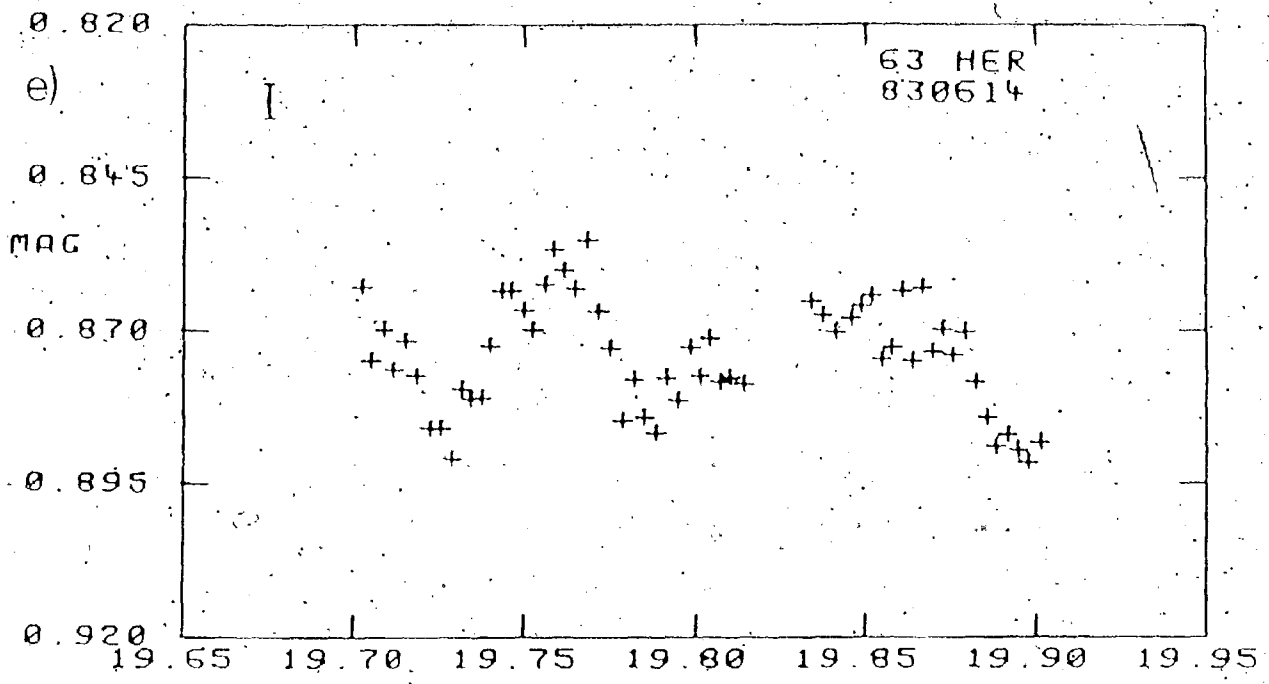
e)
63 HER
830614
0.820
0.845
MAG
0.870
0.895
0.920
19.65
19.70
19.75
19.80
19.85
19.90
19.95
JULIAN DAY

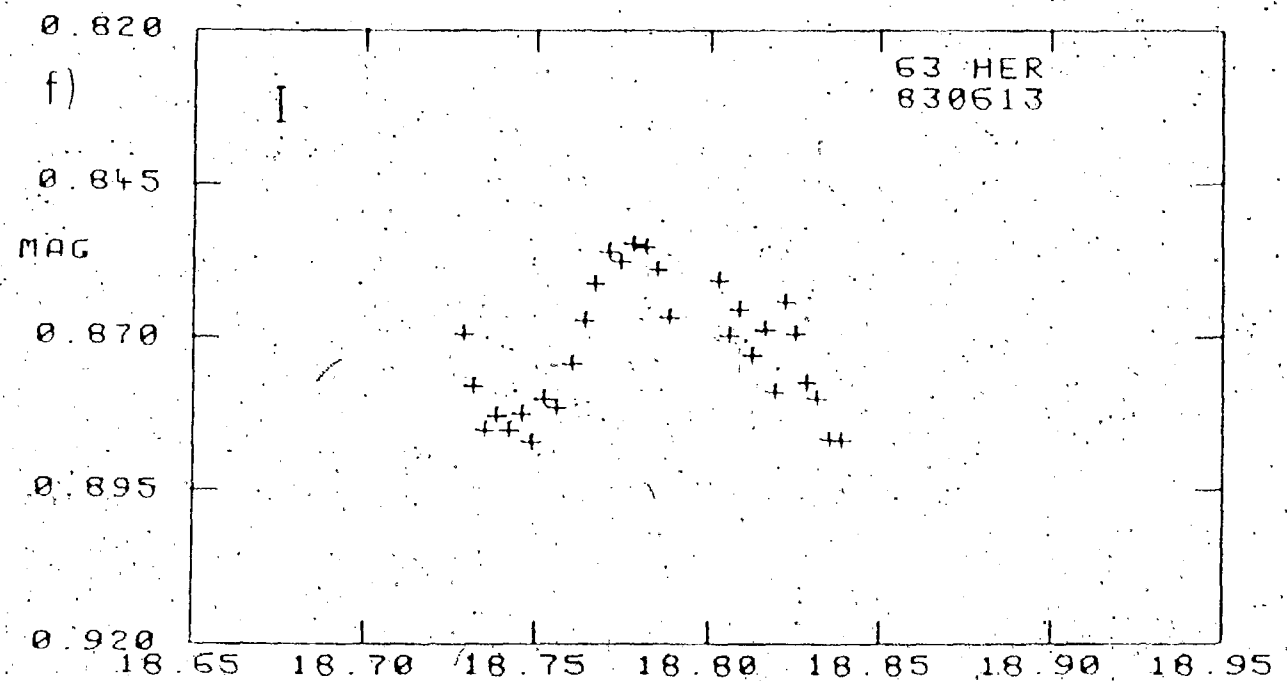
f)
63 HER
830613
0.820
0.845
MAG
0.870
0.895
0.920
18.65
18.70
18.75
18.80
18.85
18.90
18.95
JULIAN DAY

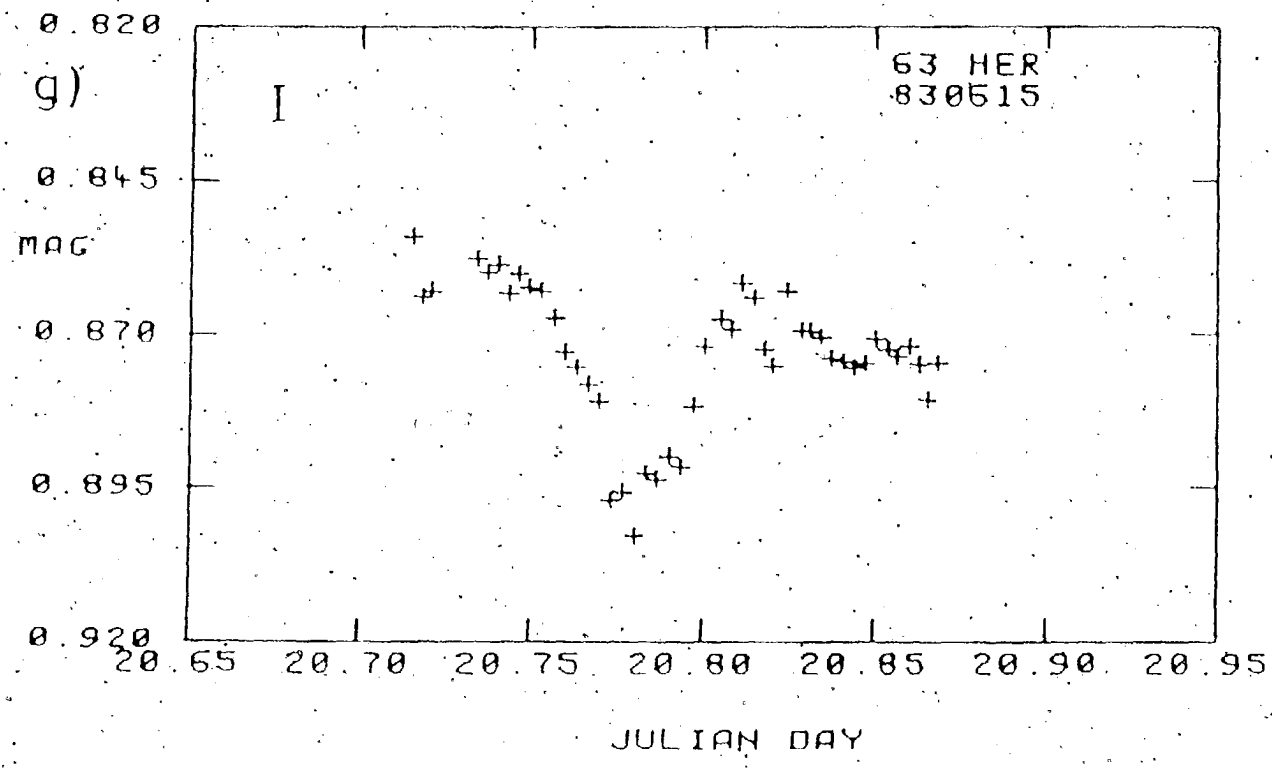
0.820
g)
I
63 HER
830615
0.845
MAG
0.870
0.895
0.920
20.65
20.70
20.75
20.80
20.85
20.90
20.95
JULIAN DAY

Chapter III: Data Reduction Procedures

1. The Jurkevich Method of Period Searching

The Jurkevich (1971) period search technique was developed as an aid in determining periodicities contained in irregularly-spaced, time-dependent observational data. Many previous authors have discussed this method in detail (Jurkevich 1971; Morris 1979; Morris and DuPuy 1980; Swingler 1985a and 1985b), so only a brief outline of the technique will be given here.

Consider a set of N (time, magnitude) data points (x_i, y_i, i = 1 to N). These points have an overall mean magnitude of zero for simplicity, and contain a periodicity P_0 of half-amplitude A_0. For every trial period P, a magnitude versus phase diagram is constructed, where the phase, ϕ_i, associated with a data point (x_i, y_i) is given by:

$$\phi_i = \frac{\text{mod}\,(x_i - x_0)}{P}, \qquad 0 < \phi_i < 1, \qquad (1)$$

where x_0 is a convenient, arbitrary starting time. Each phase diagram is then divided into M intervals, or bins. In the kth bin there are m_k points with mean magnitude mu_k. For each trial period, the Jurkevich method assigns a magnitude index, I(P),

$$I(P) = \sum_{i=1}^{N} y_i^2 - \sum_{K=1}^{m} m_K \, mu_k^2 , \qquad (2)$$

where $\sum_{i=1}^{N} y_i^2$ = a constant for a given data set.

A Jurkevich periodogram is a plot of I(P) against P.

If $P \neq P_0$, the points on the phase diagram will be randomly scattered, and the M values of mu_k will be close to zero. If $P \approx P_0$, however, the points will delineate a wave function of period P_0 and half-amplitude A_0. In this latter case, the M values of mu_k will not be close to zero, and $\sum_{k=1}^{M} m_k mu_k^2$ will approach a maximum value, since the data within the bins will be systematically either above or below zero. In the periodogram, a minimum then appears at $I(P_0)$, since I(P) is defined as a difference. Normally, however, periodograms are simply inverted and the baseline shifted to zero, so that $I(P_0)$ is a maximum.

Figure III.1.1. is a sample frequency diagram plotted for a set of unevenly-spaced time - magnitude data points into which there has been incorporated a sine function of the form

$$y = A_0 \sin(2\pi F_{m0} x + \phi_0) + \bar{m} + s_m , \quad (3)$$

where $A_0 = 0.022$, $F_{m0} = 11.36$ cy/d, $\phi_0 = 0.000$, $\bar{m}$ = a scaling factor = 0.500, s_m = random Gaussian noise = 0.001, x = time and y = magnitude. These artificial data were generated using the routine SYNCUV (Appendix D-2) and the 327 time values from the complete set of points for the program star 63 Her. That is, new <u>artificial</u> magnitudes were calculated using observed, unevenly-spaced time values. The FORTRAN routine used to perform the Jurkevich calculations was obtained from Morris and DuPuy (1980).

Figure III.1.1. Unmodified Jurkevich frequency diagram for artificial data generated using Equation 3 (from the text). The primary envelope, which surrounds the peak at F_0, is marked with circles. The irregular system of peaks between 4 and 8 cy/d is due to the 1/2 F_0 harmonic of F_0.

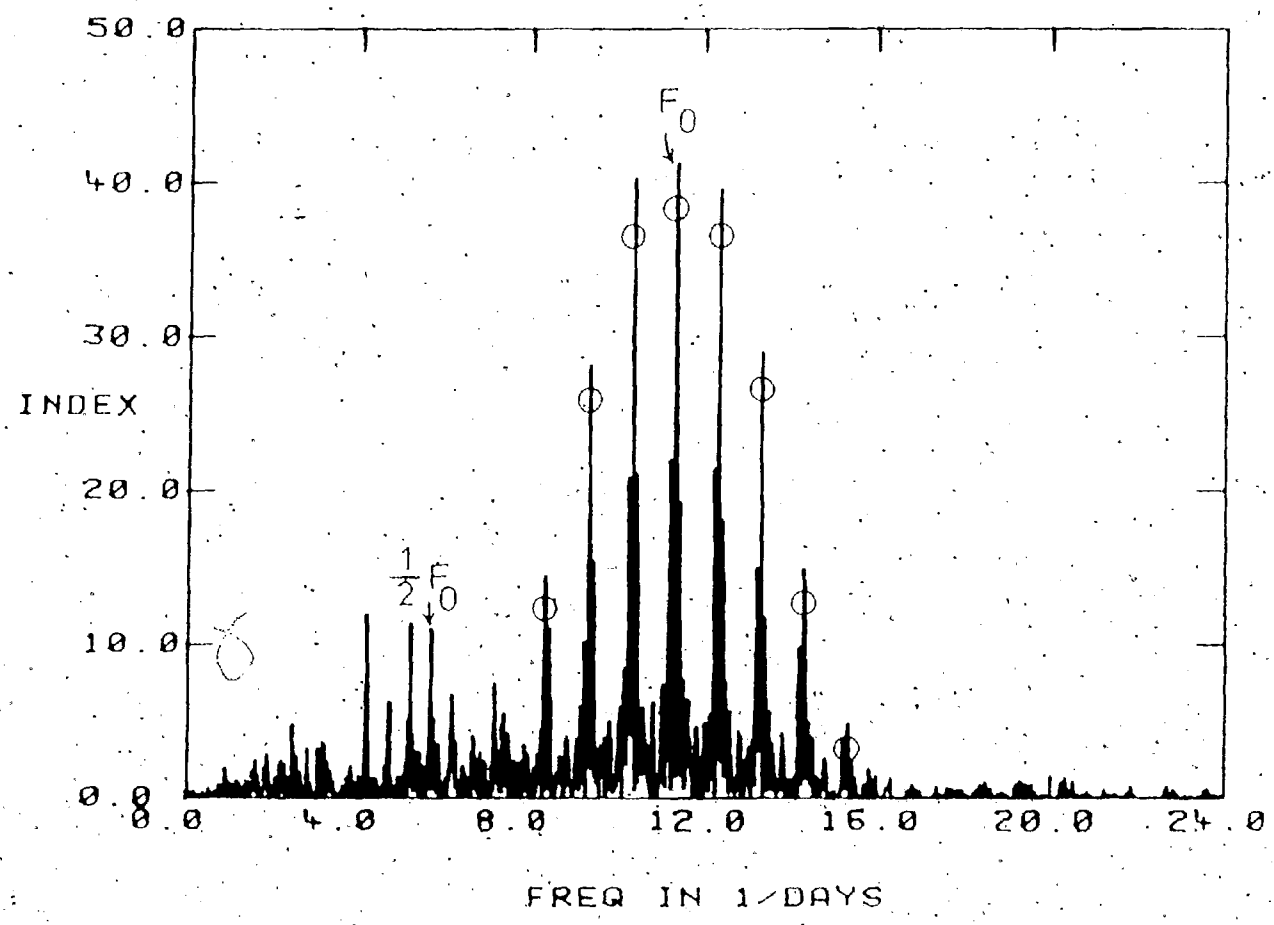
50.0
40.0
30.0
INDEX
20.0
10.0
0.0
F_0
$\frac{1}{2}F_0$
0.0
4.0
8.0
12.0
16.0
20.0
24.0
FREQ IN 1/DAYS

Frequency diagrams are shown throughout this thesis instead of periodograms; that is, frequency, not period, has been plotted along the abscissa. An Index versus Frequency diagram is easier to read because the corresponding Index versus Period diagram is not linear in frequency. Aliases (see below) of a periodicity are then simpler to pick out on a frequency diagram since they are equidistant from each other. To express Equation (3) in terms of period, P, it is necessary to remember that

$$P = \frac{1}{F}$$

Equation (3) would then be written

$$y = A_o \sin\left[\frac{2\pi x}{P_o} + \phi_o\right] + \bar{m} + s \qquad (4)$$

The frequency diagram in Figure III.1.1. illustrates two problems with the Jurkevich technique:

1) One-day aliasing tends to occur in astronomical observations since data sets are normally obtained at roughly 1-day intervals and uncertainty arises in the number of cycles which have elapsed during times of no observations. Peaks appear on the Jurkevich periodogram at values of $F = F_o \pm 1$, $F_o \pm 2$, $F_o \pm 3$, etc., but with decreasing values of I(F) since they do not fit the data as well. For uncomplicated data sets, one can ignore this quite easily. However, for data containing multiple, closely-spaced periodicities, the interaction of two or more alias envelopes in conjunction with the harmonic phenomenon discussed below can be difficult to sort out.

2) Besides the alias envelope surrounding each true frequency other systems of peaks also appear. These are centred on values of $F = n F_0$, $n = 1/2, 1/3$, etc., corresponding to harmonics of order n of the true frequency F_0. These harmonics are artifacts of the Jurkevich method and their presence only complicates the frequency diagram. For example, in Figure III.1.1., a harmonic system of F_0 appears at $F = 1/2F_0 = 5.65$ cy/d. Since data containing only one sinusoidal frequency (herein 'single-sine', or 'one-sine') are used, the maximum at F_0, its alias envelope, and the harmonics are very clearly seen.

As shown in Figure III.1.2, the situation becomes even more complicated when another sine function (of the same form as above), with frequency close, but not exactly equal to $1/2F_0$, is added to the original artificial data. The resulting periodogram shows a complicated structure of peaks between 0 cy/d and 9 cy/d due to the interaction between the harmonics and the newly introduced overtone period, $F_1 = 5.26$ cy/d. Note the misleading height of the peak at 7.14 cy/d, occurring because an alias of the overtone period happens to coincide exactly with an alias of the $2F_0$ harmonic. The two peaks simply add algebraically, resulting in a spurious peak of "false" height, indicating a strong periodicity where one does not really exist. Further experimentation showed that the confusion becomes worse when additional periodicities are introduced.

Figure III.1.2. Unmodified Jurkevich frequency diagram for two-sine artificial data (see text). Symbols are used as in Fig. III.1.1. The unmarked arrow indicates a spurious peak due to the proximity of the secondary frequency envelope surrounding the peak at F_1 to the 1/2 F_0 harmonic envelope.

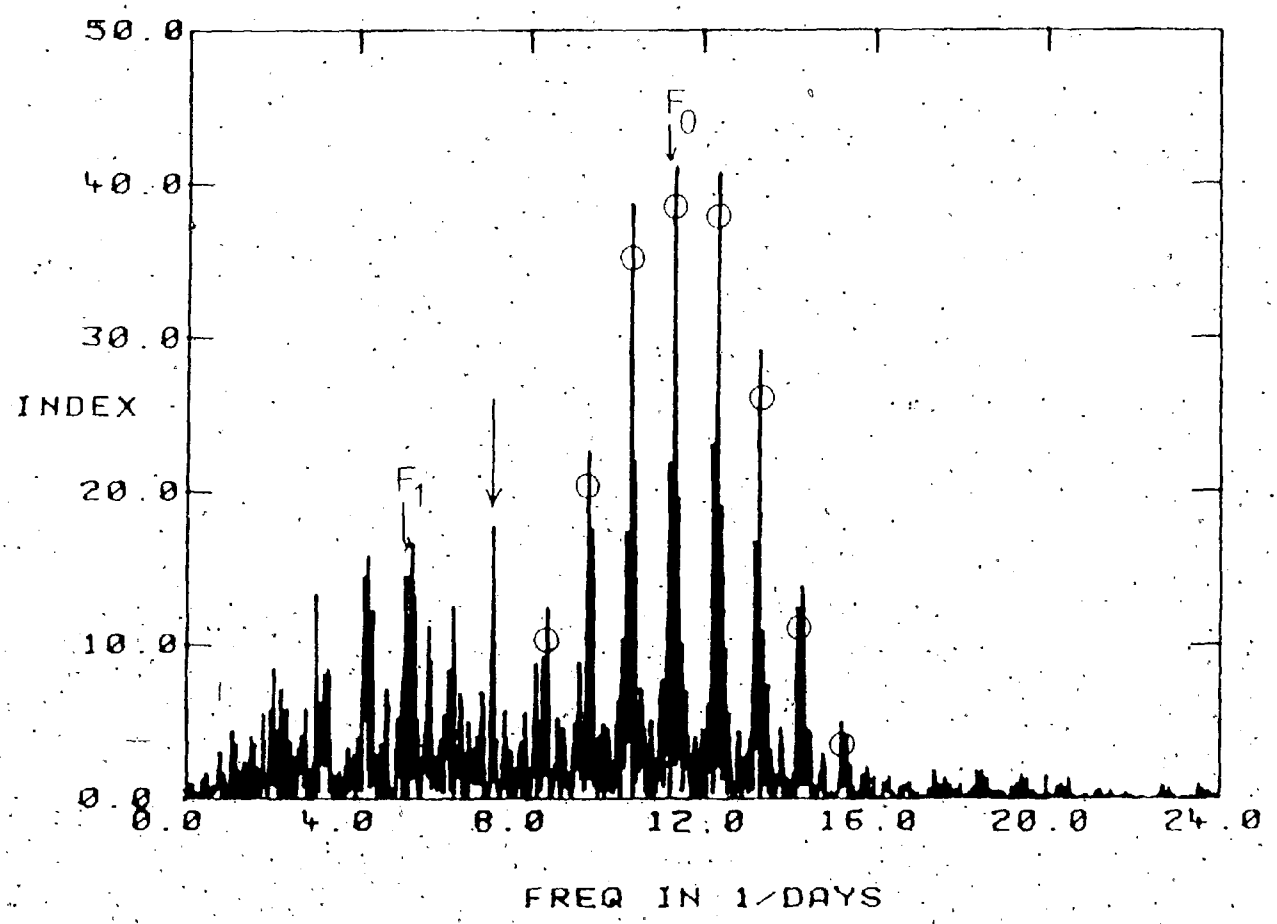
50.0
40.0
30.0
INDEX
20.0
10.0
0.0
F0
F1
0.0
4.0
8.0
12.0
16.0
20.0
24.0
FREQ IN 1/DAYS

From past experience with the Jurkevich method (DuPuy and Burgoyne, 1983), as well as from additional attempts to use it in the reduction of both real and other more complicated artificial data, we decided that Swingler's (1985b) modification of the Jurkevich method would be more suitable in circumstances where multiple periods might be expected. The complicating harmonic peaks introduced by the Jurkevich technique tend to hinder attempts at straightforward, accurate period searching.

2. Swingler's Modification of the Jurkevich Method

As demonstrated in the previous section, each periodicity contained in the data will contribute multi-peak harmonic structures to the Jurkevich periodogram. The shape of the M-bin Jurkevich periodogram is essentially the same as that of a classical Fourier frequency spectrum of a rectangular waveform of 1:M-1 mark-to-space ratio. The confusing multi-harmonic nature of the Jurkevich method (that is, the harmonic peaks themselves) can be eliminated by replacing this rectangular waveform by a waveform of some other shape (Swingler 1985). The problem of aliasing remains, however, since it is inherent to the observational data. It will be shown (here and in Chapter IV) that once the harmonic peaks are removed, the aliasing alone is no longer as difficult to interpret.

A modification of the Jurkevich technique in which a new index, I (F), is defined can be constructed as follows

(Swingler 1985b). The usual Jurkevich technique determines the points in the phase diagram for each trial frequency F. Then, for each time-magnitude data point (x_i, y_i), the products Q_i and R_i are defined:

$$Q_i = y_i \cos (2\pi F x_i)$$

and (5)

$$R_i = y_i \sin (2\pi F x_i)$$

Q_i and R_i are then separately summed over all data points and the squares of their sums are added. A scale factor involving the total number of data points is then introduced. The resulting equation defines the new index $I_s(F)$ at trial frequency F:

$$I_s(F) = \left(\frac{2}{N}\right)^2 \left[\left(\sum_{i=1}^{N} Q_i\right)^2 + \left(\sum_{i=1}^{N} R_i\right)^2\right]$$

$$= \left(\frac{2}{N}\right)^2 \left[\left(\sum_{i=1}^{N} y_i \cos 2\pi F x_i\right)^2 + \left(\sum_{i=1}^{N} y_i \sin 2\pi F x_i\right)^2\right]. \quad (6)$$

One does not know initially how the data are distributed across the magnitude versus phase diagram since, because of the uncertainty in phase, the points can appear to delineate either a sine or a cosine function. Therefore, when replacing the rectangular wave, both sine and cosine functions must be considered, that is, one must multiply by one full cycle of <u>both</u> types of functions. When $F \neq F_0$, the multiplication and summation process yields zero output, and (ideally) only gives a non-zero result when $F = F_0$. Figures III.2.1. and III.2.2. illustrate examples of modified-Jurkevich (hereinafter 'Jurkevich - Swingler')

Figure III.2.1. Jurkevich-Swingler frequency diagram for the same one-sine artificial data as in Fig. III.1.1. As before, circles are used to indicate the envelope due to the primary periodicity. Compare to Fig. III.1.1.

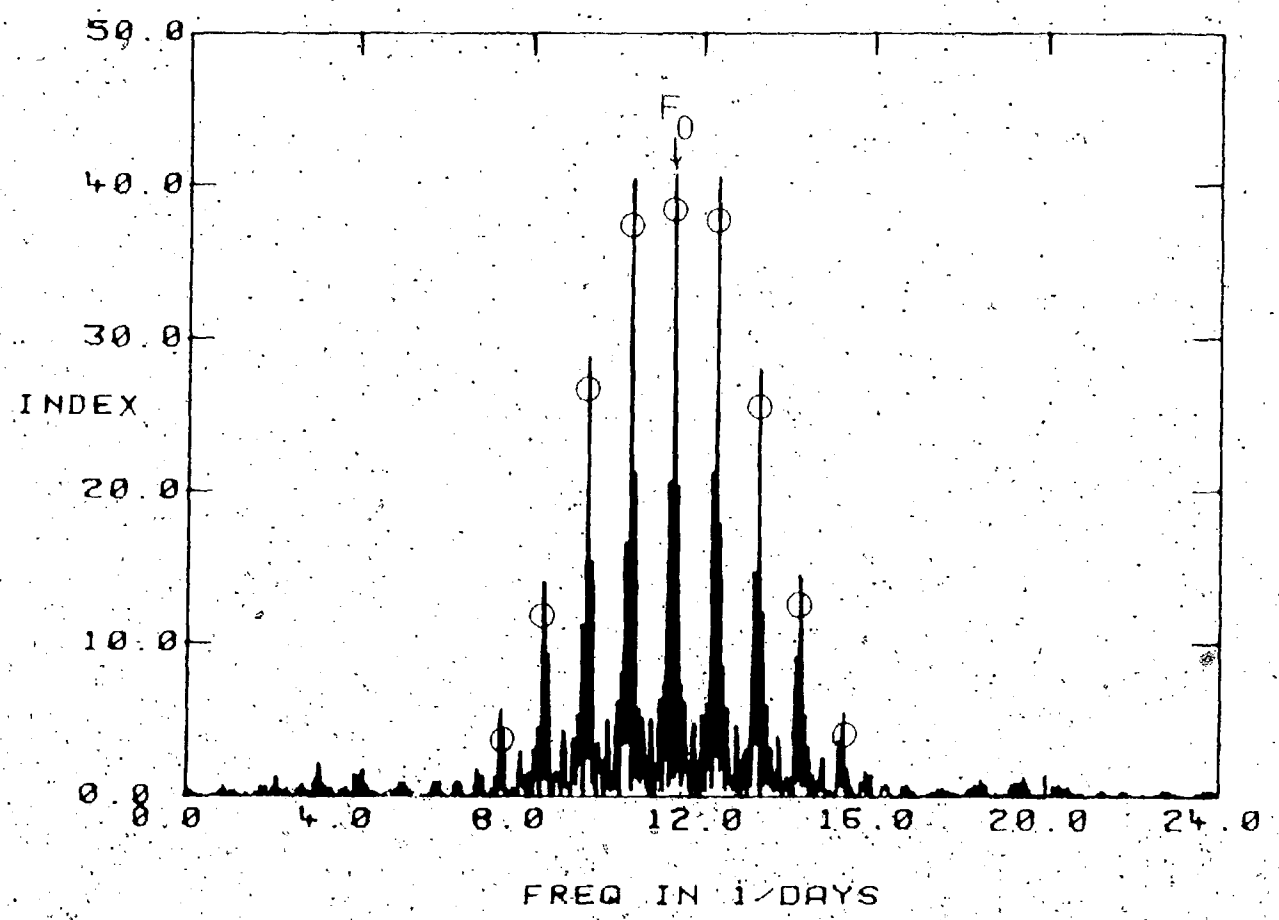
50.0
40.0
30.0
INDEX
20.0
10.0
0.0
F_0
0.0
4.0
8.0
12.0
16.0
20.0
24.0
FREQ IN 1/DAYS

Figure III.2.2. Jurkevich-Swingler frequency diagram for the same two-sine artificial data as in Fig. III.1.2. Circles are used as in previous frequency diagrams and squares are used to indicate the envelope due the secondary frequency, F_1. Compare to Fig. III.1.2.

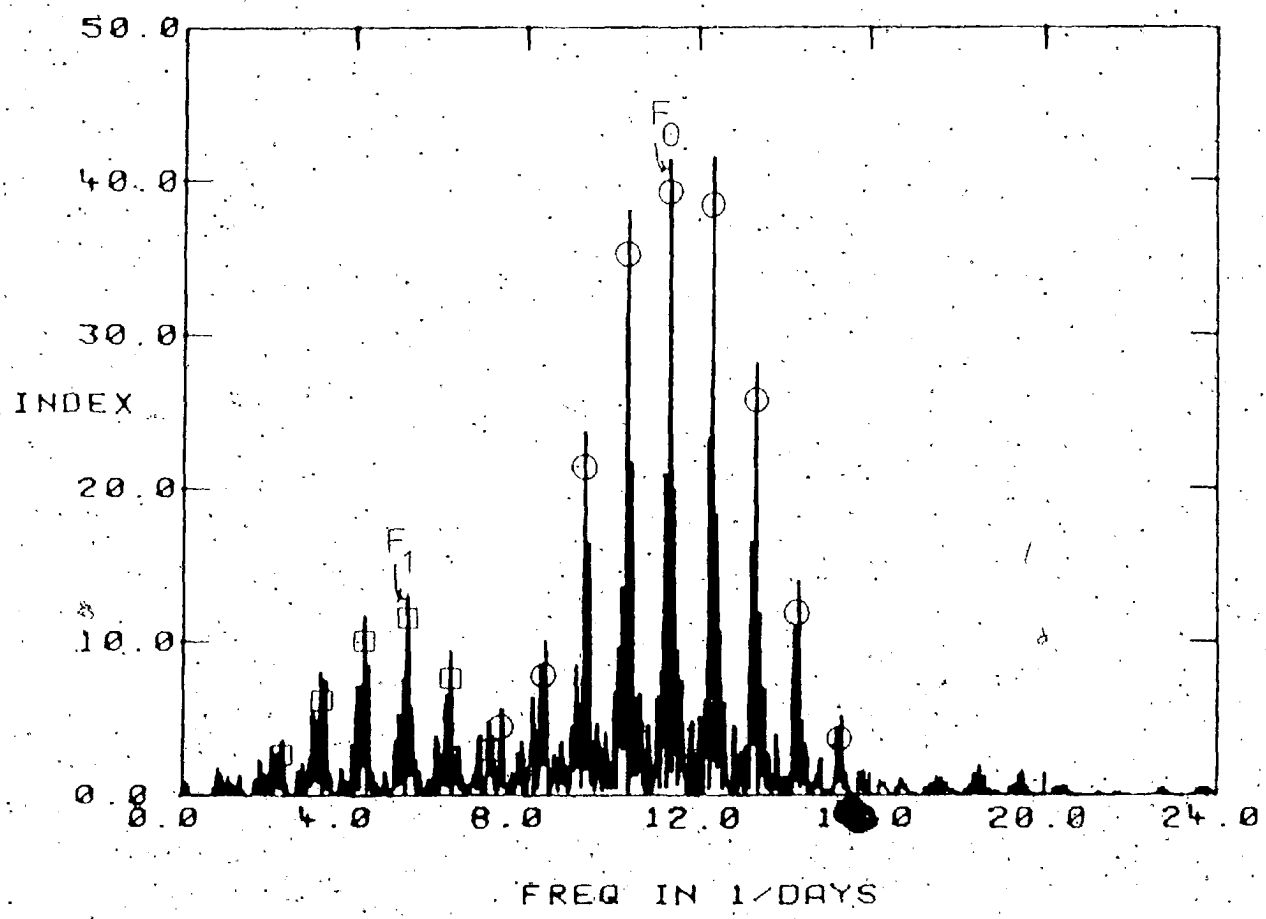
50.0
40.0
30.0
INDEX
20.0
10.0
0.0
F0
F1
0.0
4.0
8.0
12.0
20.0
24.0
FREQ IN 1/DAYS

periodograms for the same single- and double-sine artificial data used in Figures III.1.1. and III.1.2., respectively. Note the dramatic differences in the modified frequency diagrams compared to Figures III.1.1. and III.1.2., respectively. The 'new' diagrams are much cleaner and easier to interpret. The alias envelopes stand out much more clearly and, since the harmonics are gone, no spurious, misleading, peaks occur. It appears that this modified technique is more accurate and, hence, a superior period-searching tool for our data. The FORTRAN algorithm developed for this method is listed in Appendix D-3.

Equation (6) is very similar in form to that used in a classical Fourier analysis. The only difference between the two is that the Jurkevich-Swingler technique multiplies phase - magnitude data by a single period of both a sine and cosine function, whereas the usual Fourier method multiplies the original time - magnitude data by sine and cosine functions. In both cases, the resulting index $I_s(F)$ is the same (Swingler 1985b).

The new modified index, $I_s(F)$, as defined in Equation (6), can be used to obtain a direct estimate for the amplitude of a periodicity that appears as a peak in a frequency diagram. To illustrate the relationship between index and amplitude, a series of 15 artificial (time, magnitude) data sets were created, each containing the same one-sine periodicity, F_o, which in each case had a

different half-amplitude, A. A periodogram of each data set was plotted and the index, $I_s(F)$ corresponding to the peak at F was recorded. A $\log I_s(F)$ versus log A diagram (see Figure III.2.3.) for these 15 test cases exhibits a linear relationship for which linear least-squares fitting yields

$$\log I_s(F) = -0.0090\ (\pm 0.0046) + 2.0068\ (\pm 0.0026) \log A\ .$$

In other words, $I_s(F)$ is closely related to the square of amplitude corresponding to a periodicity, F. This $\log I_s(F)$ versus log A diagram will be used again in Chapter IV to determine values of A corresponding to the indices of selected peaks that appear on frequency diagrams. That is, one can use this $\log I_s(F)$ versus log A diagram to obtain initial "guesses" for the parameter A which corresponds to a variation of frequency F (cf. Chapter IV).

3. The Non-linear Least Squares Fitting Technique

A non-linear least squares fit is needed to determine the other parameters associated with a periodicity once the Jurkevich-Swingler method has been used to provide a reliable guess for that periodicity. The quantities half-amplitude, A, phase, ϕ, and an average magnitude scaling factor, m, are needed to completely describe the sine function corresponding to each frequency:

$$y(I) = A \cdot \sin(2\pi F\ x(I) + \phi) + \bar{m}\ , \qquad (7)$$

where I = 1,...N data points.

Figure III.2.3. Plot of log Modified Index versus log Amplitude

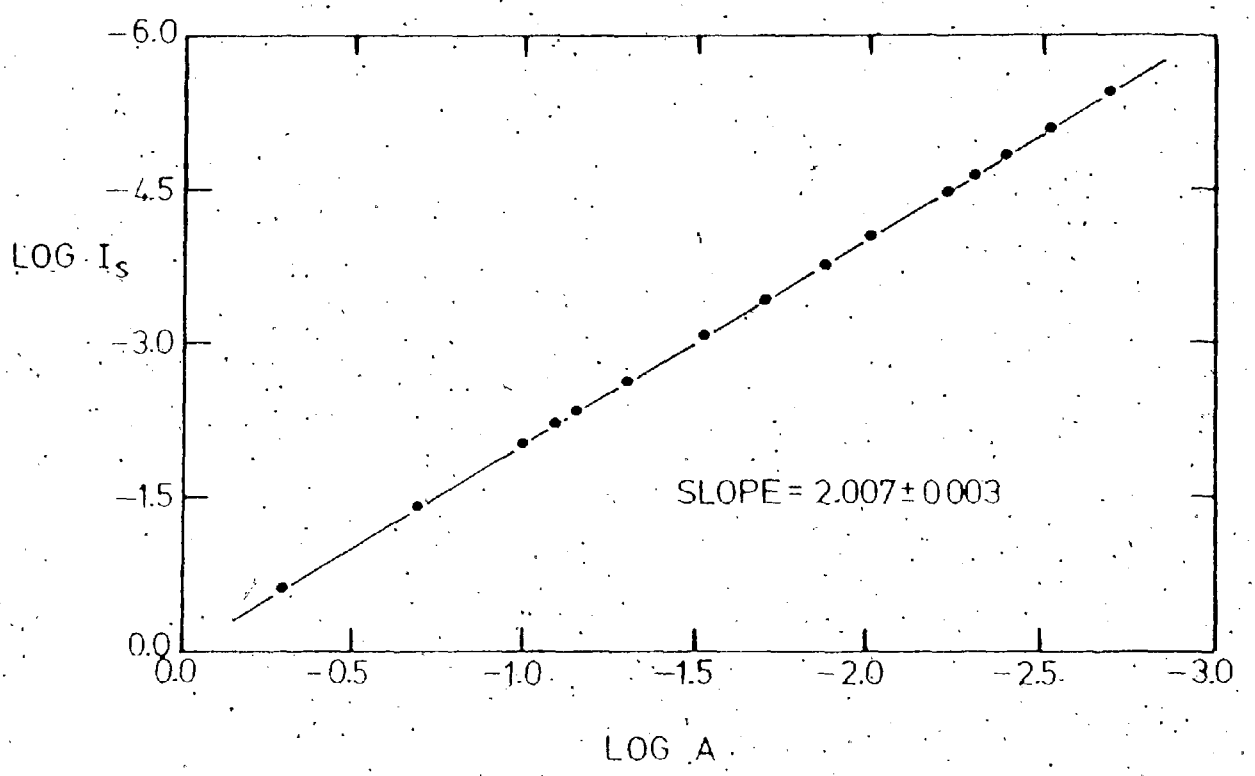
-6.0
-4.5
-3.0
-1.5
0.0
LOG I_S
SLOPE = 2.007 ± 0.003
0.0
-0.5
-1.0
-1.5
-2.0
-2.5
-3.0
LOG A

The fits were made using P3R, a library program in the Biomedical Statistical Package from the University of California, Los Angeles (see Morris, 1979 for a program listing), in conjunction with the Dalhousie University CYBER 6600 computer. P3R requires that the user make reasonably accurate (to within a few percent) initial guesses for frequency, phase, and average magnitude; initial estimates for half-amplitude turn out to be less critical to the success of the fit. P3R can be used to determine the parameters of up to six sine functions occurring simultaneously within a single data set, although in this work it was never used in anything more complex than a four-sine fit. The type of output generated by P3R (including parameter error estimates and "best-fit" residual mean square values) will be discussed in detail in Chapters IV and V.

A basic flowchart for the complete period-search procedure used on all three program stars is shown in Figure III.3.1. For a given set of data points, the most dominant frequency is chosen from a plotted Jurkevich-Swingler frequency diagram. The routine P3R is then used to perform a non-linear, single-sine, least squares fit on the data, using the dominant frequency and guesses for A, ϕ, and m. The best (lowest RMS deviation) converged fit is then subtracted from the data, that is, the data are "prewhitened". Next, a new frequency diagram is plotted using the prewhitened data to see if any secondary

Figure III.3.1.: Rough Flowchart for the Complete Period-Search Procedure Used in This Thesis

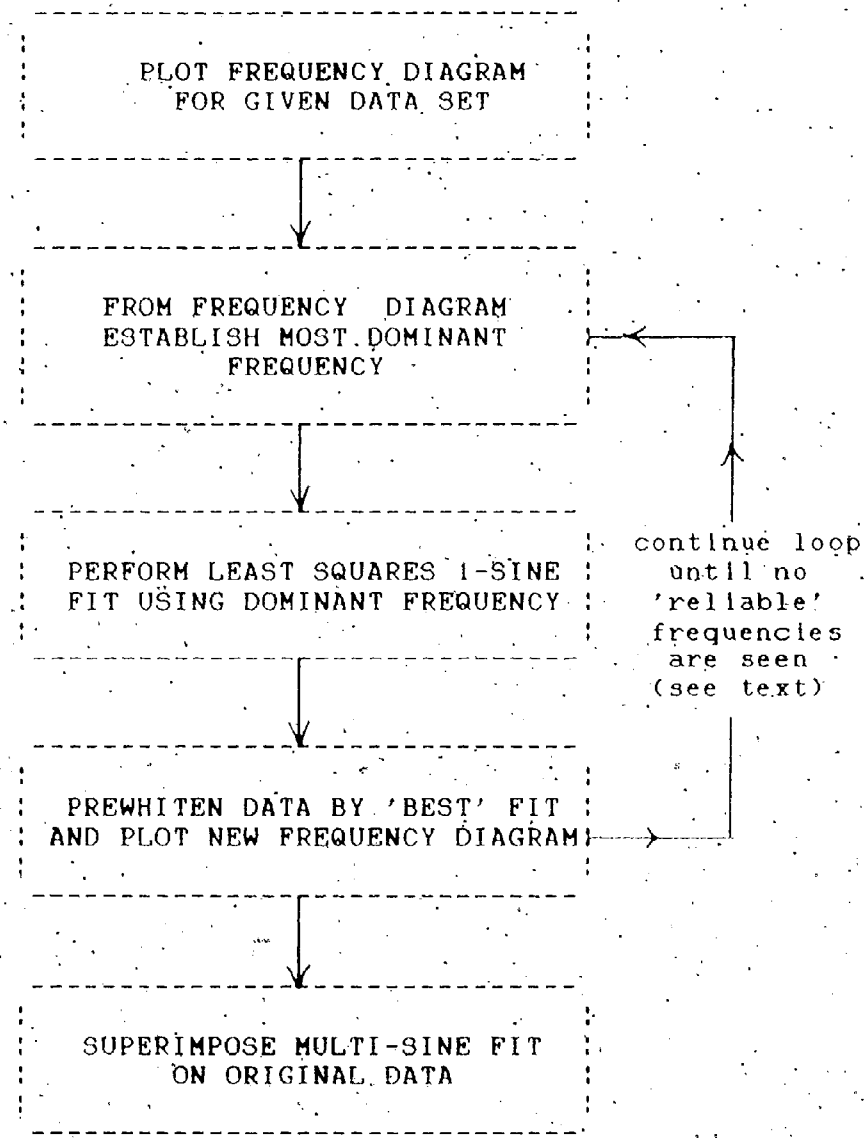

periodicities have become apparent in the absence of the dominant variation. If any further periodicities are present, they are individually fitted with a single-sine equation using P3R, and also removed from the data.

This procedure is repeated until no further periodicities of reliable amplitude (that is, amplitude larger than the previously discussed observational error) are seen. Finally, the total multi-sine fit is superimposed on the original differential data, and final residuals are calculated.

Chapter IV: The Period Searches and Their Results

1. 63 Herculis

As stated in Chapter II, the data for 63 Her consist of 327 observations obtained during seven nights spread over 12 days. The initial Jurkevich-Swingler frequency diagram formed from the data is shown in Figure IV.1.1.

Note the horizontal line drawn across the frequency diagram at Index = 1.38. It was decided that the frequency diagram (shown in Figure IV.1.2.) formed from the 63 Her comparison minus check data would be a good indicator of the expected (observational) noise level seen in Figure IV.1.1. There is only one major system of peaks seen in Figure IV.1.2.; the envelope centred at approximately 20 cy/d indicates that the highest peaks due to expected observational uncertainty should have a maximum index of 1.38. Hence, the line drawn across Figure IV.1.1. (and all other 63 Her frequency diagrams) at Index = 1.38 indicates the limiting index, I_1, such that any peaks not having an index at least as large as I_1 are to be eliminated or regarded with suspicion. Similar arguments shall be carried out for V1208 Aql and LT Vul. The Index in Figure IV.1.1. has been plotted only for the frequency interval of 0 to 24 cy/d since analysis of the same data at frequencies greater than 24 cy/d shows no peaks above the

Figure IV.1.1. Jurkevich-Swingler frequency diagram of 63 Her data. Symbols for this and all following frequency diagrams are: ◯ - primary envelope, □ - secondary envelope, and △ - tertiary envelope. The dashed line indicates the limiting Index, I

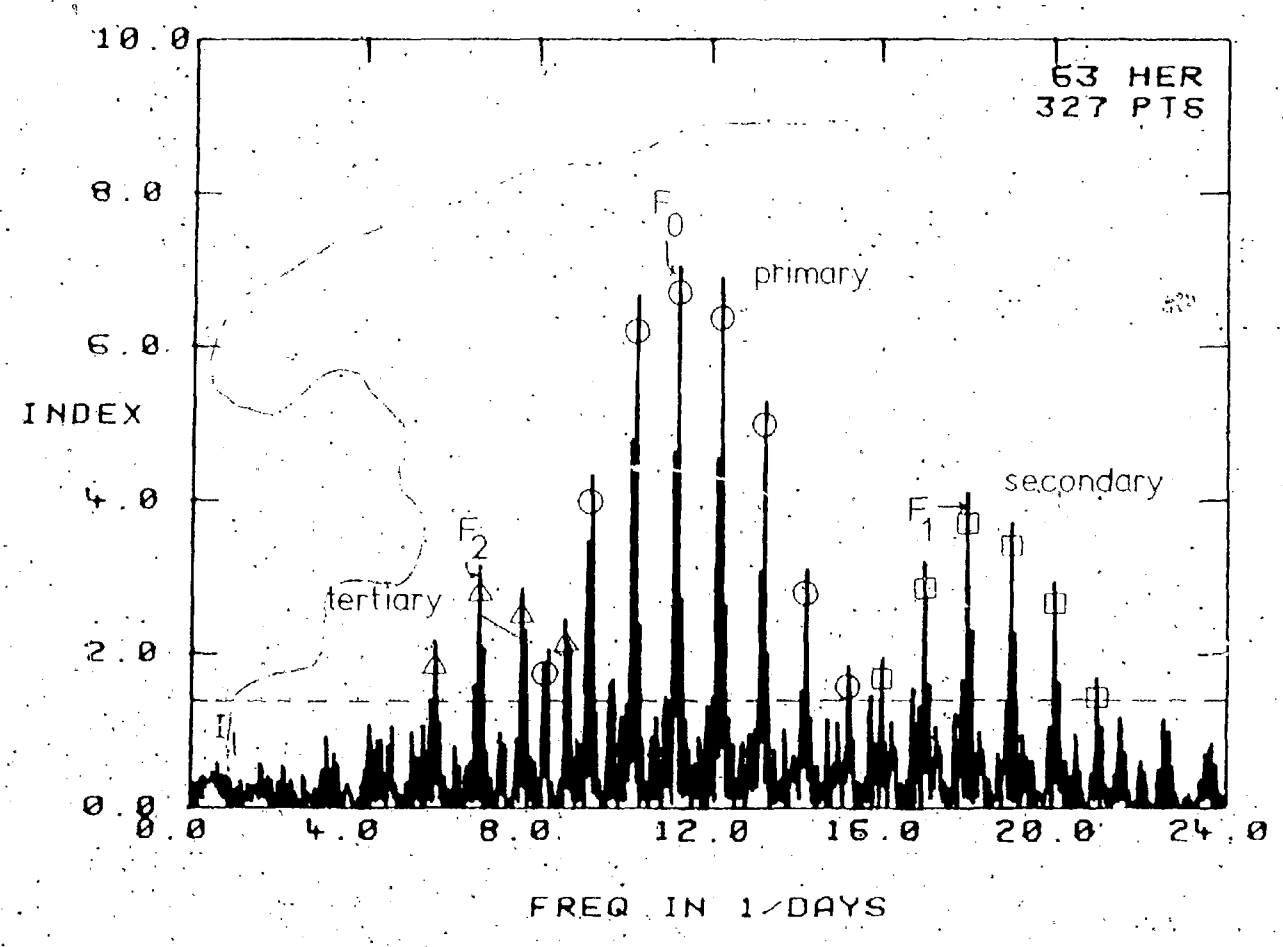
63 HER
327 PTS
INDEX
10.0
8.0
6.0
4.0
2.0
0.0
0.0
4.0
8.0
12.0
16.0
20.0
24.0
F0
primary
F2
F1
secondary
tertiary
FREQ IN 1/DAYS

Figure IV.1.2. Frequency diagram of 63 Her comparison star minus check star data. The largest envelope has a maximum index of 1.38, which defines the limiting index, I_1, for the 63 Her data. Similar procedures are followed for V1208 Aql and LT Vul to determine I_1.

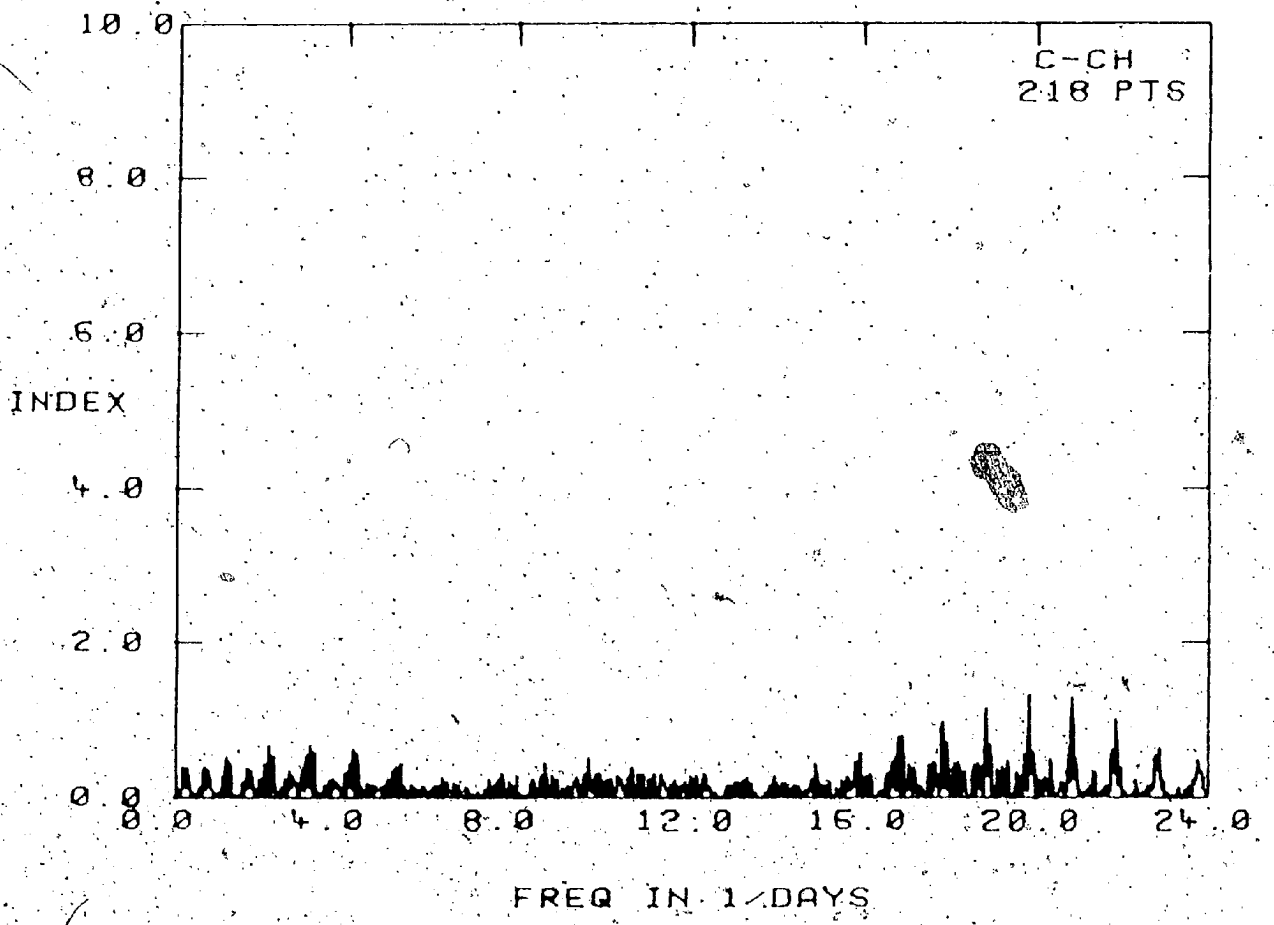
C-CH
218 PTS
10.0
8.0
6.0
INDEX
4.0
2.0
0.0
0.0
4.0
8.0
12.0
16.0
20.0
24.0
FREQ IN 1/DAYS

limiting index of 1.38.

Three distinct systems of peaks are visible against the background noise. The most prominent envelope, designated 'primary', is centred on the tallest peak at F_A = 11.33 cy/d. The envelope itself is composed of seven one-day aliases of F_A appearing on either side of the central peak.

The secondary envelope consists of six peaks centred around F_B = 18.10 cy/d. The tertiary envelope, the least prominent of the three, consists of a central peak at F_C = 7.74 cy/d and five aliases. The index of the F_C peak is only of the order of $2I_1$, hence, it is the least reliable of the three frequencies.

From this preliminary frequency diagram, then, one may conclude that 63 Her appears to be pulsating in at least two and possibly three distinct frequencies: F_A = 11.33 cy/d; F_B = 18.10 cy/d; and F_C = 7.74 cy/d.

At this stage it is interesting to note that an envelope of peaks centred on the one frequency of 12.98 cy/d seen by Breger (1969) does not appear in Figure IV.1.1. The reason for this could be simply that his small number of observations (50) were not adequate to accurately indicate the presence of one or more frequencies for this obviously complicated star. That is, since the data obtained here are considerably more comprehensive than Breger's observations, more confidence should be placed in these results.

The next step in the reduction is to use the non-linear least squares routine P3R to accurately determine the parameters for the primary frequency and to aid in the determination of F_B and F_C. Figures IV.1.1. and III.2.3. were used to obtain initial guesses of A_A and F_A. Initial guesses for the remaining two parameters, ϕ_A and $\bar{m}$, were set to zero, since ϕ_A was completely unknown and could be anything between 0 and 2π, while $\bar{m}$ is just the average magnitude of the data, which the routine calculates regardless.

After nine iterations the program converged on the following parameters:

$$A_A = 0.0086 \pm 0.0007,$$
$$F_A = 11.3176 \pm 0.0030 \text{ cy/d},$$
$$\phi_A = 0.6910 \pm 0.2570,$$
$$\text{and } \bar{m} = 0.8718 \pm 0.0050,$$

with a root mean square (RMS) of 8.482×10^{-3} magnitudes. The output generated by this first run of P3R has been included in Appendix D-4 to show the comprehensive nature of this routine.

It should be mentioned that once this first run was complete, several further runs of P3R were made using the above parameters, slightly varied, as initial guesses. The reason for this was to determine if the parameters could be further refined on successive 'passes' through P3R. The results in every case, however, remained unchanged to well within half of one percent.

As well, several runs of P3R were made using the converged values of A, ϕ_A, and $\bar{m}$ as initial guesses, while attempting to use nearby aliases of the primary frequency as initial guesses for F_A. Although the program usually converged, both N, the number of iterations needed to achieve convergence, and the RMS values increased dramatically.

Also, several runs were made using the converged values of A, F_A, and $\bar{m}$ as initial guesses, while varying the initial guesses for ϕ_A between 0 and 2π. While frequency is of course the most important parameter here, the starting value for phase can also influence the convergence of the run (DuPuy and Burgoyne 1983). Results for these runs showed that although converged values of ϕ_A changed, the results for A, F_A, m and RMS remained virtually identical. However, as before, the number of iterations rose dramatically, as did the RMS values. It was decided, therefore, to adopt the original converged values for the four parameters. All non-linear least squares results for 63 Her are summarized in Table IV.1.1.

Figure IV.1.3. shows the periodogram resulting from the original data after it was prewhitened by the parameters for the primary frequency. Note that the primary envelope has been completely removed, leaving the secondary and tertiary envelopes very slightly weakened in index, but unchanged in all other aspects. Similar procedures involving P3R were followed for the remaining

Figure IV.1.3. Frequency diagram of 63 Her data prewhitened by:

$$y(I) = {}^{m}0.0086 \sin(2\pi 11.3176\ cy/d\ x(I) + 0.691) + {}^{m}0.8718$$

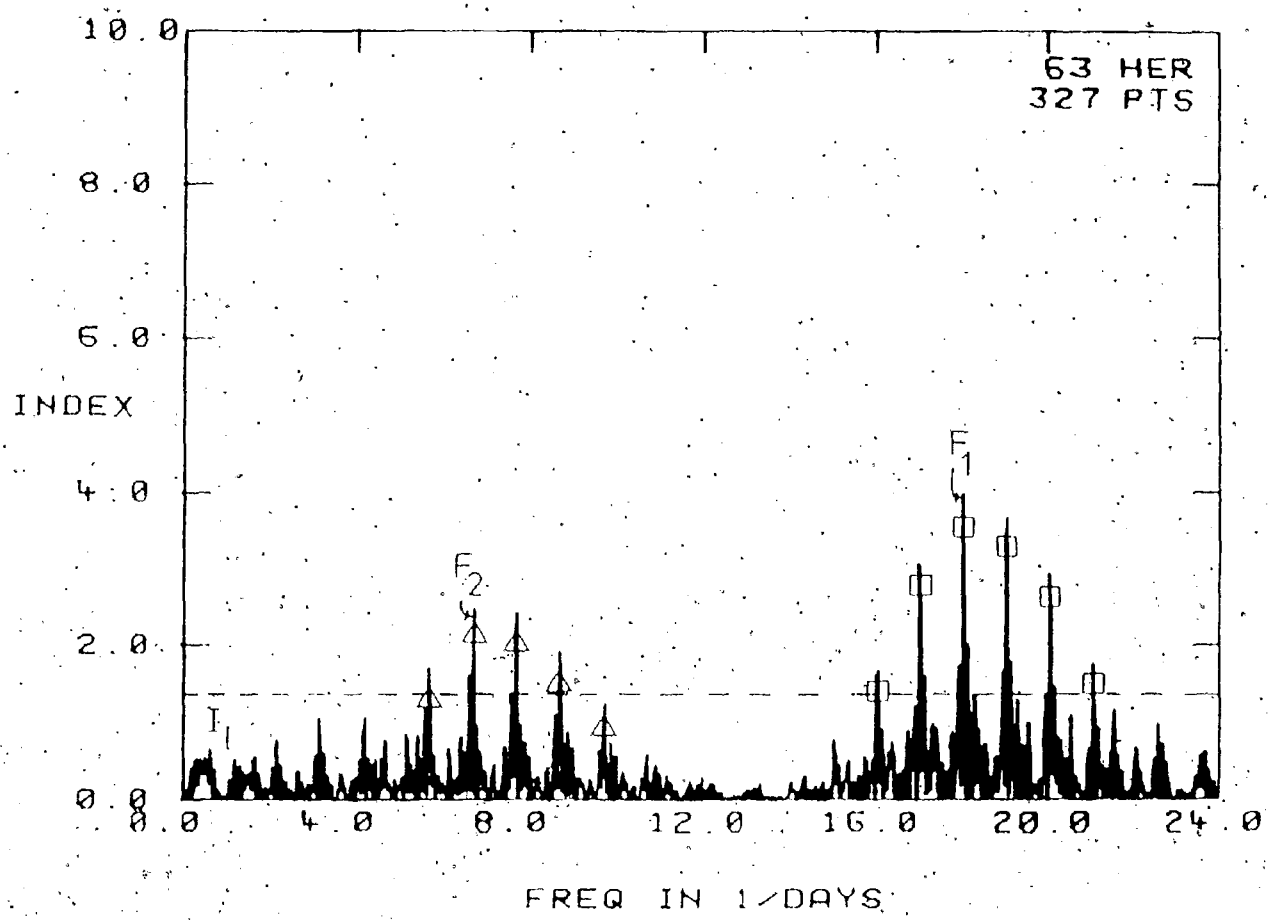
63 HER
327 PTS
INDEX
10.0
8.0
6.0
4.0
2.0
0.0
F1
F2
I1
0.0
4.0
8.0
12.0
16.0
20.0
24.0
FREQ IN 1/DAYS

periodicities in the data of 63 Her.

Table IV.1.1. summarizes the converged parameters and their errors resulting from the runs of P3R for all three periodicities in 63 Her. Figures IV.1.4. and IV.1.5. show periodograms for data prewhitened by the frequencies F_A and F_B, and F_A, F_B, and F_C respectively.

It is interesting to note here that the converged value of F_B is actually a one-day alias of the tallest peak in the secondary envelope. P3R converged on F_B = 19.07 cy/d and would at no time converge on 18.1 cy/d despite several attempt to force a solution at this frequency.

As discussed above, F_C is considered the least reliable periodocity of the three determined for 63 Her. This contention is now reinforced by the fact that its converged amplitude, $A_C = 0^m.0048 \pm 0^m.0005$, is actually less than the observational uncertainty determined for this star. We cannot be confident, then, that F_C is real.

Since all three periodicities have been removed from the 63 Her data in Figure IV.1.5., we expect to see no peaks of importance, which in fact turns out to be the case.

The last step in the reduction of the 63 Her data is to superimpose the converged fits on top of the original data to see how they compare. The top diagrams in Figures IV.1.6 a) to g) show these comparisons.

For each night, the data used to produce the superimposed lines have been calculated in the following

Table IV.1.1.: P3R results for 69 Her

Run	Converged Parameters A (mag)	F (cy/d) / P (d)	ϕ (rad)	$\bar{m}$ (mag)	N	RMS x 10 (mag)
A	0.0086 ±0.0007	11.3176 ±0.0026 / 0.0884 ±0.0002	0.6910 ±0.2569	0.8718 ±0.0005	9	8.482
B	0.0064 ±0.0006	19.0704 ±0.0030 / 0.0524 ±0.0001	2.3528 ±0.2934	0.0000 ±0.0004	10	7.178
C	0.0048 ±0.0005	7.7233 ±0.0035 / 0.1295 ±0.0001	4.1991 ±0.3424	0.0001 ±0.0004	8	6.343

Figure IV.1.4. Frequency diagram of 63 Her data prewhitened by:

$$y(I) = 0^{m}.0086 \sin(2\pi 11.3176 \text{ cy/d } x(I) + 0.691) + 0^{m}.0064 \sin(2\pi 19.0704 \text{ cy/d } x(I) + 2.353) + 0^{m}.8718$$

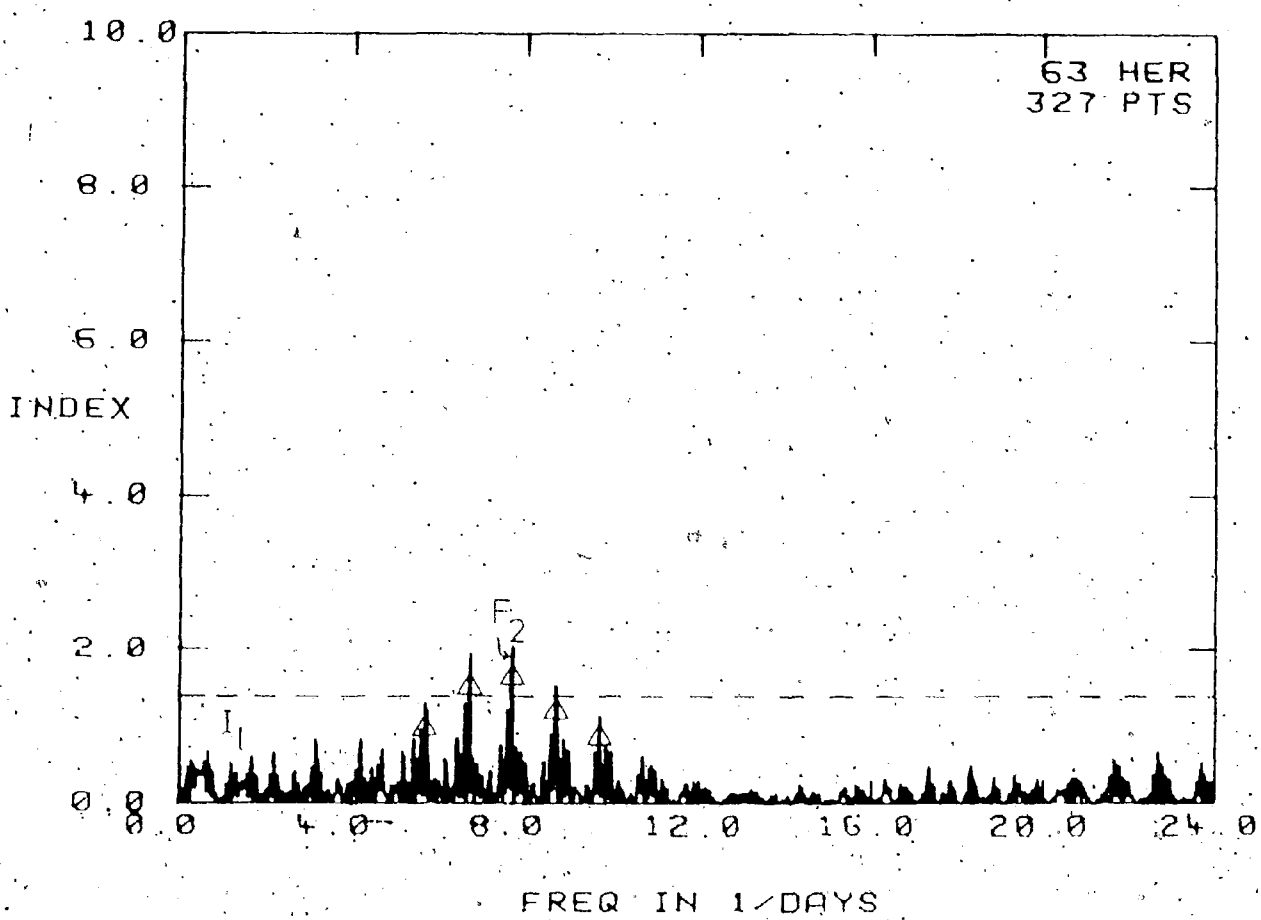
63 HER
327 PTS
10.0
8.0
6.0
INDEX
4.0
2.0
0.0
F_2
I_1
0.0
4.0
8.0
12.0
16.0
20.0
24.0
FREQ IN 1/DAYS

Figure IV.1.5. Frequency diagram of 63 Her data prewhitened by:

$$y(I) = 0^{m}.0086 \sin(2\pi\, 11.3176\ \mathrm{cy/d}\ x(I) + 0.691) + 0^{m}.0064 \sin(2\pi\, 19.0704\ \mathrm{cy/d}\ x(I) + 2.353) + 0^{m}.0048 \sin(2\pi\, 7.7233\ \mathrm{cy/d}\ x(I) + 4.199) + 0^{m}.8718$$

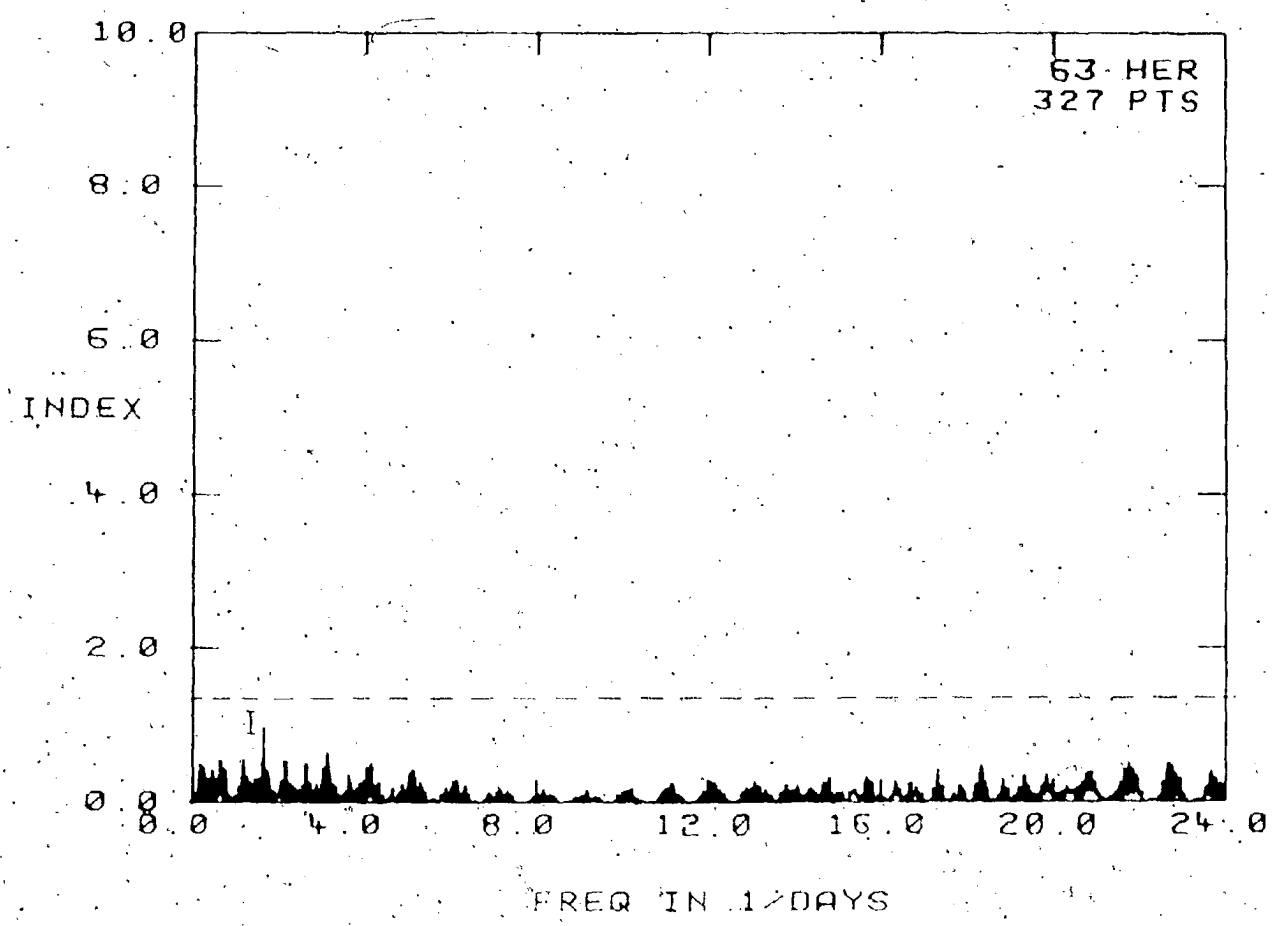
10.0
8.0
6.0
INDEX
4.0
2.0
0.0
63 HER
327 PTS
0.0
4.0
8.0
12.0
16.0
20.0
24.0
FREQ IN 1/DAYS

Figure IV.1.6. a) - g) top: Differential photometry of 63 Her with three-sine fit superimposed (see Table IV.1.1.).
bottom: Residuals of above three-sine fit.

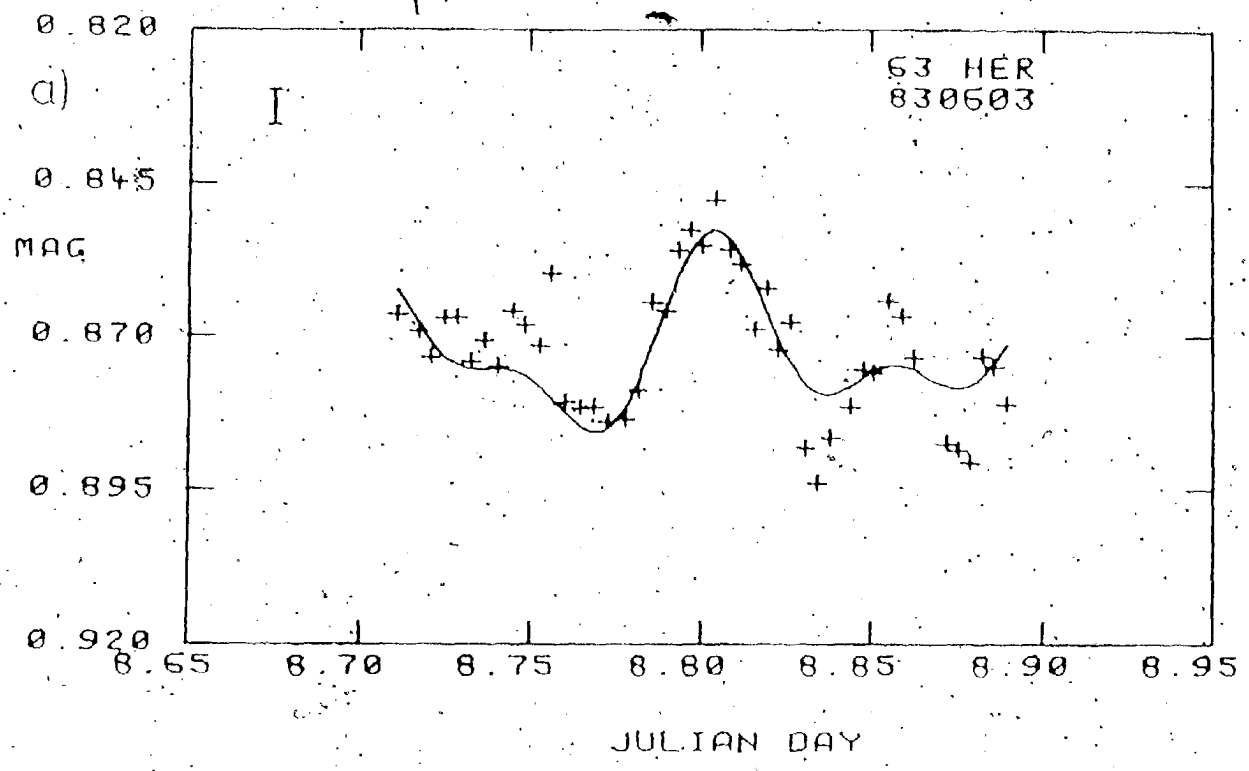
a)
I
63 HER
830603
0.820
0.845
0.870
0.895
0.920
MAG
8.65
8.70
8.75
8.80
8.85
8.90
8.95
JULIAN DAY

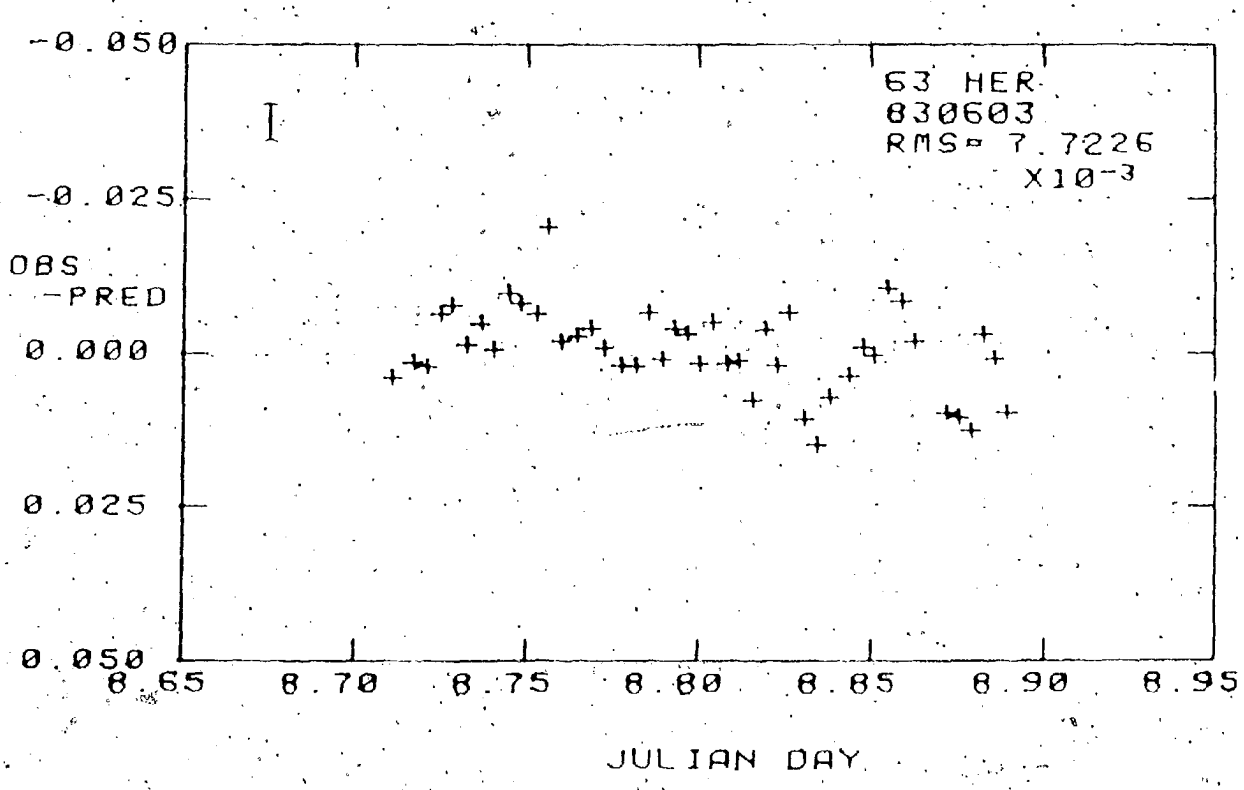
I
63 HER
830603
RMS= 7.7226
X10⁻³
-0.050
-0.025
0.000
0.025
0.050
OBS
-PRED
8.65
8.70
8.75
8.80
8.85
8.90
8.95
JULIAN DAY

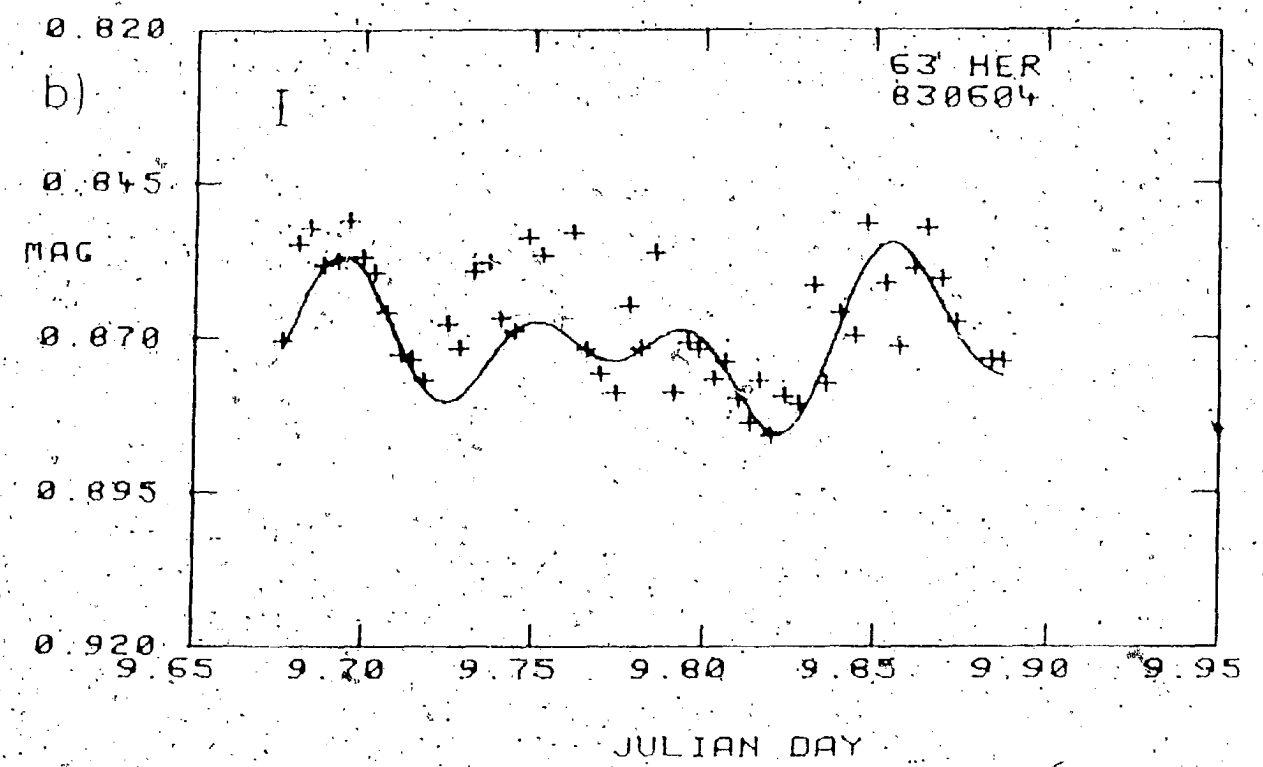
b)
I
63' HER
830604
0.820
0.845
MAG
0.870
0.895
0.920
9.65
9.70
9.75
9.80
9.85
9.90
9.95
JULIAN DAY

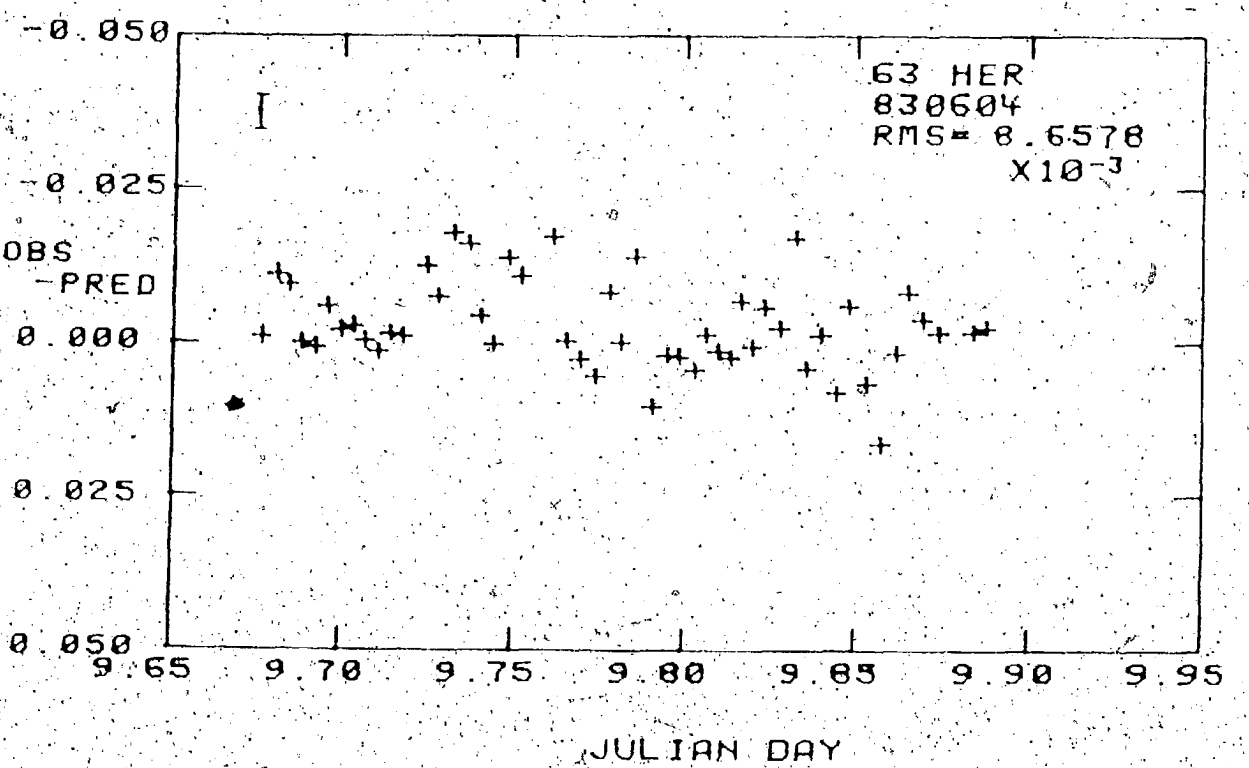
I
63 HER
830604
RMS= 8.6578
X10⁻³
-0.050
-0.025
OBS
-PRED
0.000
0.025
0.050
9.65
9.70
9.75
9.80
9.85
9.90
9.95
JULIAN DAY

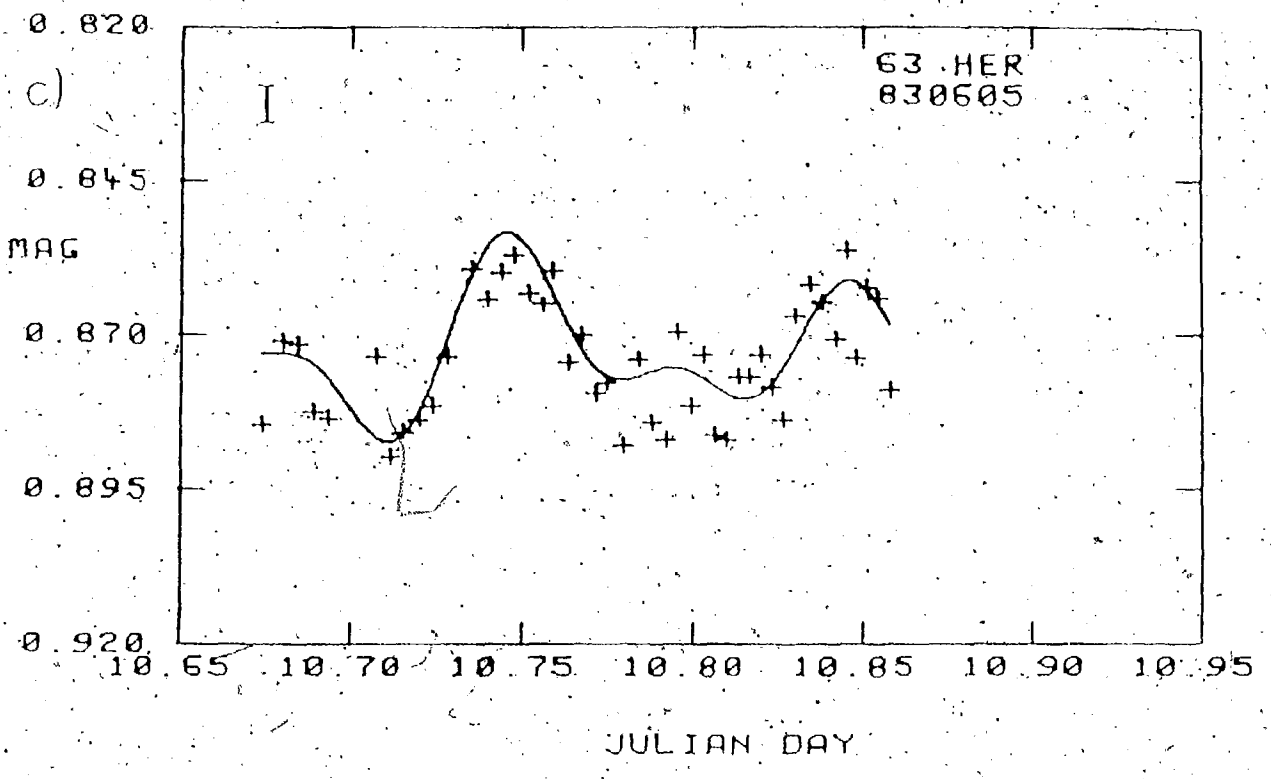
c)
63 HER
830605
0.820
0.845
MAG
0.870
0.895
0.920
10.65
10.70
10.75
10.80
10.85
10.90
10.95
JULIAN DAY

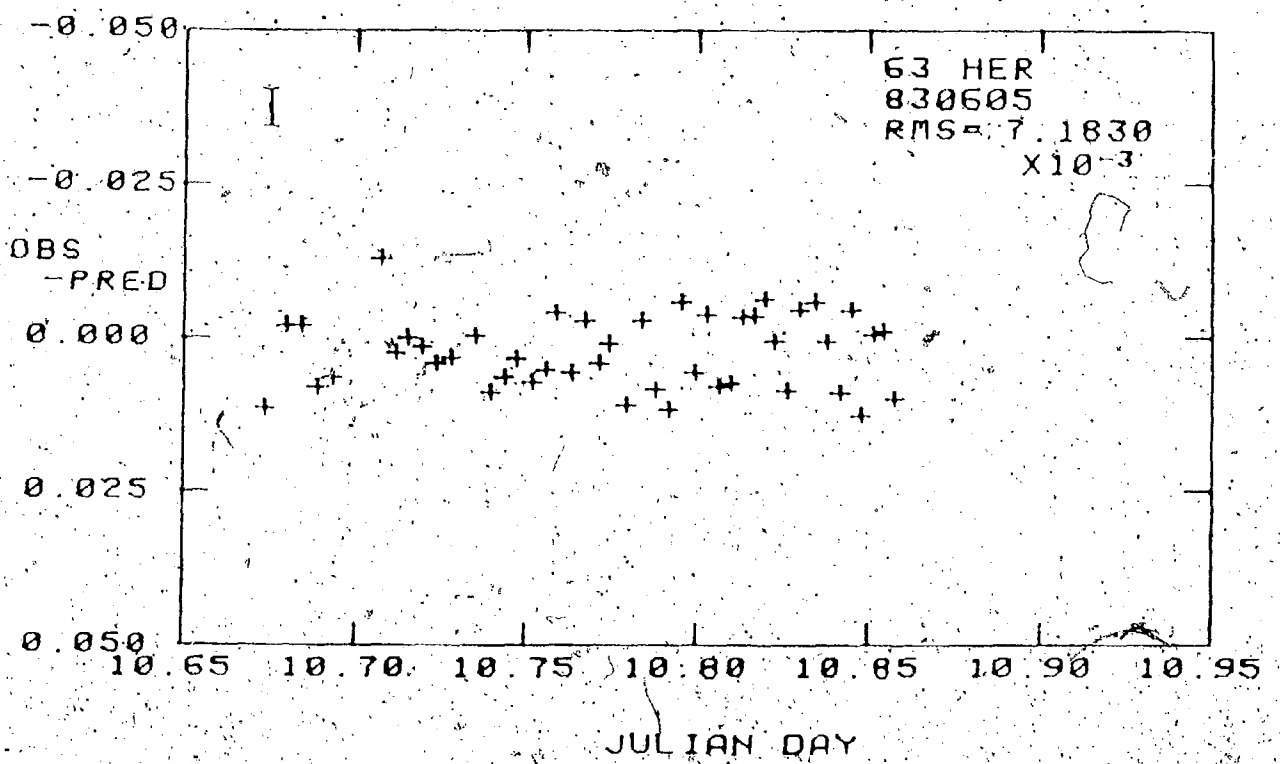
63 HER
830605
RMS= 7.1830
X10-3
-0.050
-0.025
OBS
-PRED
0.000
0.025
0.050
10.65
10.70
10.75
10.80
10.85
10.90
10.95
JULIAN DAY

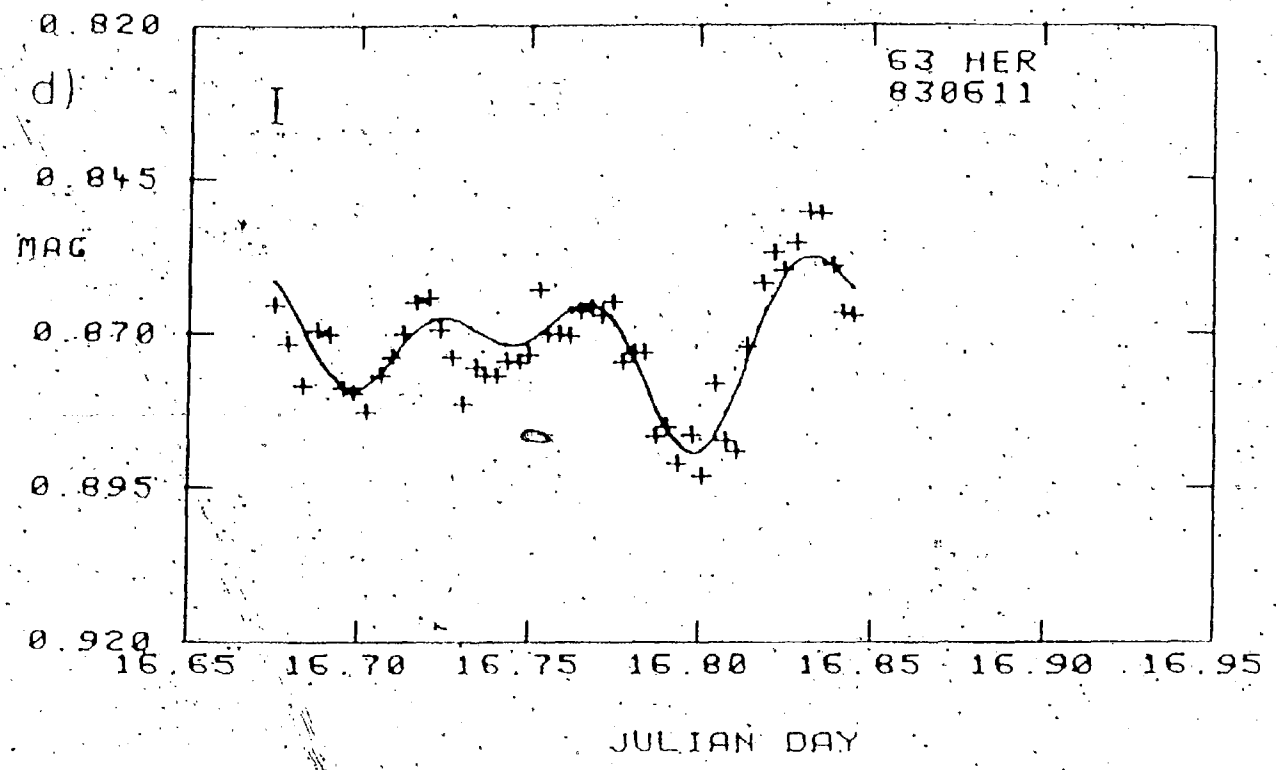
d)
63 HER
830611
0.820
0.845
0.870
0.895
0.920
MAG
16.65
16.70
16.75
16.80
16.85
16.90
16.95
JULIAN DAY

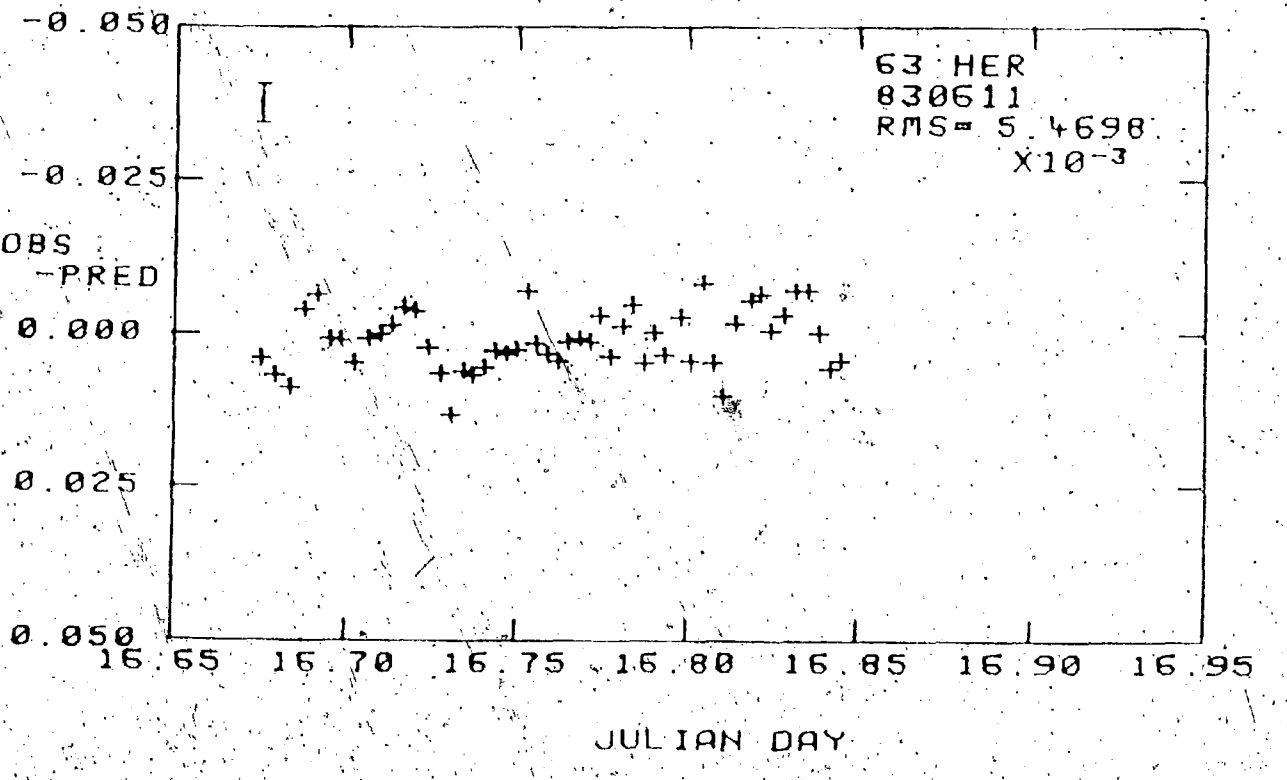
63 HER
830611
RMS= 5.4698
X10-3
-0.050
-0.025
0.000
0.025
0.050
OBS
-PRED
16.65
16.70
16.75
16.80
16.85
16.90
16.95
JULIAN DAY

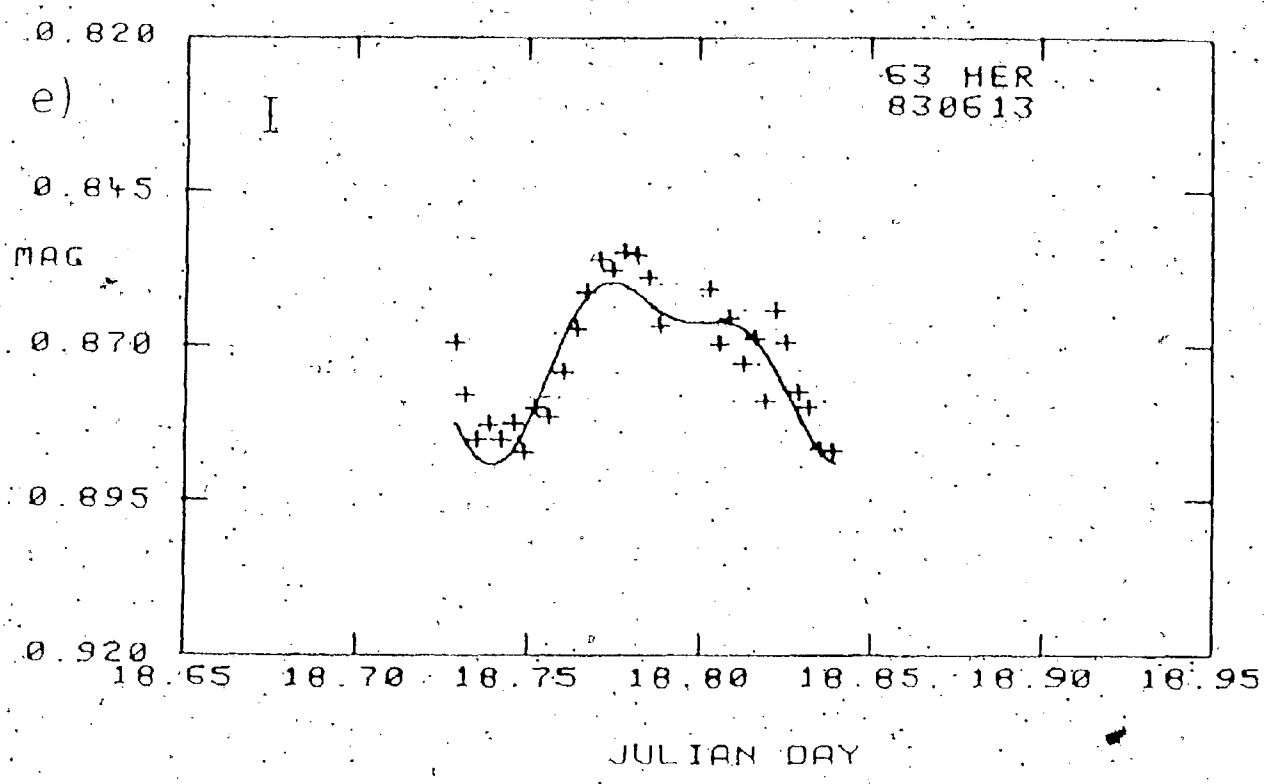
e)
63 HER
830613
0.820
0.845
0.870
0.895
0.920
MAG
18.65
18.70
18.75
18.80
18.85
18.90
18.95
JULIAN DAY

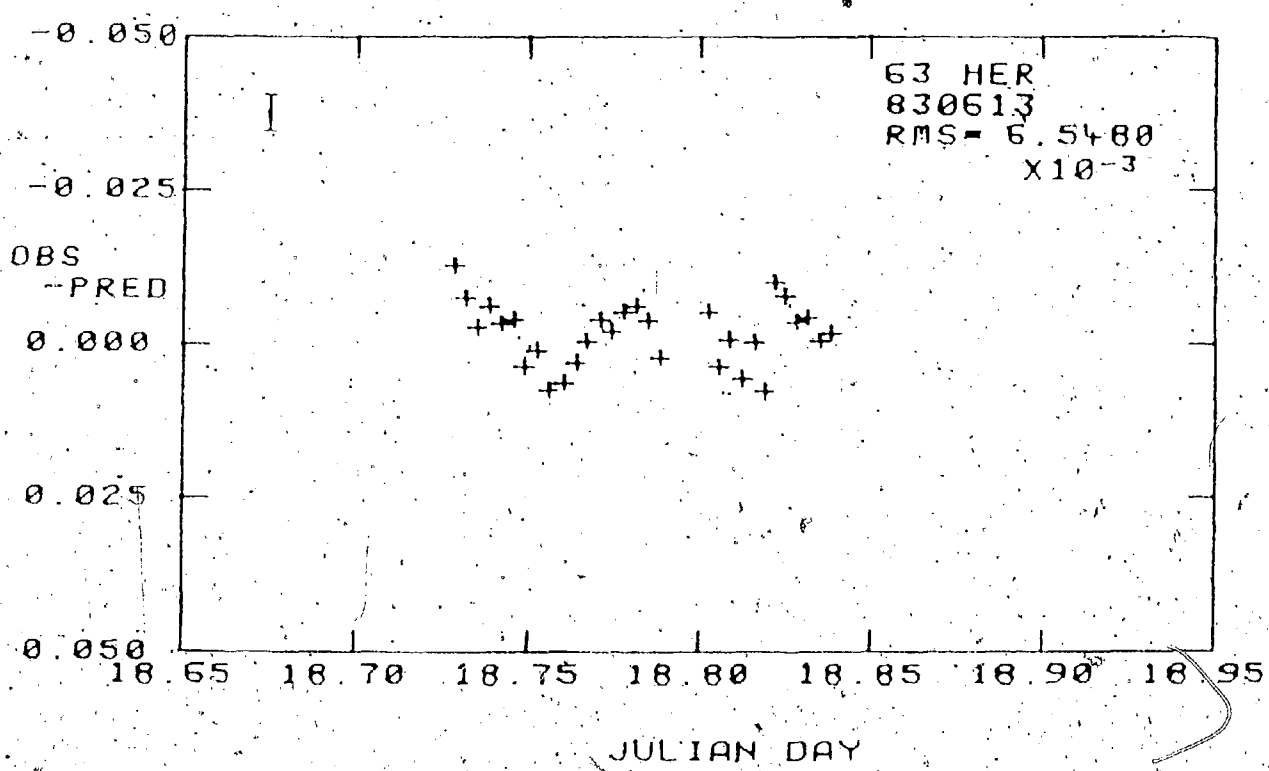
63 HER
830613
RMS= 6.5480
X10-3
-0.050
-0.025
0.000
0.025
0.050
OBS
-PRED
18.65
18.70
18.75
18.80
18.85
18.90
18.95
JULIAN DAY

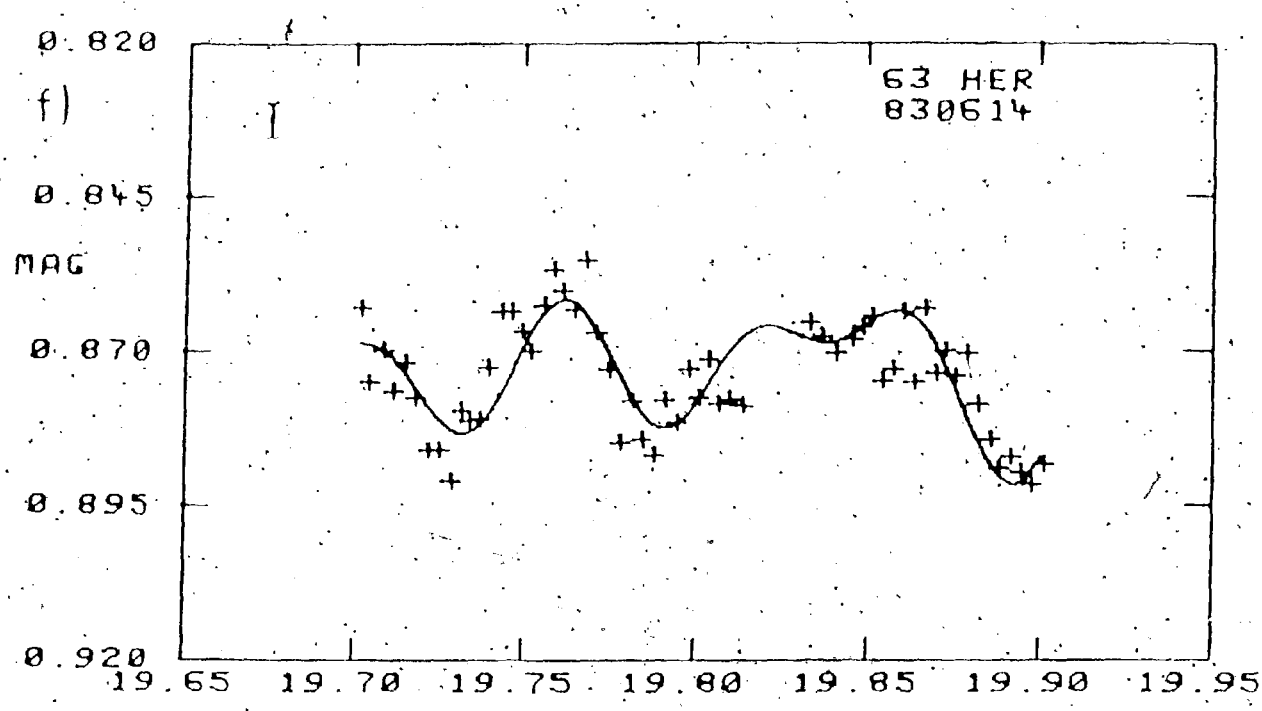
f)
63 HER
830614
0.820
0.845
MAG
0.870
0.895
0.920
19.65
19.70
19.75
19.80
19.85
19.90
19.95
JULIAN DAY

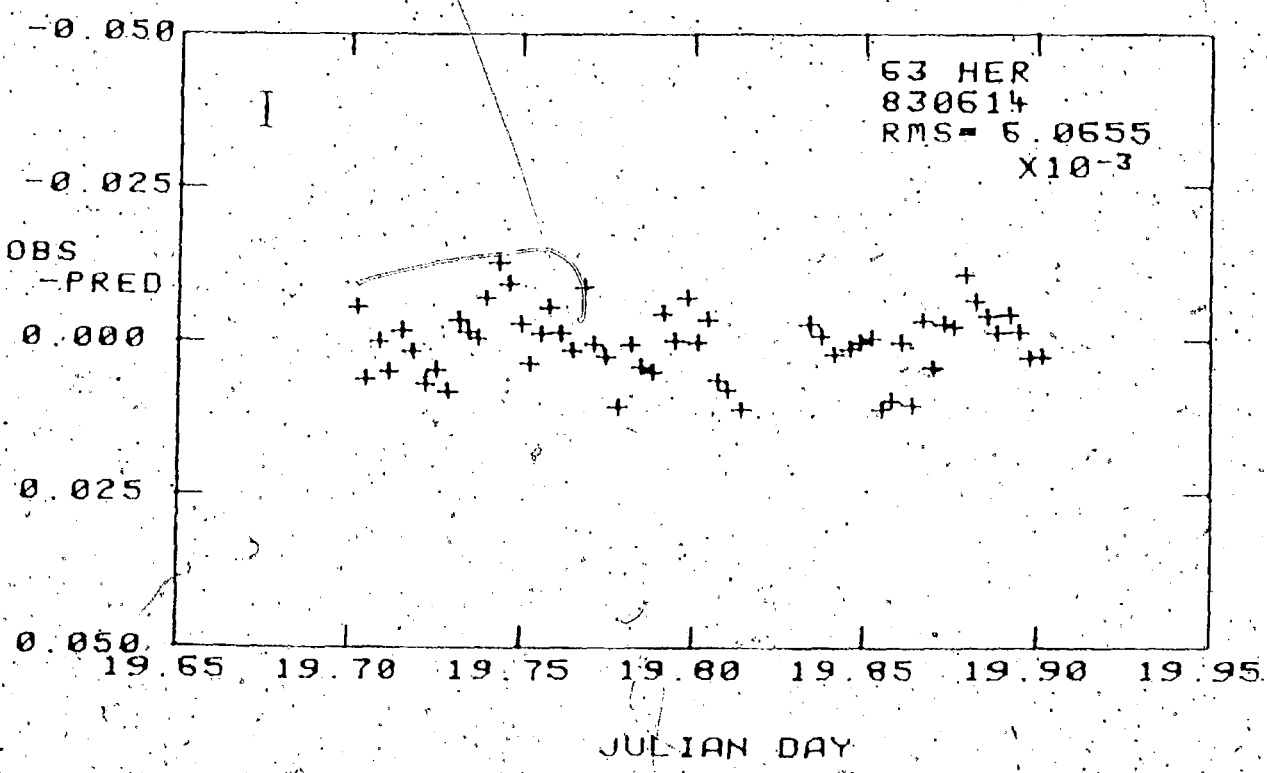
63 HER
830614
RMS= 6.0655
X10-3
-0.050
-0.025
OBS
-PRED
0.000
0.025
0.050
19.65
19.70
19.75
19.80
19.85
19.90
19.95
JULIAN DAY

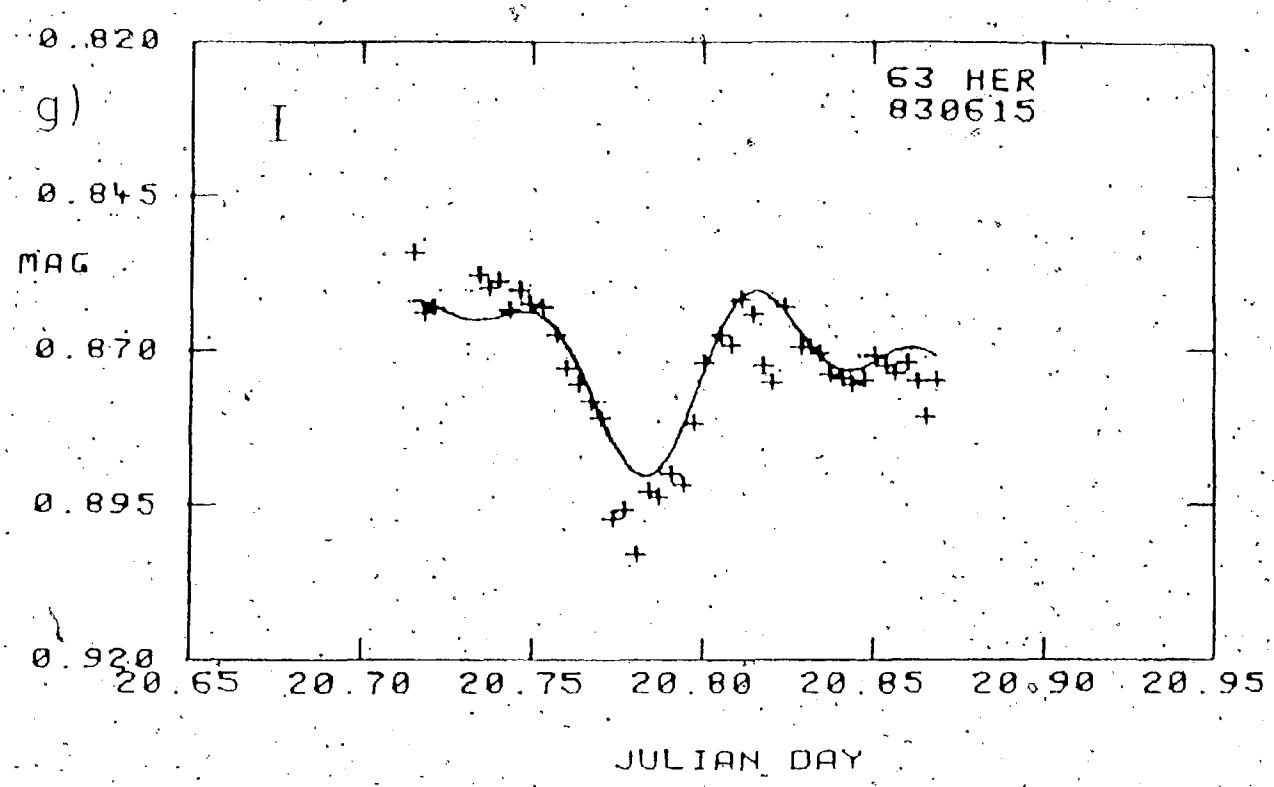
g)
I
63 HER
830615
0.820
0.845
MAG
0.870
0.895
0.920
20.65
20.70
20.75
20.80
20.85
20.90
20.95
JULIAN DAY

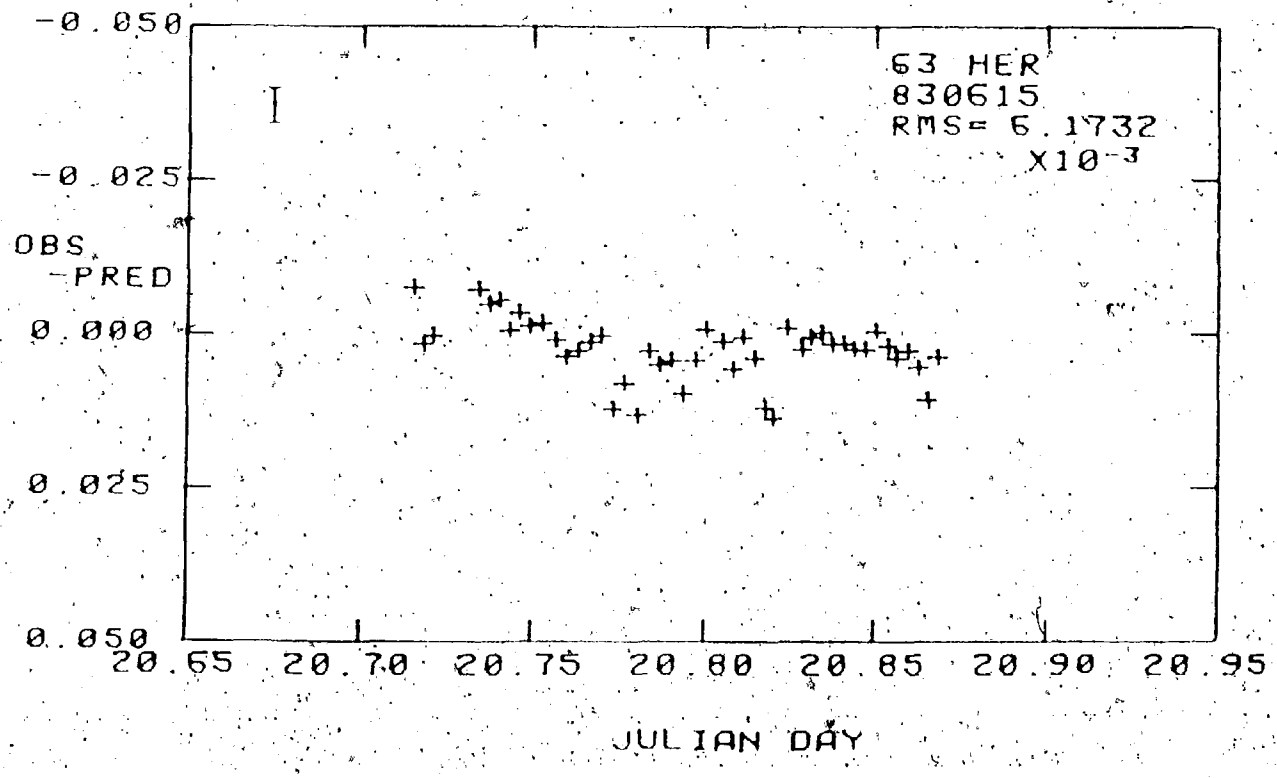
I
63 HER
830615
RMS= 6.1732
X10-3
-0.050
-0.025
OBS
-PRED
0.000
0.025
0.050
20.65
20.70
20.75
20.80
20.85
20.90
20.95
JULIAN DAY

way: the time interval between the first and last observations was divided into 1000 increments, and for each of these 1000 points, new magnitude values were calculated using the equation:

$$y_{line}(I) = A_A \sin(2 F_A x(I) + \phi_A) + A_B \sin(2 F_B x(I) + \phi_B) + A_C \sin(2 F_C x(I) + \phi_C) + \bar{m},$$

where $I = 1,2,\ldots,1000$, $x(I)$ is the Julian date corresponding to the Ith increment, and the parameters correspond to those in Table IV.1.1.

The (observed - predicted) residuals, including an RMS residual for each night, are shown in the bottom diagrams of Figure IV.1.6. As is apparent from all 14 diagrams, the three-sine fit as shown above is a fairly accurate one. RMS residuals ranged from 5.47×10^{-3} to 8.66×10^{-3} magnitudes over the seven nights, being consistent with the residuals stated above for the three individual periodicities (cf. Table IV.1.1.).

Previous work on 63 Her (Breger 1969) had revealed only one frequency (period) of 12.98 cy/d (0.077 d). Because of the larger data set and improved period search technique used here, however, the two and perhaps three converged frequencies derived in this work must be considered the more reliable fit to this star's pulsation. These new results for 63 Her will be discussed in detail in Chapter V.

2. V1208 Aquilae

Data for V1208 Aql consist of 140 observations taken during three nights spread over seven days. Figure IV.2.1. shows the initial Jurkevich-Swingler frequency diagram. Here, as in the case of 63 Her, the magnitude index has been plotted only for the short frequency interval from 0 to 15 cy/d since no peaks of index greater than the limiting index of 4.30 were seen beyond F = 15 cy/d.

Only one system of peaks is immediately apparent in Figure IV.2.1. The primary frequency seems to be F_A = 6.90 cy/d, and four one-day aliases are seen on each side of this central peak.

P3R was used to determine F_A and its parameters accurately, using F_A = 6.9 cy/d and A_m = 0.02 from Figures IV.2.1. and III.2.3., and ϕ_A = m_A = 0.0 as discussed above for starting values. The program converged on the parameters shown in the first row of Table IV.2.1.

As in the case of 63 Her, several other series of runs of P3R were made both with the initial phase varied between 0 and 2π; and also with the initial frequency slightly changed. The results showed, however, that either the routine converged on values essentially the same as above or on totally different values that were considered spurious because of their high RMS residuals and/or an unacceptable value for the frequency (as judged from Figure IV.2.1.). Figure IV.2.2. shows the periodogram

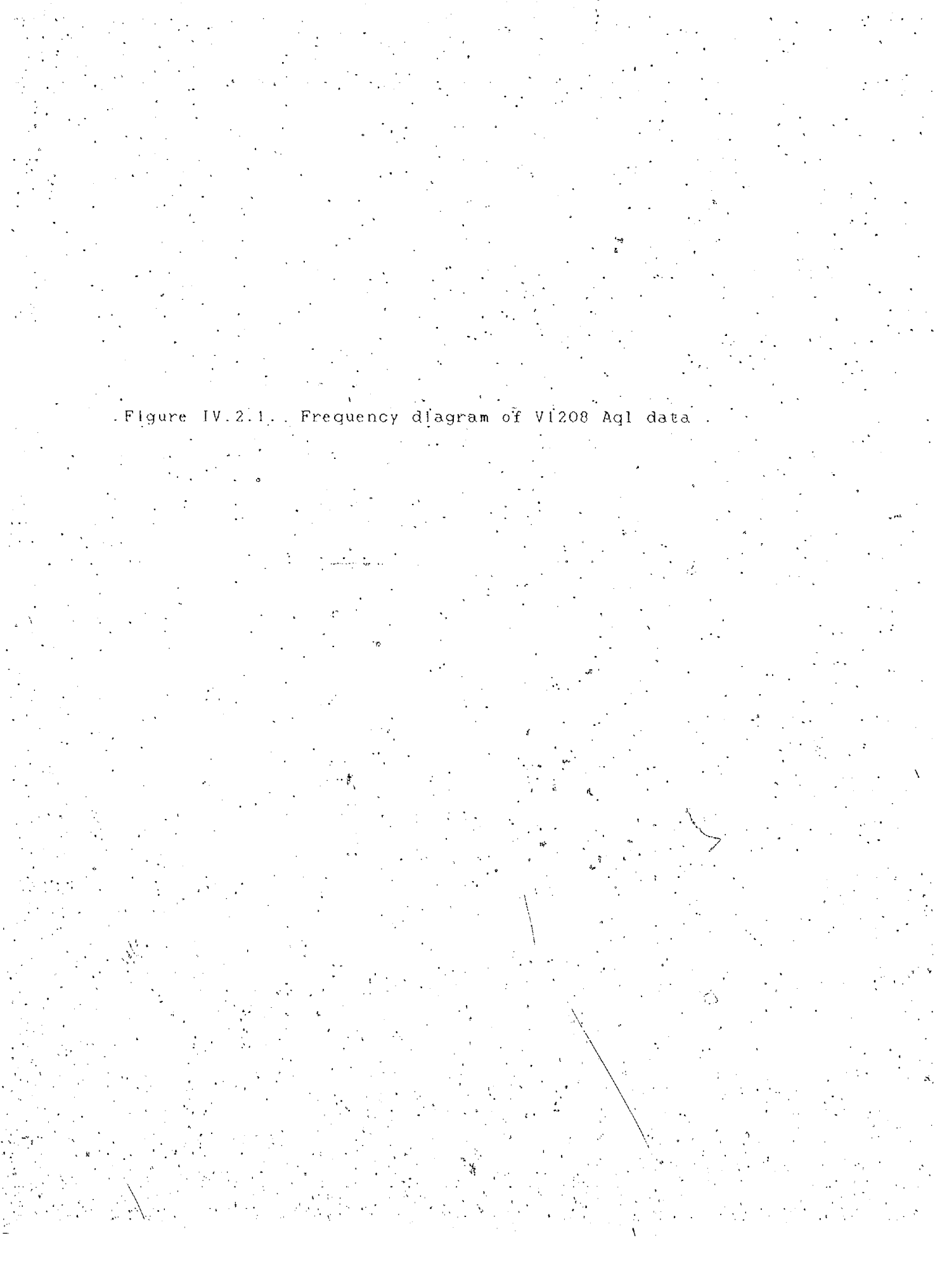

Figure IV.2.1. Frequency diagram of V1208 Aql data

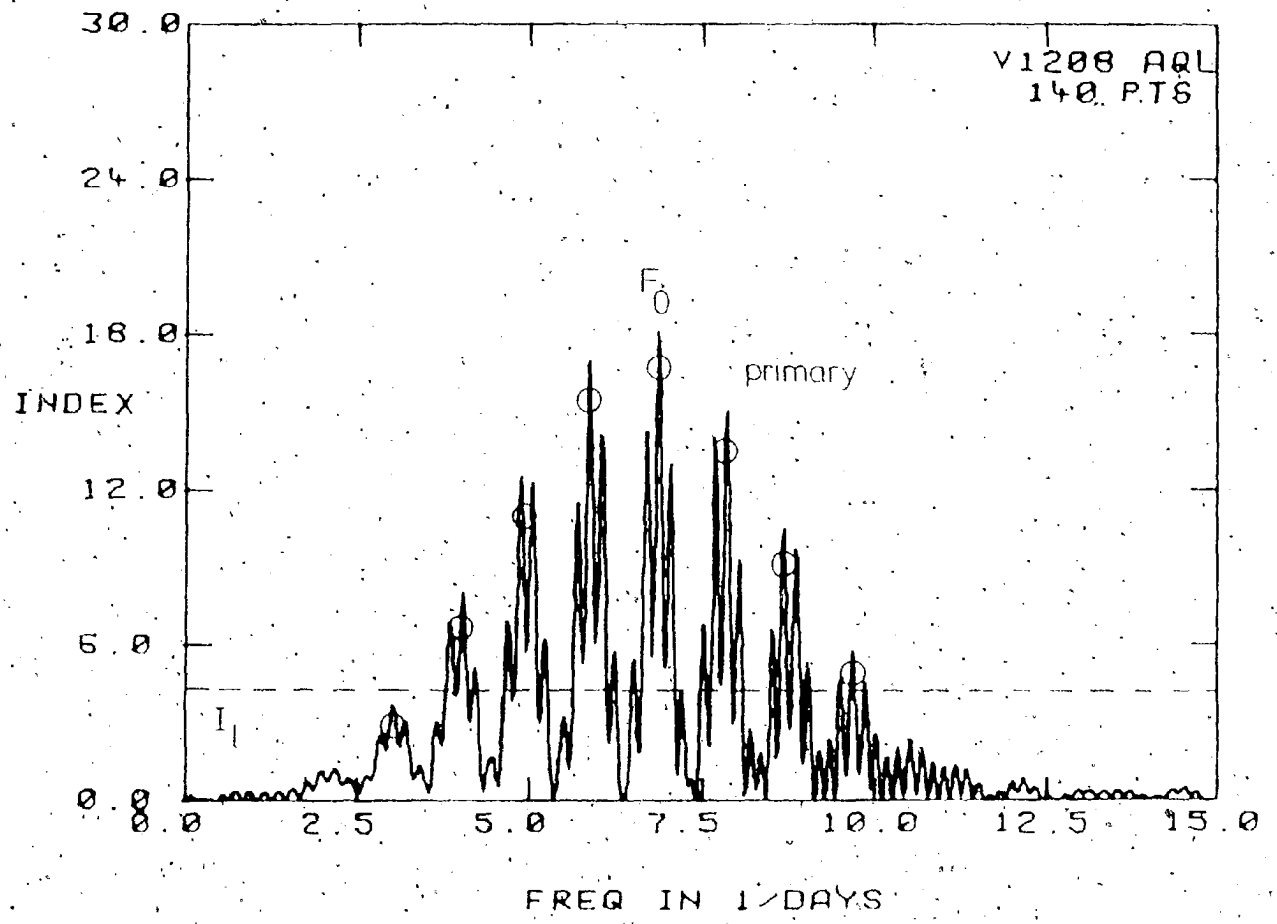
V1208 AQL
140 PTS
30.0
24.0
18.0
12.0
6.0
0.0
INDEX
F_0
primary
I_1
0.0
2.5
5.0
7.5
10.0
12.5
15.0
FREQ IN 1/DAYS

Table IV.2.1.: P3R results for V1208 Aql

Run	Converged Parameters A (mag)	F (cy/d) / P (d)	ϕ (rad)	$\bar{m}$ (mag)	N	RMS x 10 (mag)
A	0.0134 ±0.0008	6.8669 ±0.0037 / 0.1456 ±0.0001	4.9810 ±0.1632	0.5107 ±0.0006	12	6.965
B	0.0039 ±0.0007	9.4093 ±0.0115 / 0.1063 ±0.0001	1.6166 ±0.4757	0.0005 ±0.0005	10	6.033
C	0.0032 ±0.0007	5.1515 ±0.0127 / 0.1941 ±0.0001	0.9955 ±0.5494	0.0002 ±0.0005	8	5.603

Figure IV.2.2. Frequency diagram of V1208 Aql data prewhitened by:

$$y(I) = {}^{m}_{0}.0134 \sin(2\pi\, 6.8669\ cy/d, x(I) + 4.981) + {}^{m}_{0}.5107$$

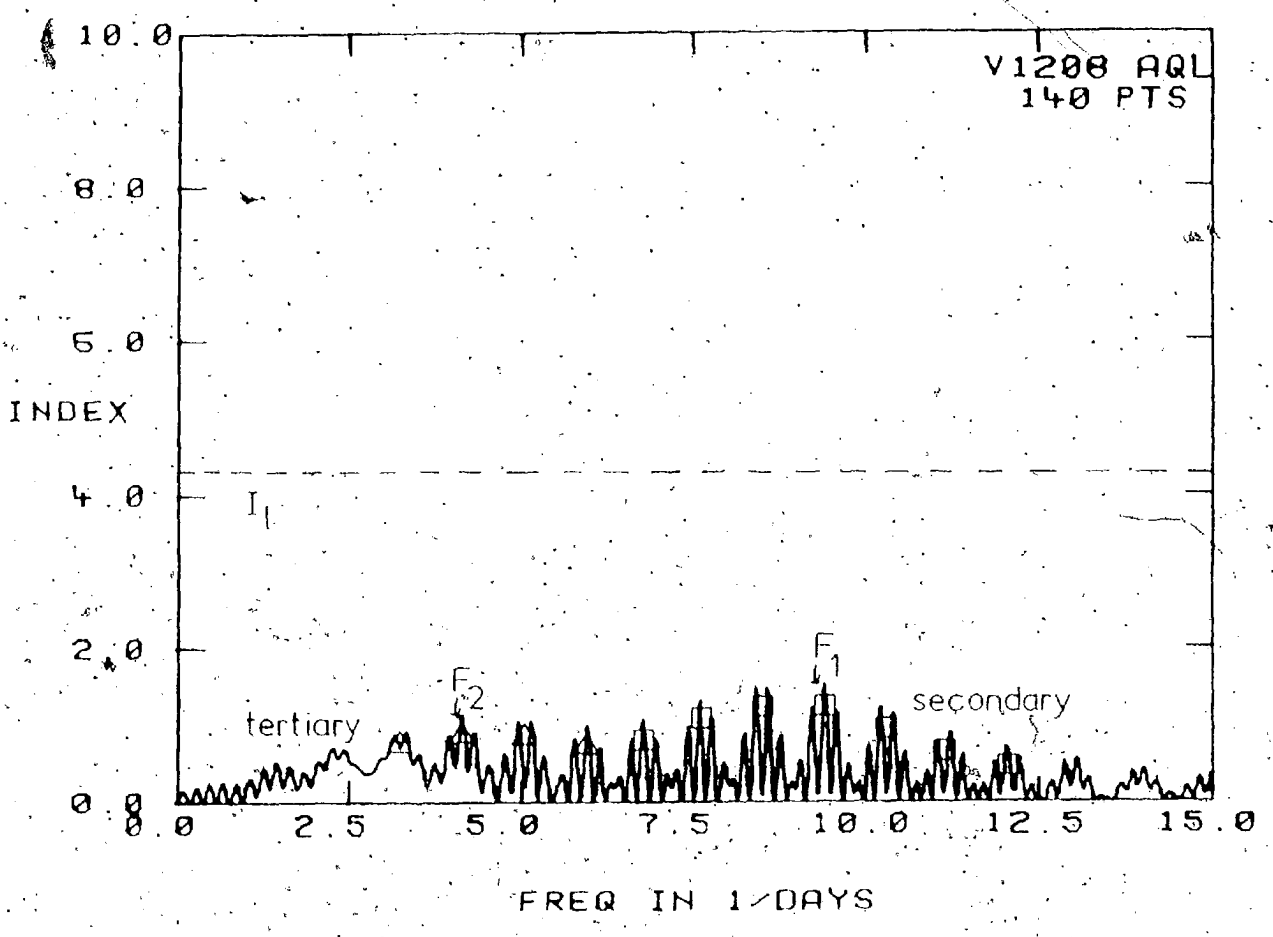
V1208 AQL
140 PTS
10.0
8.0
6.0
INDEX
4.0
I_1
2.0
0.0
F_1
F_2
tertiary
secondary
0.0
2.5
5.0
7.5
10.0
12.5
15.0
FREQ IN 1/DAYS

resulting from the prewhitening of the V1208 Aql data by the parameters for the dominant variability. Note that the index interval on the y-axis has been expanded by a factor of three since the remaining peaks have much smaller, insignificant amplitudes.

The most prominent peak seen in Figure IV.2.2. is the one at F_B = 9.40 cy/d, which appears to have three aliases on each side. A second, less prominent envelope of five peaks can be seen centred on the peak at F_C = 4.15 cy/d. However, the peaks at F_B and F_C do not exceed the limiting index, and hence, must be considered less significant.

The top diagrams in Figure IV.2.3. a) to c) show the resulting one-sine fit superimposed on the data for V1208 Aql, where the line has been generated using the parameters for F_A in Table IV.2.1. as discussed earlier. The (observed - predicted) residuals shown below each fit yielded RMS values ranging from 6.08×10^{-3} to 7.72×10^{-3} magnitudes.

Although F_B and F_C are considered less significant, the reduction procedure was completed for them (cf. Table IV.2.1.). All three frequencies were then included in a three-sine fit to compare with the fit shown in Figure IV.2.3. This three-sine fit is shown in Figure IV.2.4., and yields RMS residuals ranging from 4.99×10^{-3} to 6.58×10^{-3} magnitudes. Based on the RMS residuals, this three-sine fit does appear to be better than the one-sine fit, but we cannot be positive that F_B and F_C really exist,

Figure IV.2.3: a) - c) top: Differential photometry of V1208 Aql with one-sine fit superimposed (see text and Table IV.2.1.). Compare with Figure IV.2.4.
bottom: Residuals of above one-sine fit.

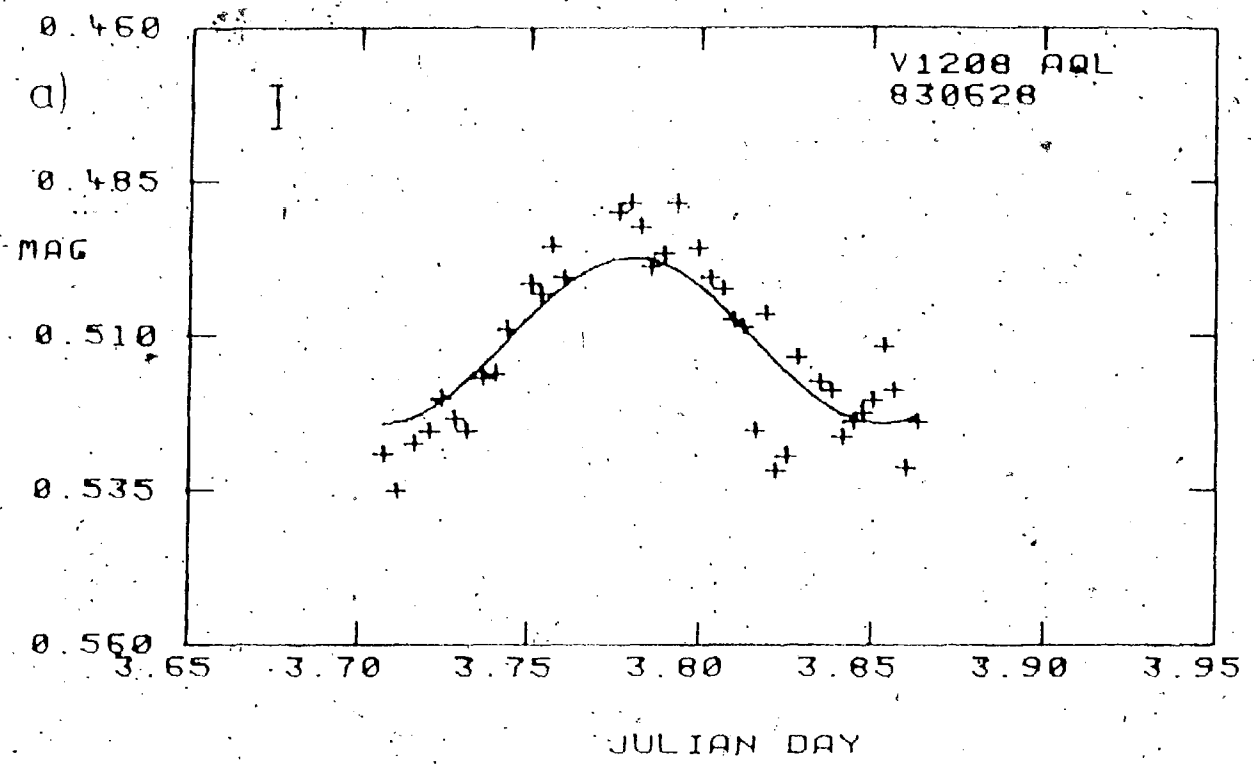
a)
V1208 AQL
830628
0.460
0.485
0.510
0.535
0.560
MAG
3.65
3.70
3.75
3.80
3.85
3.90
3.95
JULIAN DAY

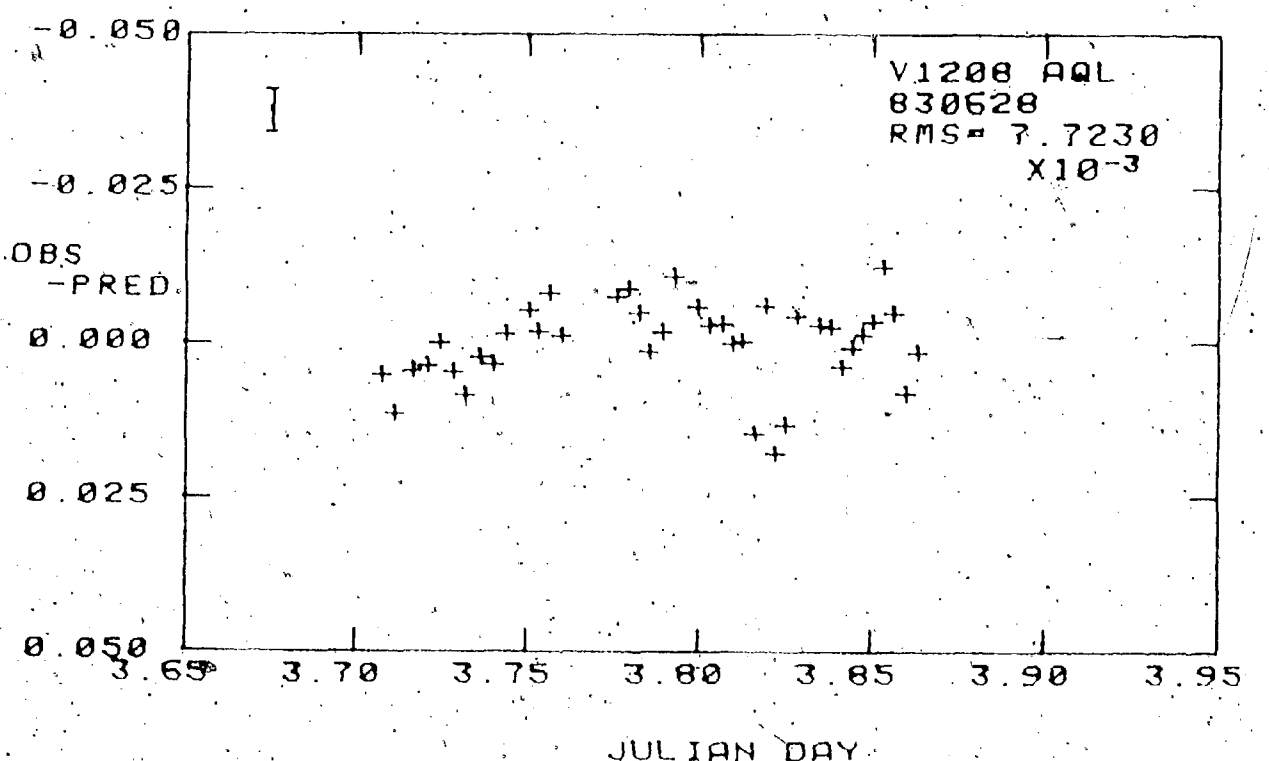
V1208 AQL
830628
RMS= 7.7230
X10-3
-0.050
-0.025
0.000
0.025
0.050
OBS
-PRED
3.65
3.70
3.75
3.80
3.85
3.90
3.95
JULIAN DAY

b)

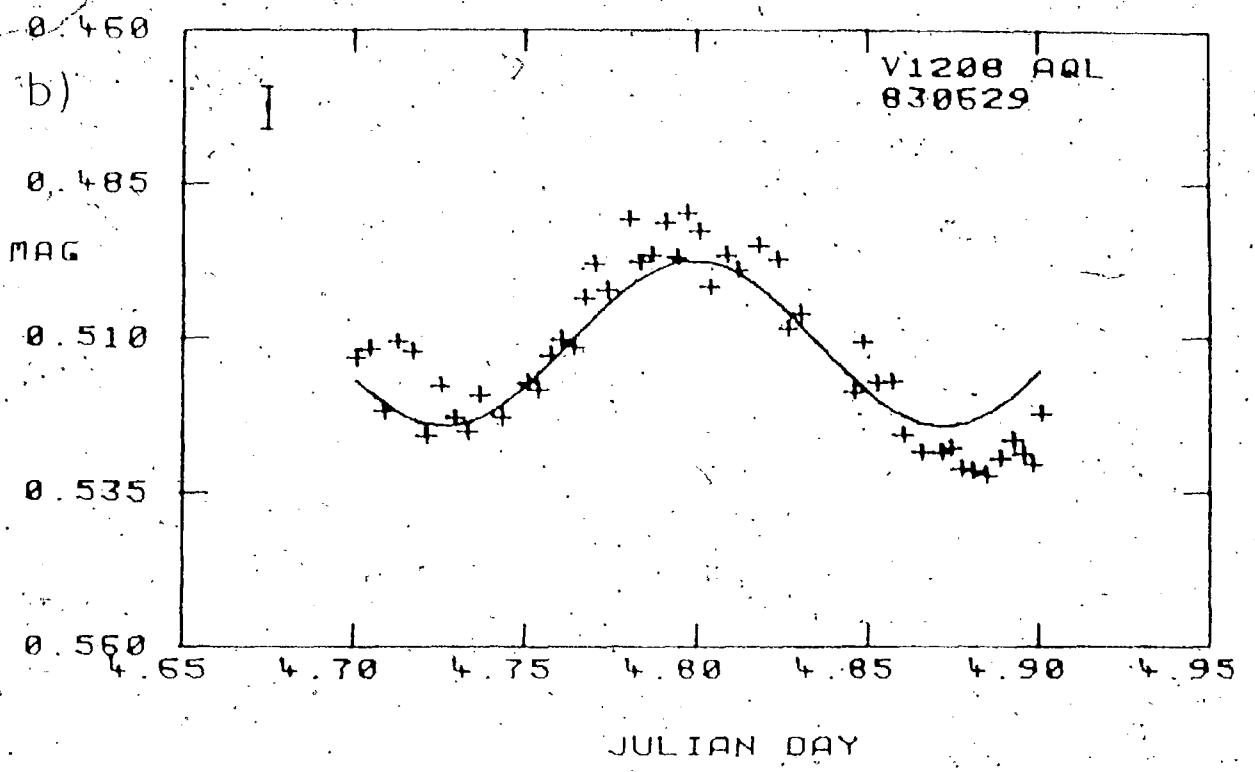
V1208 AQL
830629
0.460
0.485
MAG
0.510
0.535
0.560
4.65
4.70
4.75
4.80
4.85
4.90
4.95
JULIAN DAY

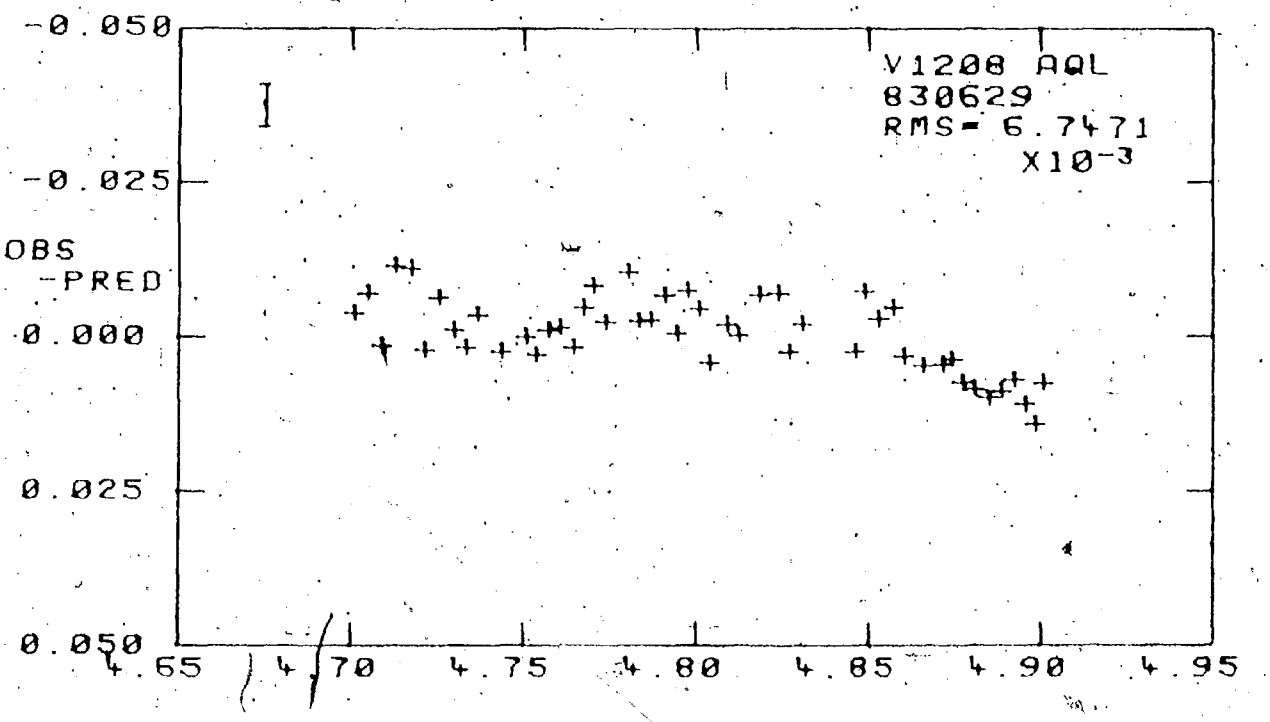
V1208 AQL
830629
RMS= 6.7471
X10-3
-0.050
-0.025
OBS
-PRED
0.000
0.025
0.050
4.65
4.70
4.75
4.80
4.85
4.90
4.95
JULIAN DAY

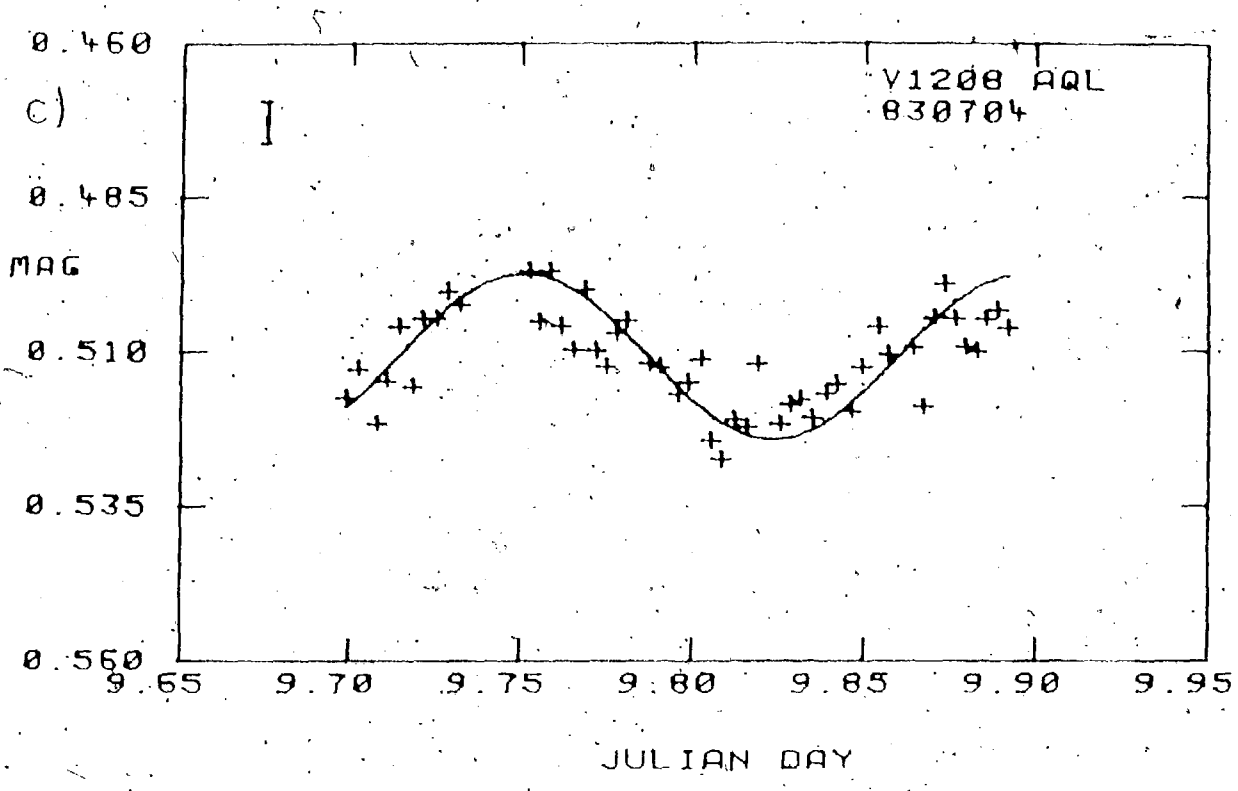
c)
V1208 AQL
830704
0.460
0.485
MAG
0.510
0.535
0.560
9.65
9.70
9.75
9.80
9.85
9.90
9.95
JULIAN DAY

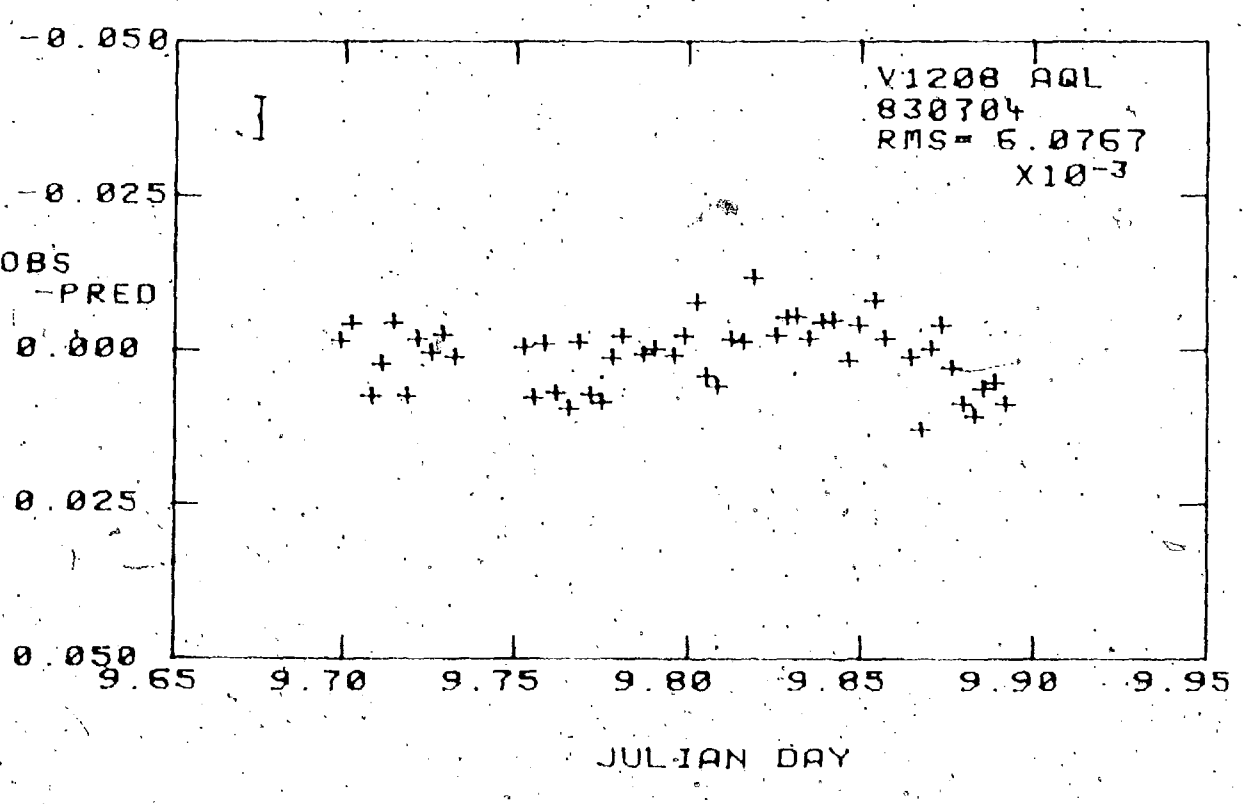
V1208 AQL
830704
RMS= 6.0767
X10-3
-0.050
-0.025
OBS
-PRED
0.000
0.025
0.050
9.65
9.70
9.75
9.80
9.85
9.90
9.95
JULIAN DAY

Figure IV.2.4. a) - c) top: Differential photometry of V1208 Aql with three-sine fit superimposed (see Table IV.2.1.). Compare with Figure IV.2.3.
bottom: Residuals of above three-sine fit.

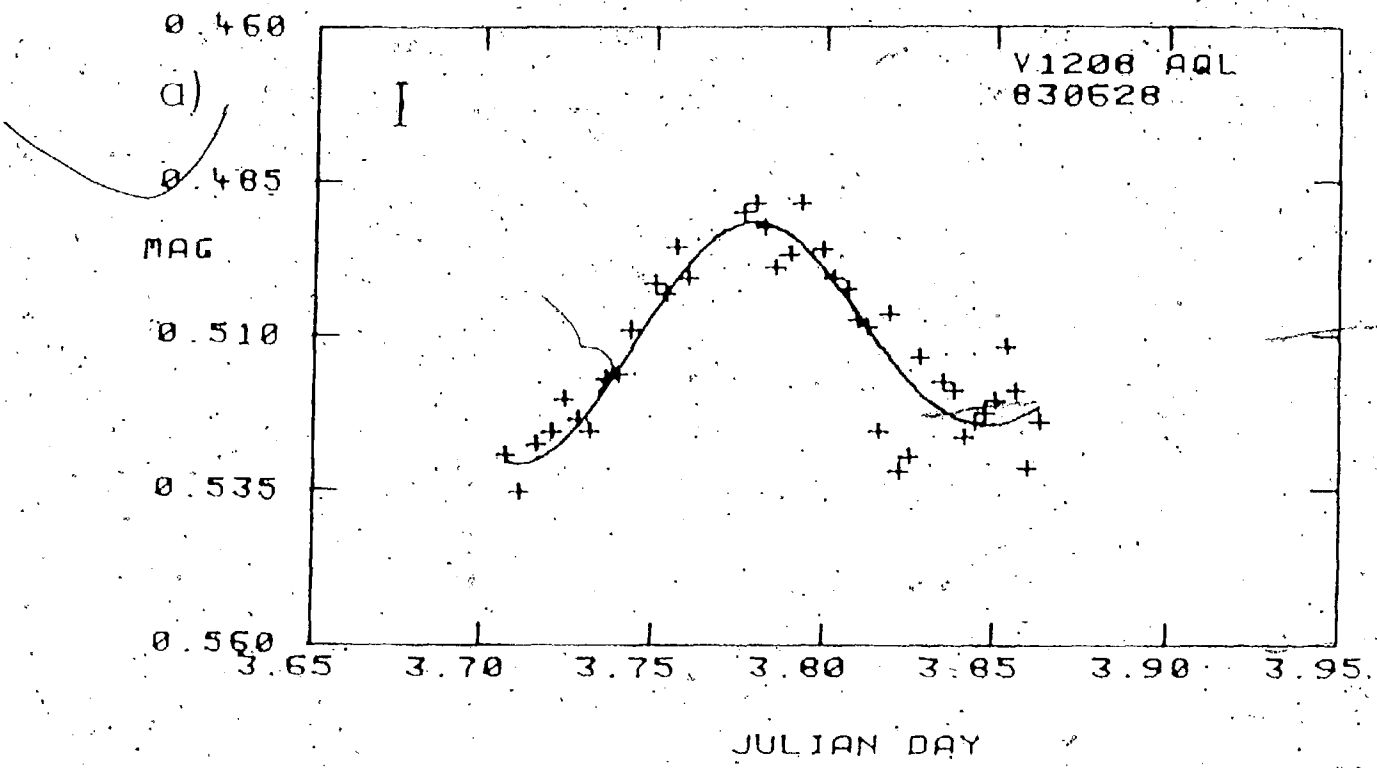
a)
V1208 AQL
830628
0.460
0.485
MAG
0.510
0.535
0.560
3.65
3.70
3.75
3.80
3.85
3.90
3.95
JULIAN DAY

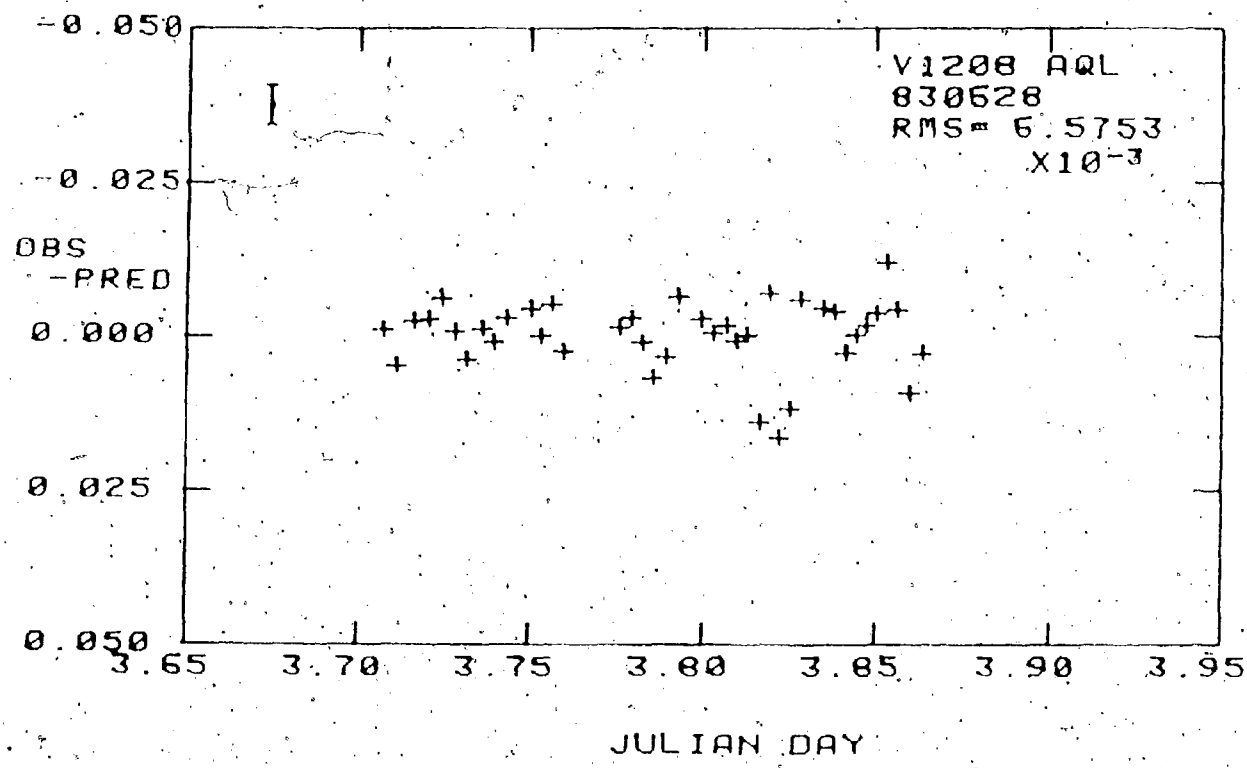
-0.050
V1208 AQL
830628
RMS= 6.5753
X10-3
-0.025
OBS
-PRED
0.000
0.025
0.050
3.65
3.70
3.75
3.80
3.85
3.90
3.95
JULIAN DAY

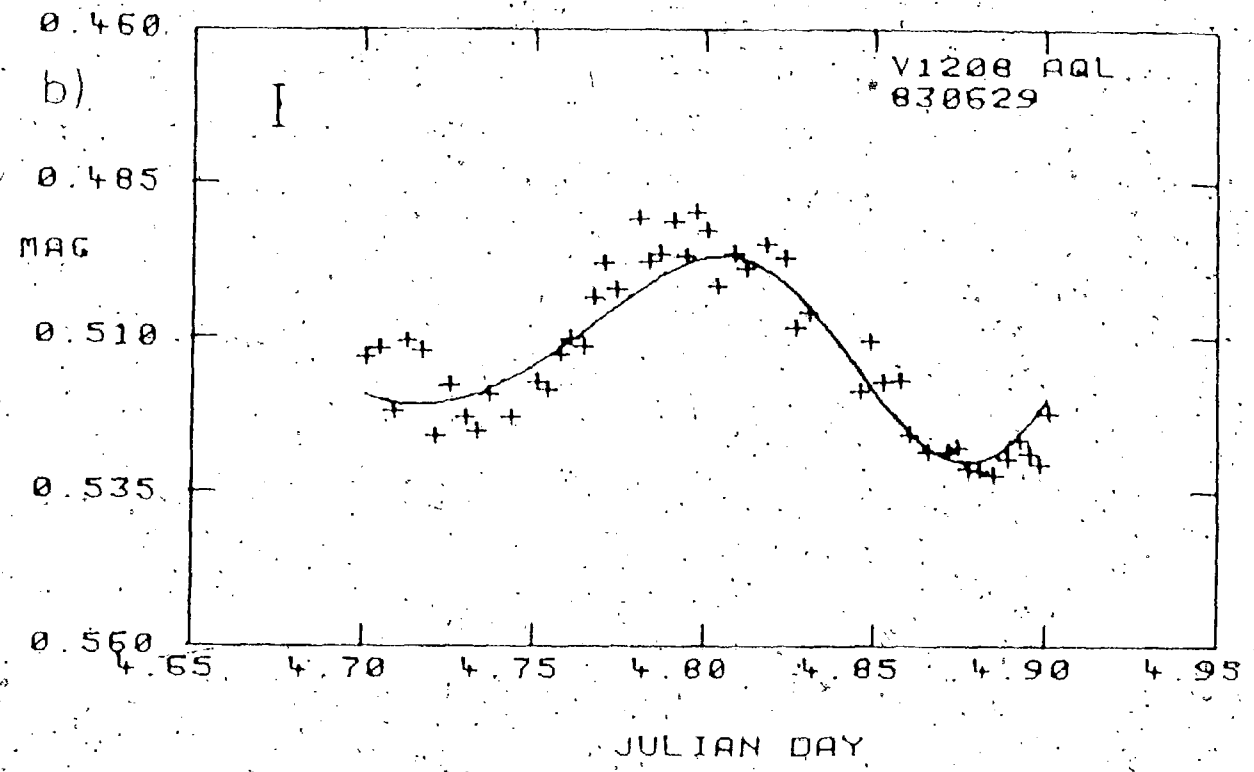
b)
V1208 AQL
830629
0.460
0.485
0.510
0.535
0.560
MAG
4.65
4.70
4.75
4.80
4.85
4.90
4.95
JULIAN DAY

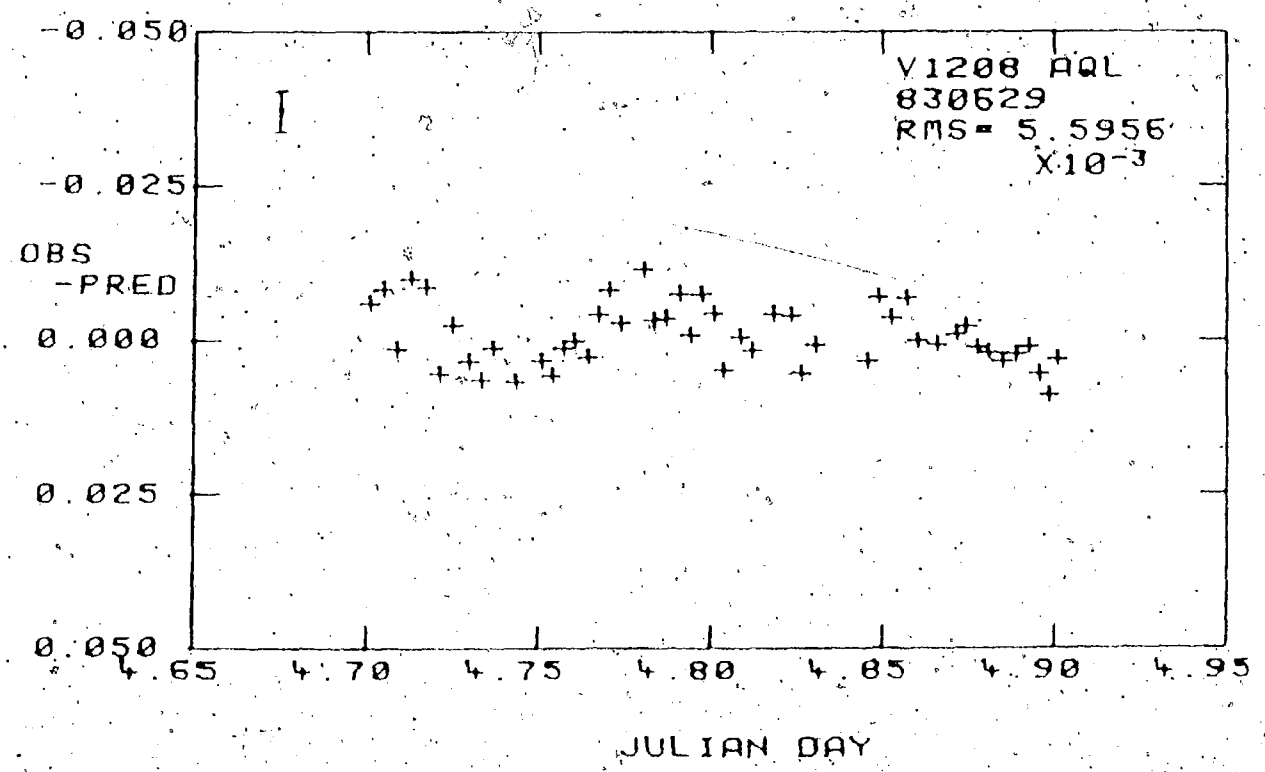
V1208 AQL
830629
RMS= 5.5956
X10-3
-0.050
-0.025
0.000
0.025
0.050
OBS
-PRED
4.65
4.70
4.75
4.80
4.85
4.90
4.95
JULIAN DAY

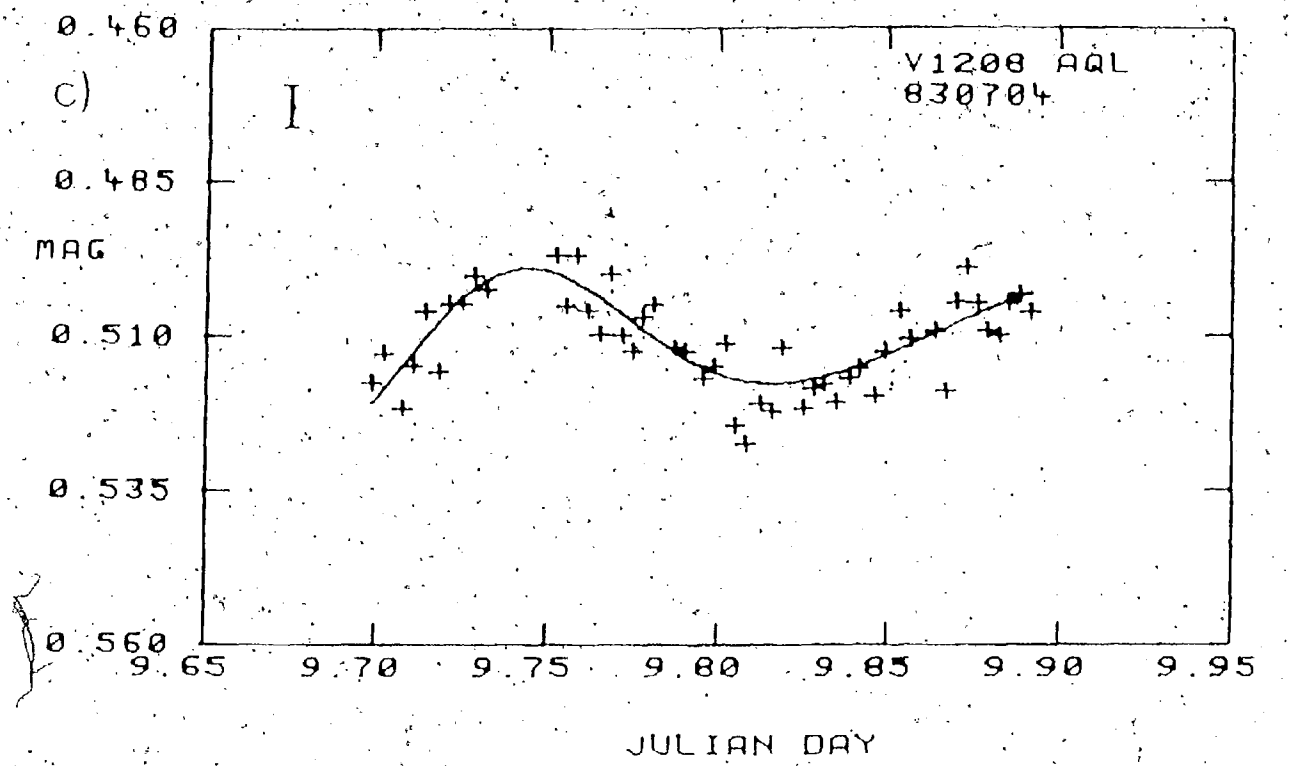
C)
V1208 AQL
830704
0.460
0.485
MAG
0.510
0.535
0.560
9.65
9.70
9.75
9.80
9.85
9.90
9.95
JULIAN DAY

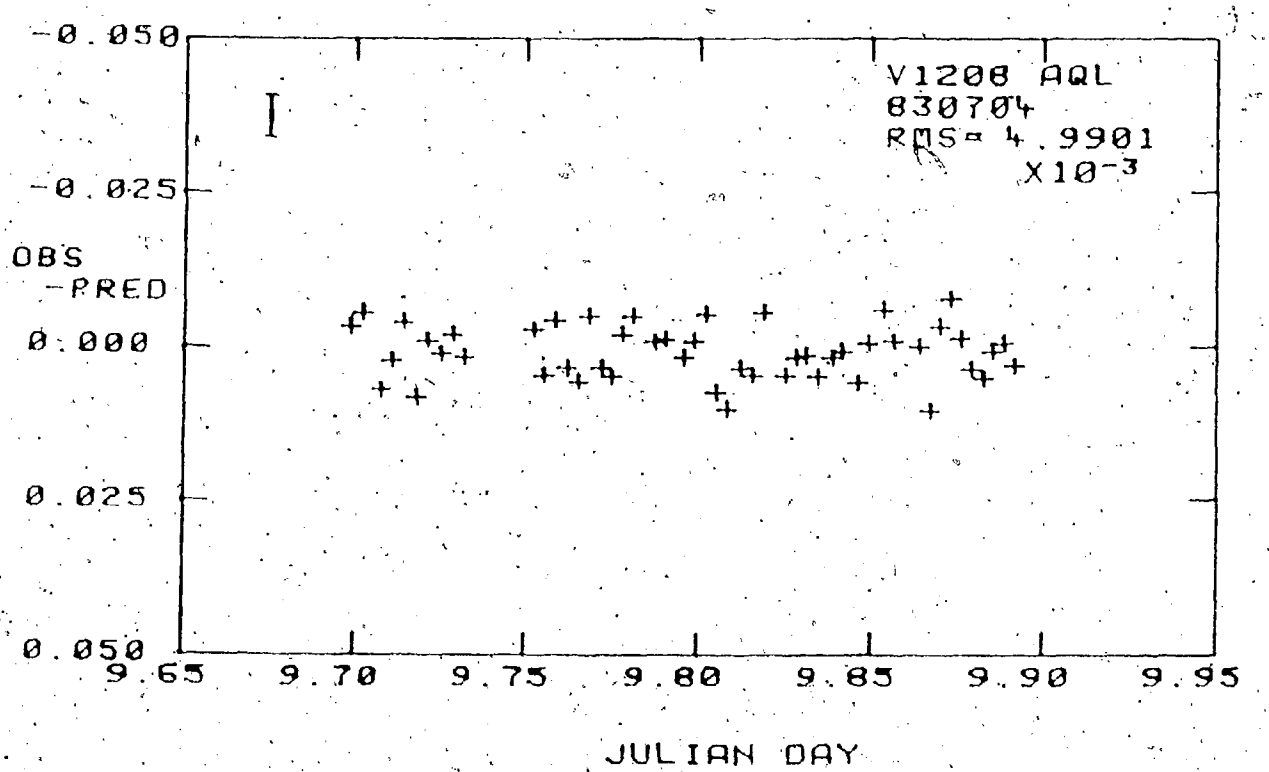
V1208 AQL
830704
RMS= 4.9901
X10-3
-0.050
-0.025
OBS
-PRED
0.000
0.025
0.050
9.65
9.70
9.75
9.80
9.85
9.90
9.95
JULIAN DAY

since their envelopes were so much less than the limiting index for this star. Therefore, one must conclude from this analysis that V1208 Aql is pulsating with only one frequency that we can be confident of, that is, F_A = 6.87 cy/d.

Recent work on V1208 Aql (Pena and Warman 1979) revealed that it was pulsating with two frequencies (periods) of 7.112 cy/d and 6.678 cy/d (0.141 and 0.15 d_d). The converged results derived here are very comparable to the previous work, with F_A being exactly midway. Please see Chapter V for a complete discussion of the periods of V1208 Aql.

3. LT Vulpeculae

Data for LT Vul consist of 66 observations obtained during two nights separated by three days. The initial Jurkevich-Swingler frequency diagram is shown in Figure IV.3.1., where the index has been plotted only for the frequency interval from 0 to 36 cy/d since no peaks of index greater than the limiting index of I_1 = 2.04 were found beyond F = 36 cy/d. This periodogram is both unusual and complex in appearance. The primary envelope, centred at about F_A = 9.74 cy/d, extends from F = 0.0 cy/d to F_A = 16.0 cy/d and is composed of 44 peaks. However, since only two nights of data separated by three days were obtained, the aliases seen here are three-day aliases. That is, the frequency interval between any two adjacent

Figure IV.3.1. Frequency diagram of LT Vul data

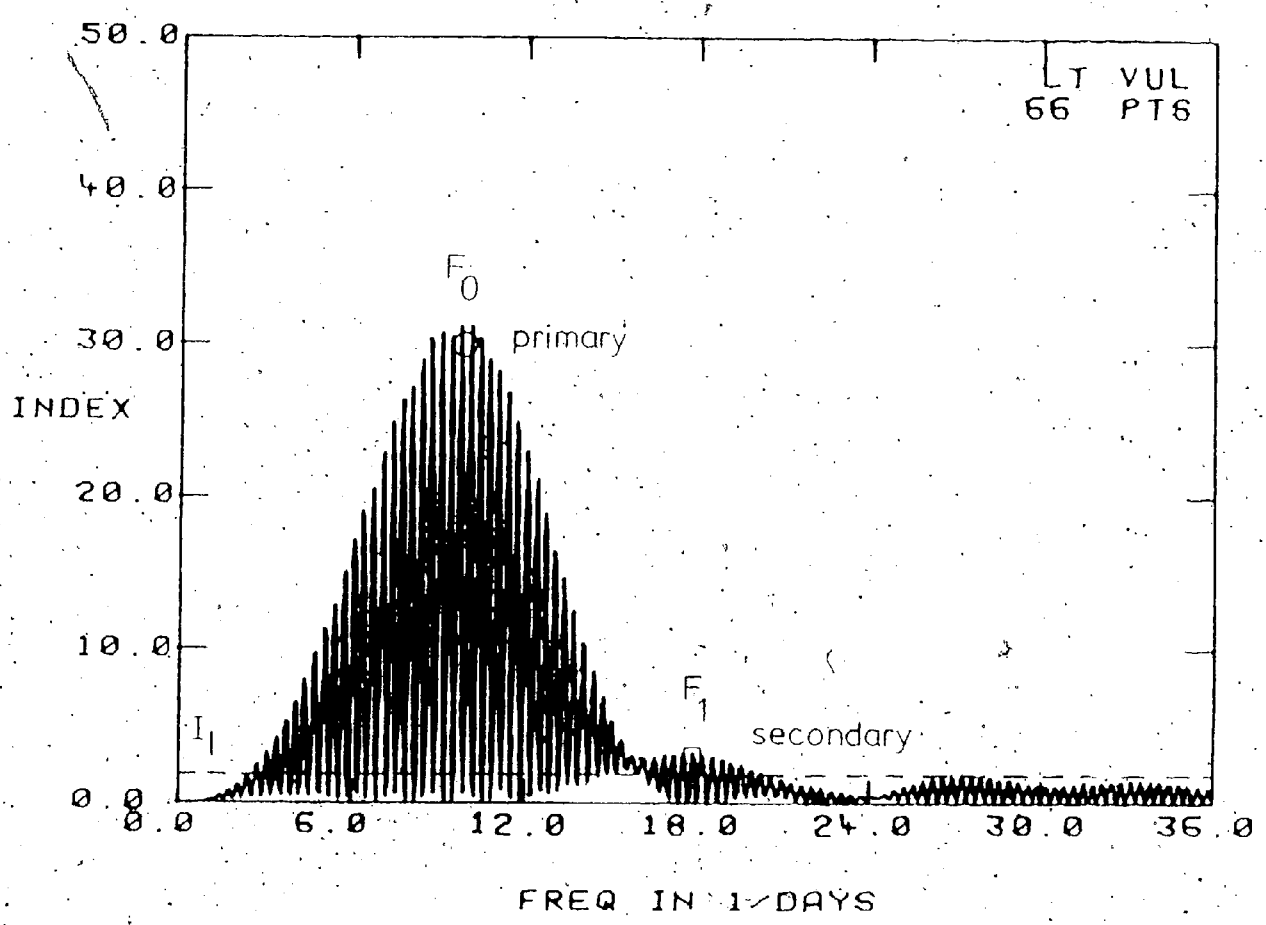
50.0
40.0
30.0
20.0
10.0
0.0
INDEX
LT VUL
66 PTS
F0
primary
F1
secondary
I1
0.0
6.0
12.0
18.0
24.0
30.0
36.0
FREQ IN 1/DAYS

peaks is 0.333 cy/d, or in terms of period, three days. A smaller, much less obtrusive secondary envelope is centred at about F_B = 17.82 cy/d.

For a dramatic illustration of the improvement brought about by the Jurkevich-Swingler method, compare Figure IV.3.1. with Figure IV.3.2., where index has been calculated using the original Jurkevich method.

Runs of P3R and successive prewhitenings, conducted as in the previous two cases reveal that LT Vul is apparently pulsating with perhaps four frequencies. Table IV.3.1. lists the converged parameters and their errors and Figures IV.3.3, IV.3.4., and IV.3.5. show periodograms of data prewhitened by F_A; F_A and F_B, and all four frequencies, respectively.

At this point, it must be noted that, as shown in the above three figures, the peaks of F_C and F_D do not exceed the limiting index for this star, implying that these two frequencies are to be treated as much less significant compared to F_A. Even F_B cannot be considered absolutely reliable, as it exceeds I_1 by a factor of only 1.3.

However, as Figures IV.3.6. a) and b) illustrate, the four combined frequencies yield a surprisingly good fit to the two nights of data. If any or all of F_B, F_C and F_D are omitted, the RMS residuals rise dramatically, and the superimposed fits simply do not look correct. Of these three frequencies, F_B would have to be considered the most reliable. Figures IV.3.7 a) and b) illustrate the fit to

Figure IV.3.2. Unmodified Jurkevich frequency diagram of LT Vul data (to compare with Figure IV.3.1).

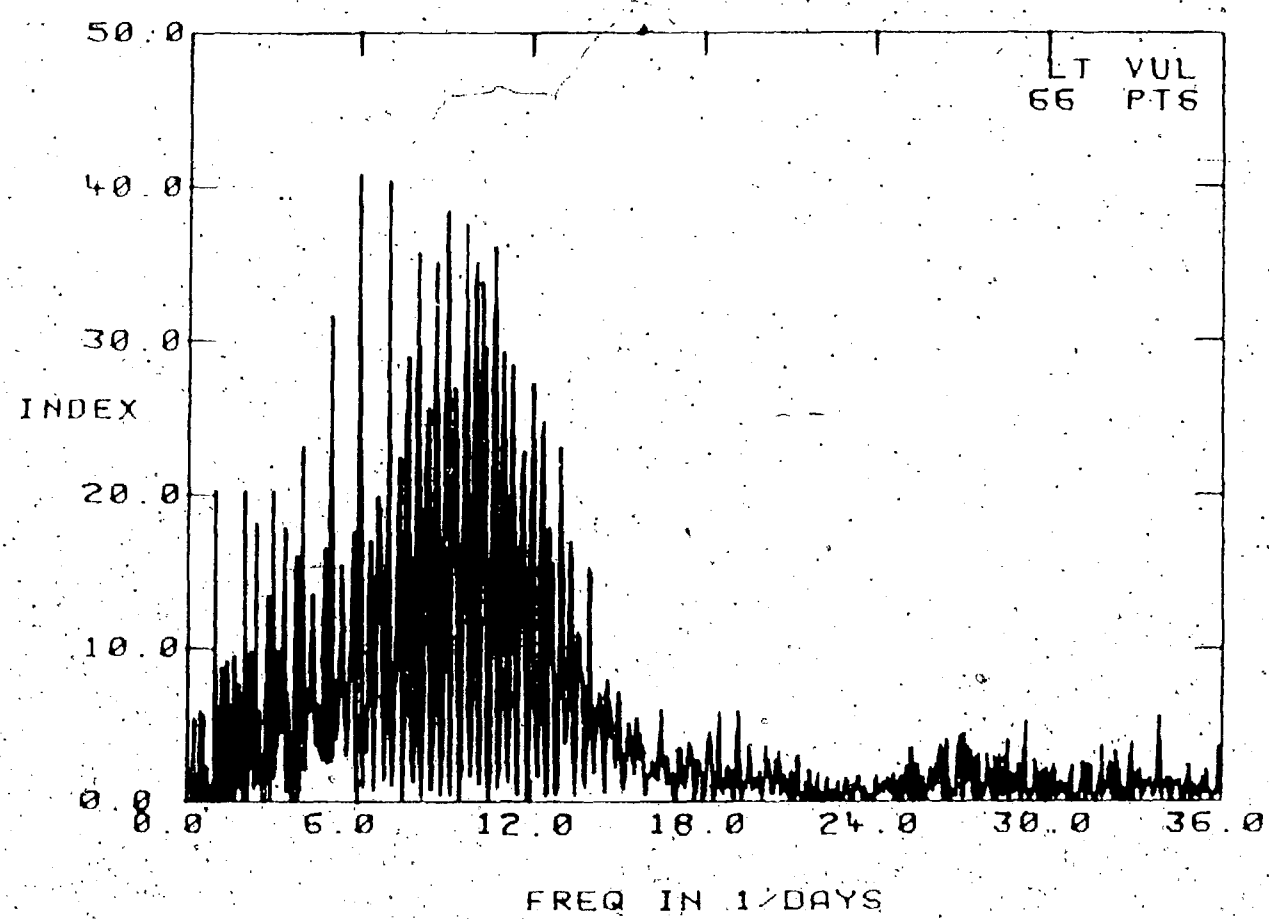
LT VUL
66 PTS
50.0
40.0
30.0
INDEX
20.0
10.0
0.0
0.0
6.0
12.0
18.0
24.0
30.0
36.0
FREQ IN 1/DAYS

Table IV.3.1.: P3R results for LT Vul

Run	Converged Parameters A (mag)	F (cy/d) / P (d)	ϕ (rad)	$\bar{m}$ (mag)	N	RMS x 10 (mag)
A	0.0195 ±0.0015	9.7474 ±0.0073 / 0.1026 ±0.0001	3.1861 ±0.2121	0.8625 ±0.0010	10	7.980
B	0.0049 ±0.0012	16.2521 ±0.0274 / 0.0615 ±0.0001	8.4730 ±0.7958	0.0004 ±0.0009	15	7.128
C	0.0029 ±0.0012	31.8270 ±0.0442 / 0.0314 ±0.0001	3.9449 ±1.3063	0.0001 ±0.0008	12	6.790
D	0.0035 ±0.0012	6.9008 ±0.0359 / 0.1449 ±0.0001	2.8706 ±1.0417	0.0003 ±0.0008	13	6.656

Figure IV.3.3. Frequency diagram of LT Vul data prewhitened by:

$$y(I) = {}^{m}_{0}.0195 \sin(2\pi\ 9.7474\ \text{cy/d}\ x(I) + 3.186) + {}^{m}_{0}.8625$$

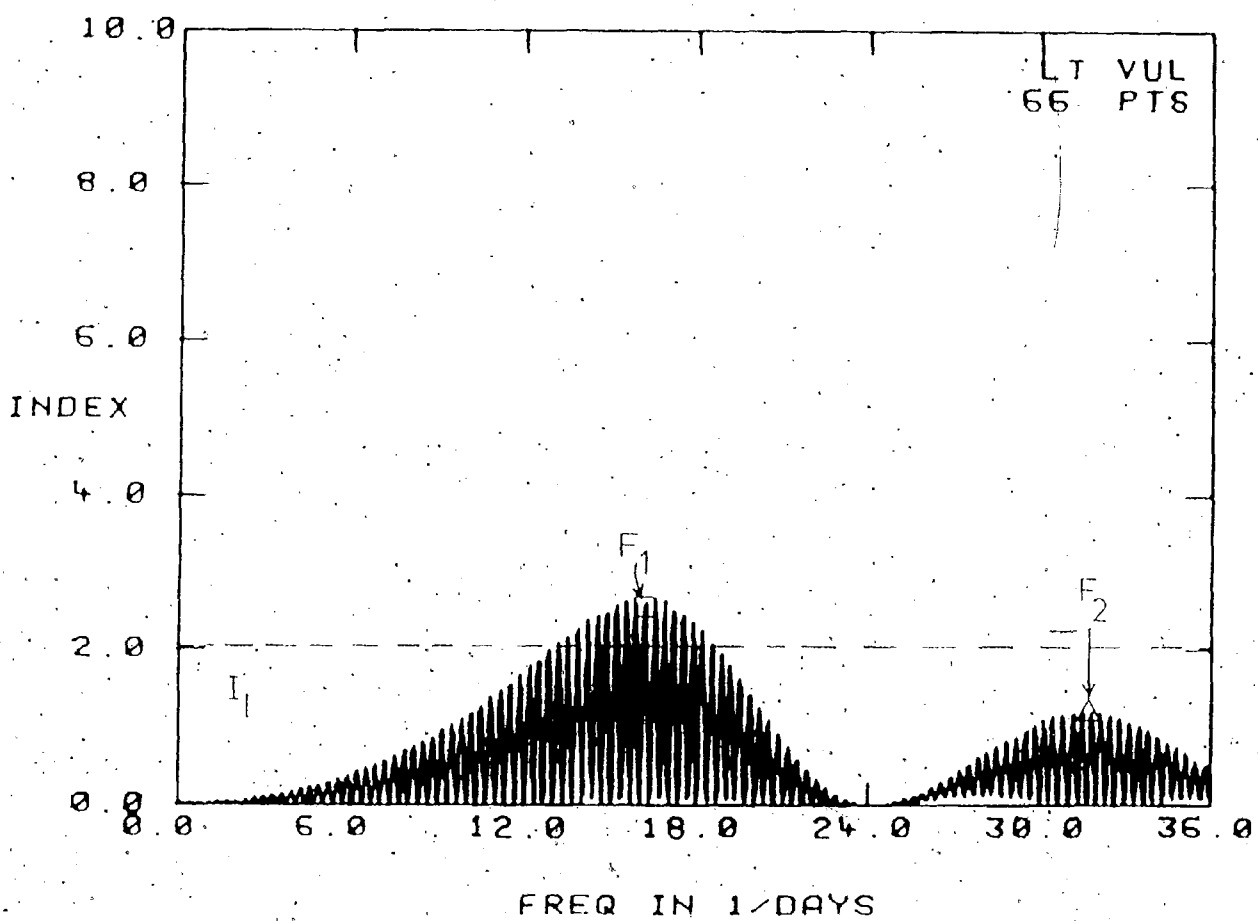
10.0
8.0
6.0
INDEX
4.0
2.0
0.0
LT VUL
66 PTS
F1
F2
I1
0.0
6.0
12.0
18.0
24.0
30.0
36.0
FREQ IN 1/DAYS

Figure IV.3.4. Frequency diagram of LT Vul data prewhitened by:

$$y(I) = {}^{m}_{0}.0195 \sin(2\pi\ 9.7474\ \text{cy/d}\ x(I) + 3.186) + {}^{m}_{0}.0049 \sin(2\pi\ 16.2521\ \text{cy/d}\ x(I) + 8.473) + {}^{m}_{0}.8625$$

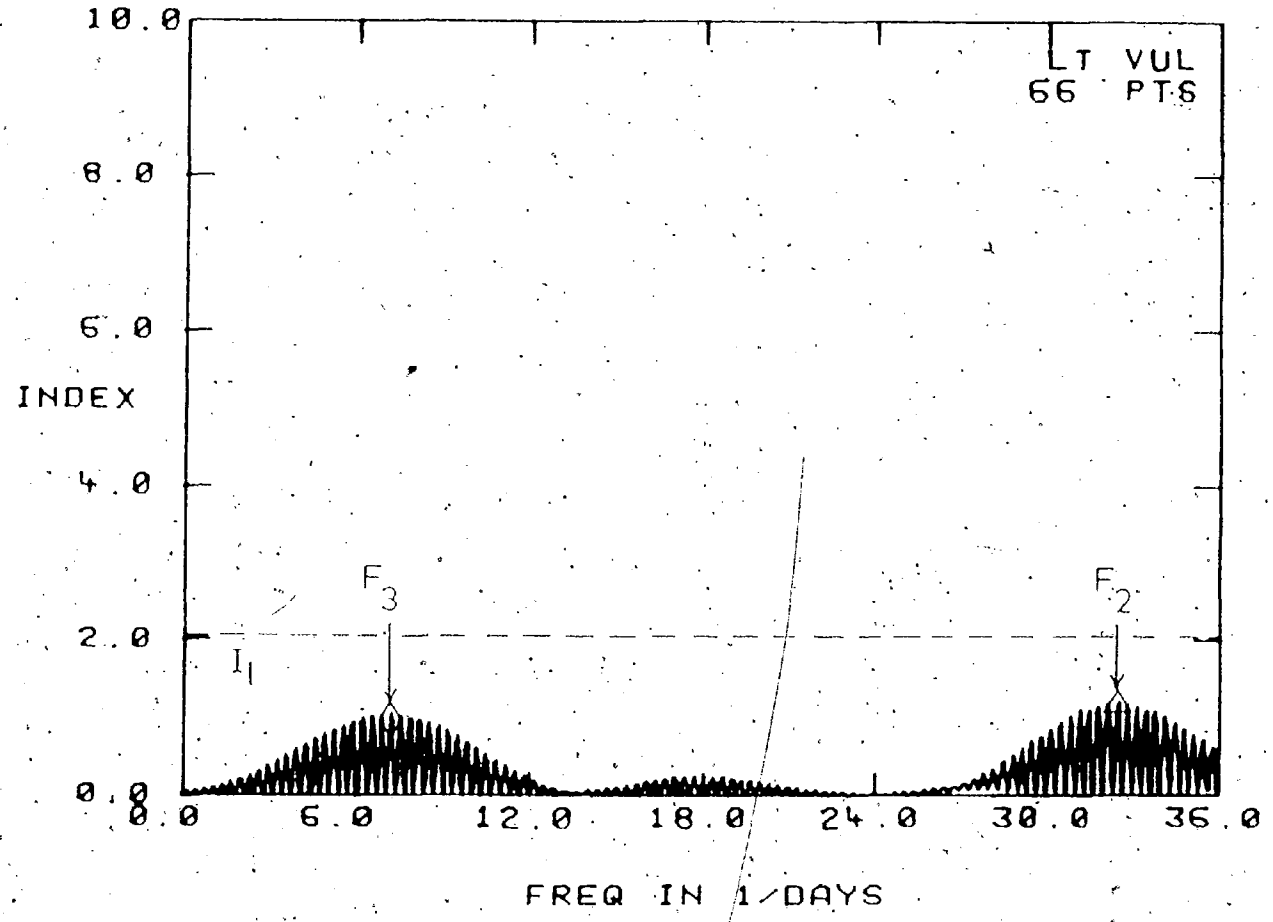
10.0
8.0
6.0
INDEX
4.0
2.0
0.0
LT VUL
66 PTS
F3
F2
I1
0.0
6.0
12.0
18.0
24.0
30.0
36.0
FREQ IN 1/DAYS

Figure IV.3.5. Frequency diagram of LT - Vul data prewhitened by:

$$y(I) = 0^{m}.0195 \sin(2\pi\ 9.7474\ \text{cy/d}\ x(I) + 3.861) + 0^{m}.0049 \sin(2\pi\ 16.2521\ \text{cy/d}\ x(I) + 8.473) + 0^{m}.0029 \sin(2\pi\ 31.8270\ \text{cy/d}\ x(I) + 3.945) + 0^{m}.0035 \sin(2\pi\ 6.9008\ \text{cy/d}\ x(I) + 2.871) + 0^{m}.8625$$

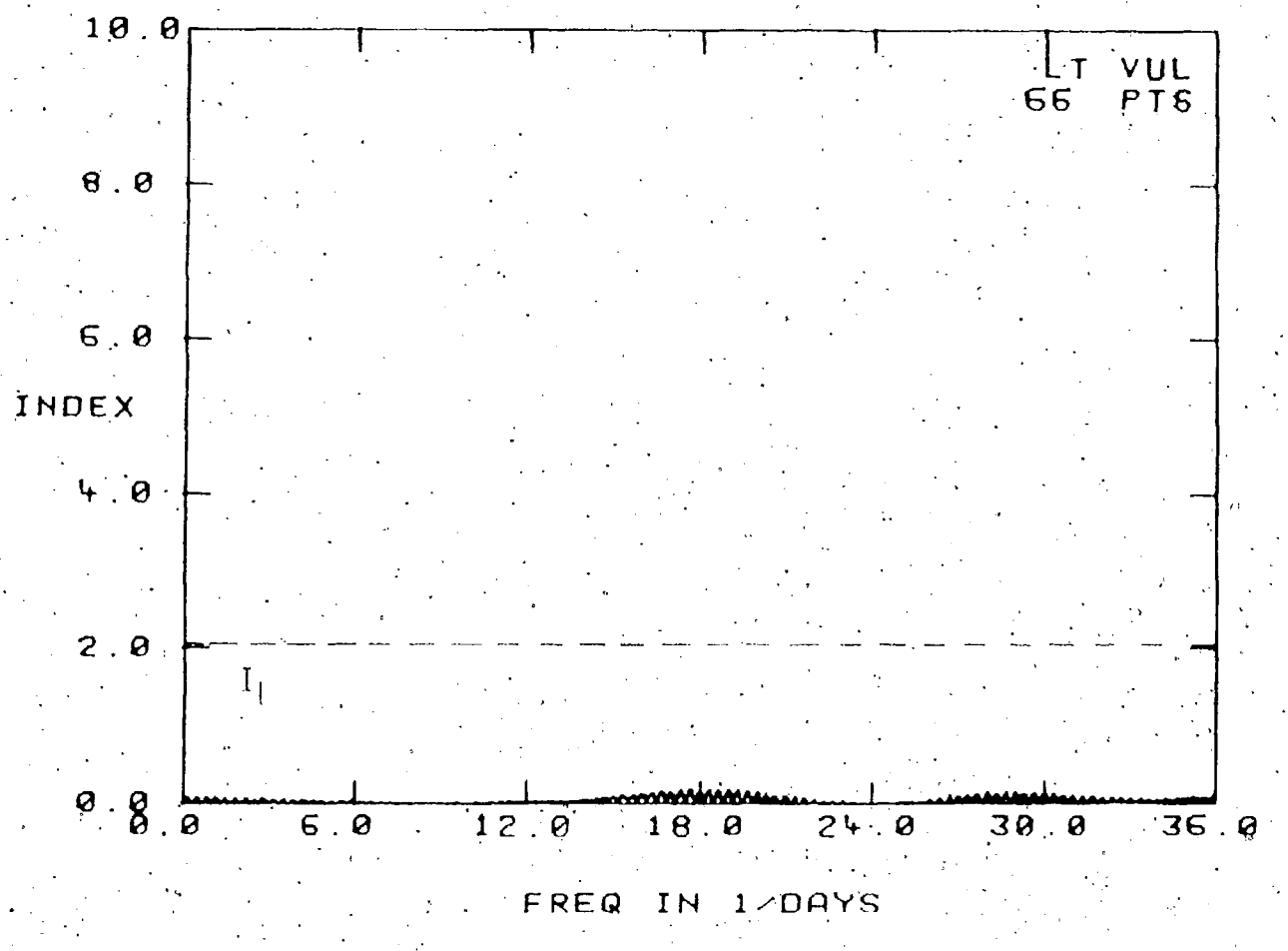
10.0
8.0
6.0
INDEX
4.0
2.0
0.0
LT VUL
66 PTS
0.0
6.0
12.0
18.0
24.0
30.0
36.0
FREQ IN 1/DAYS

Figure IV.3.6. a) - b) top: Differential photometry of LT Vul with four-sine fit superimposed (see Table IV.3.1.). bottom: Residuals of above four-sine fit.

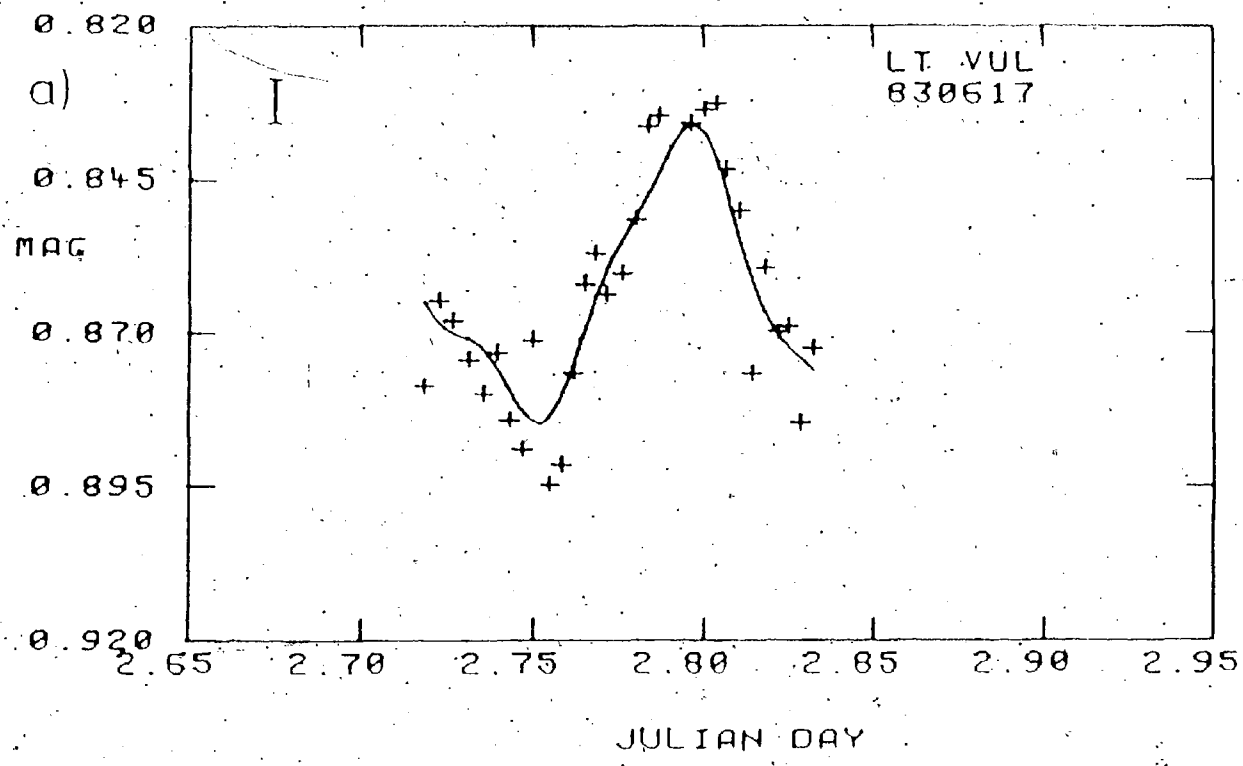
a)
LT VUL
830617
0.820
0.845
0.870
0.895
0.920
MAG
2.65
2.70
2.75
2.80
2.85
2.90
2.95
JULIAN DAY

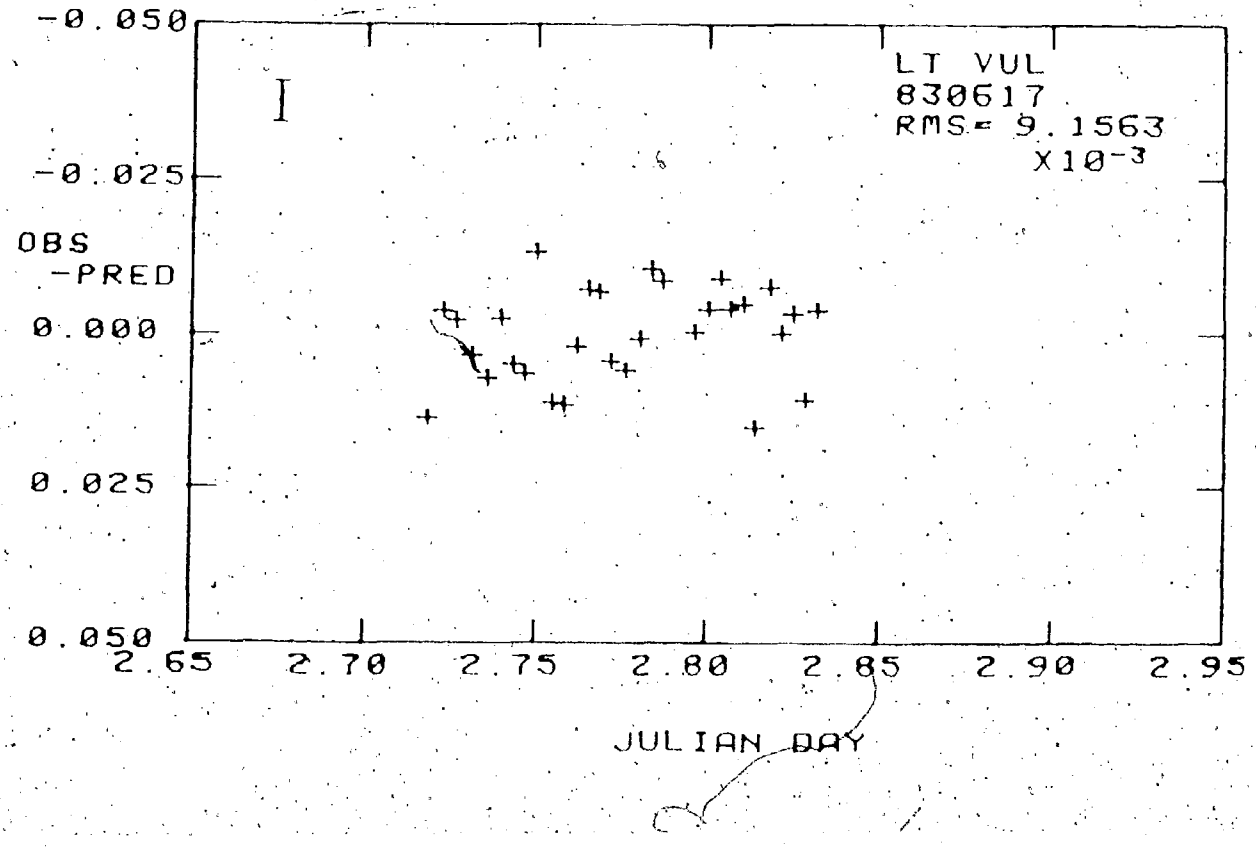
LT VUL
830617
RMS= 9.1563
X10-3
-0.050
-0.025
0.000
0.025
0.050
OBS
-PRED
2.65
2.70
2.75
2.80
2.85
2.90
2.95
JULIAN DAY

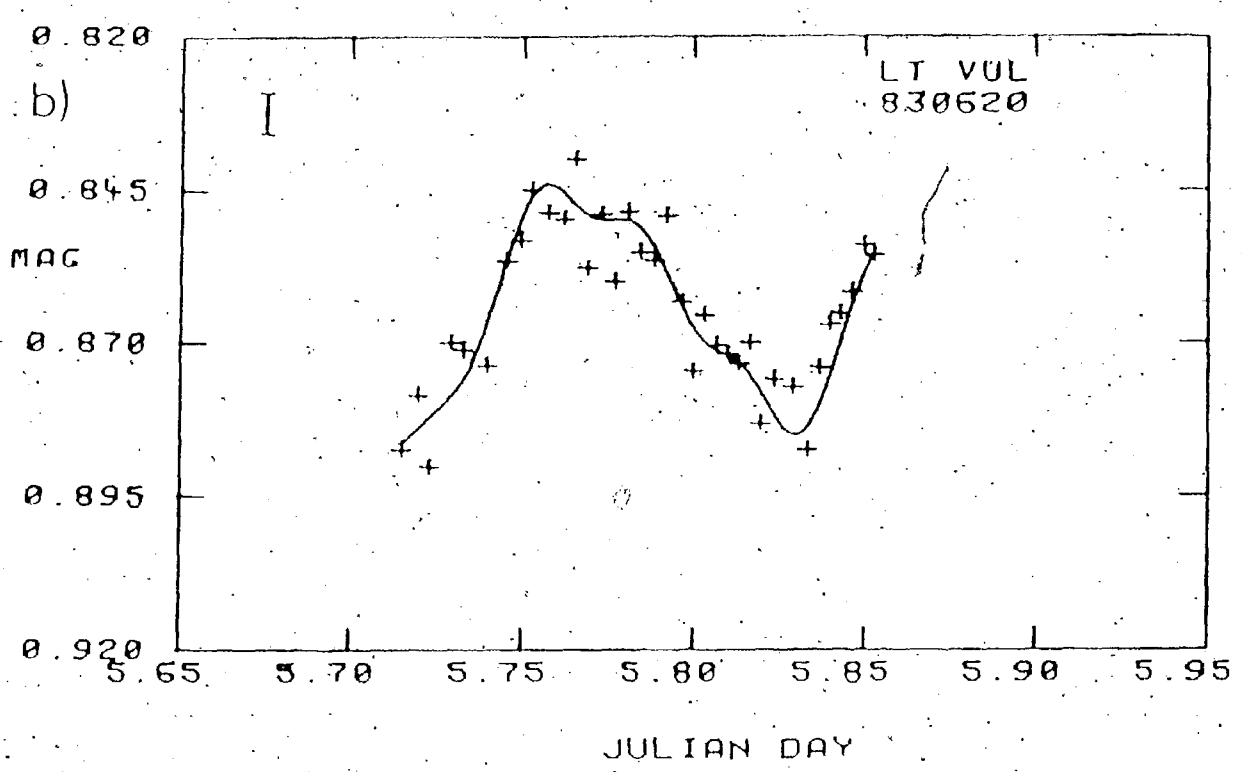
b)
I
LT VUL
830620
0.820
0.845
MAG
0.870
0.895
0.920
5.65
5.70
5.75
5.80
5.85
5.90
5.95
JULIAN DAY

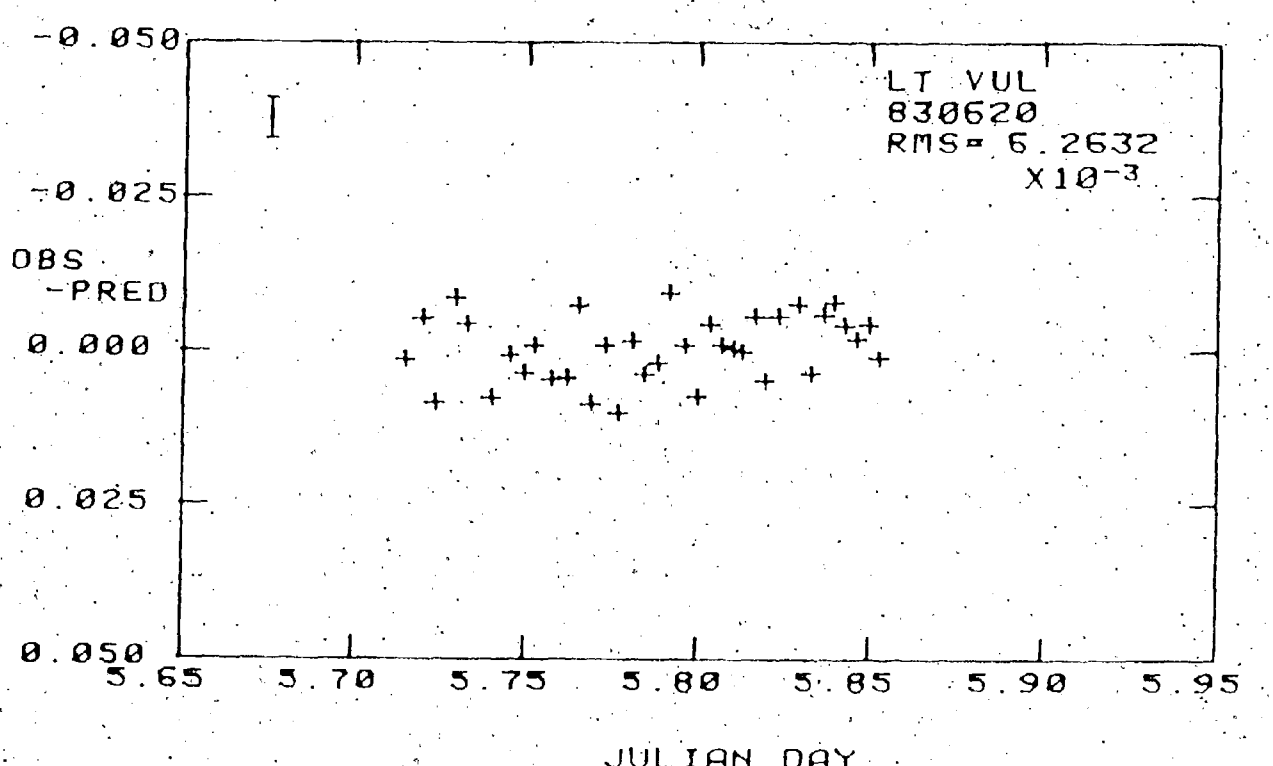
I
LT VUL
830620
RMS= 6.2632
X10-3
-0.050
-0.025
OBS
-PRED
0.000
0.025
0.050
5.65
5.70
5.75
5.80
5.85
5.90
5.95
JULIAN DAY

Figure IV.3.7. a) - b) top: Differential photometry of LT Vul with two-sine fit superimposed (see text).
Compare to Figure IV.3.6:
bottom: Residuals of above two-sine fit.

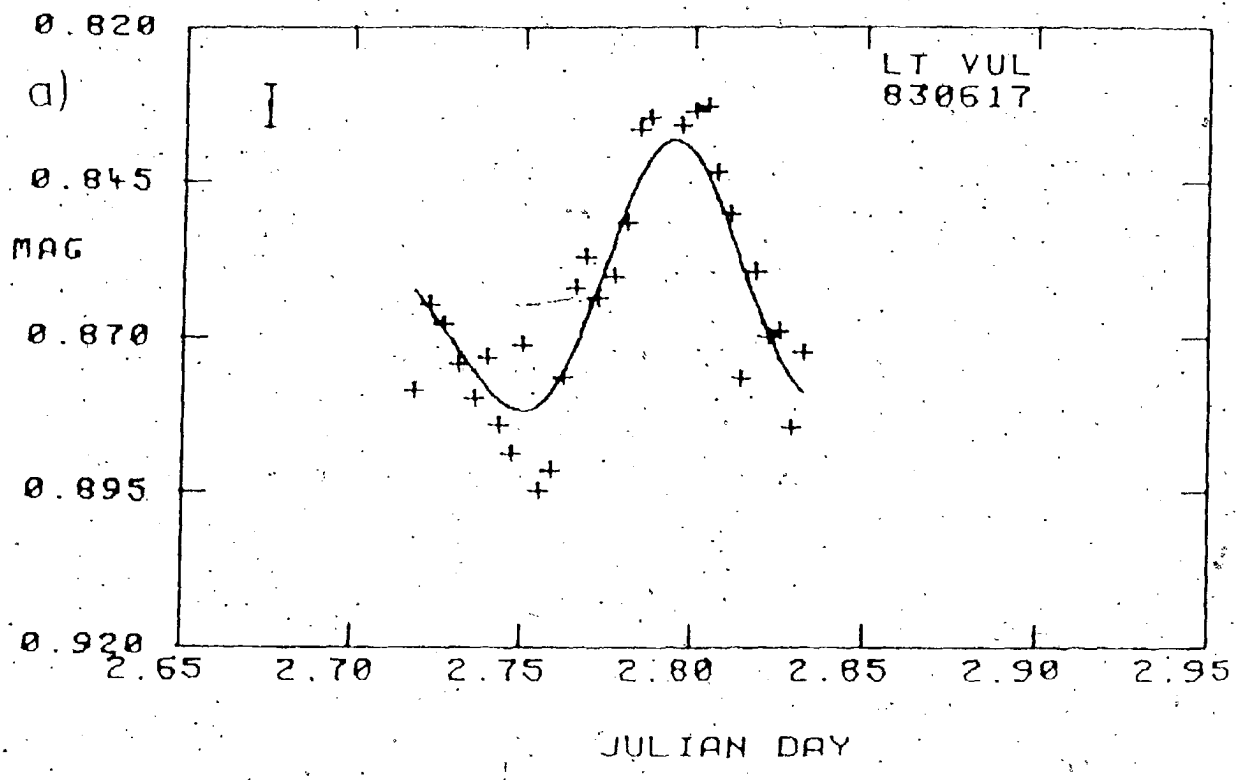
a)
LT VUL
830617
0.820
0.845
MAG
0.870
0.895
0.920
2.65
2.70
2.75
2.80
2.85
2.90
2.95
JULIAN DAY

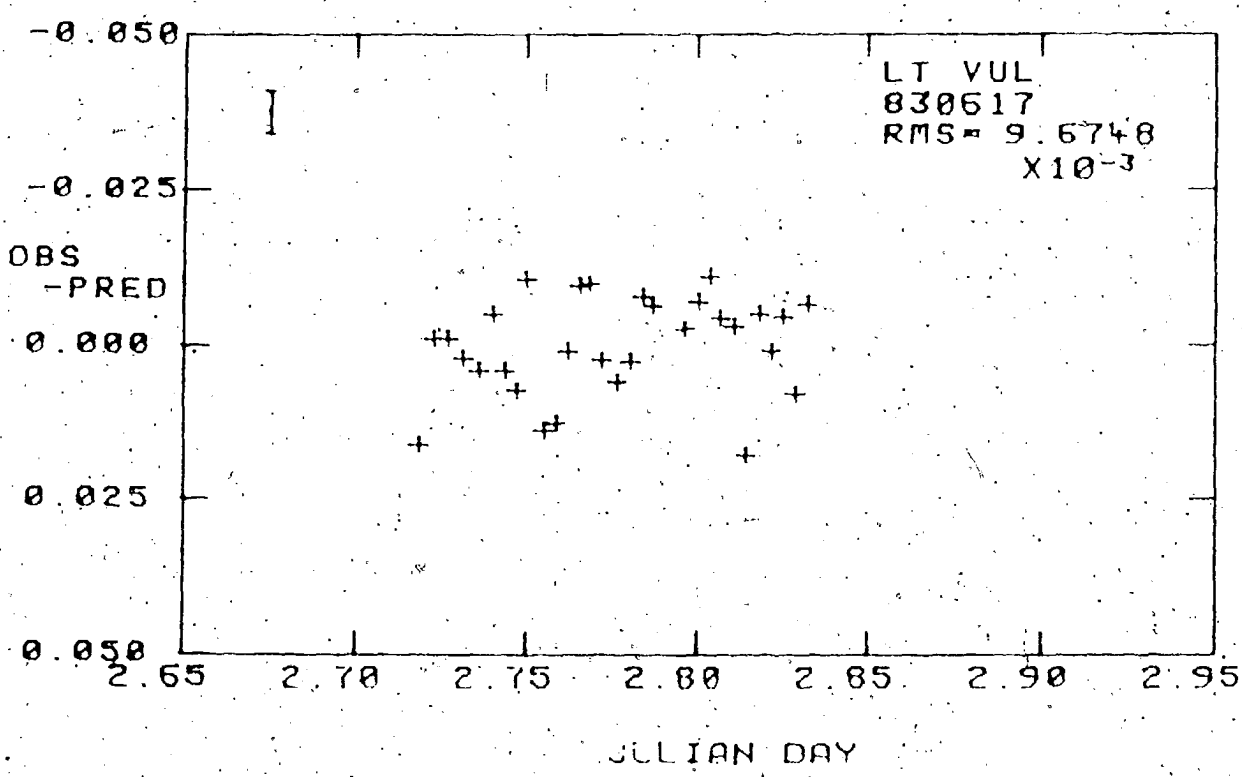
LT VUL
830617
RMS= 9.6748
X10-3
-0.050
-0.025
OBS
-PRED
0.000
0.025
0.050
2.65
2.70
2.75
2.80
2.85
2.90
2.95
JULIAN DAY

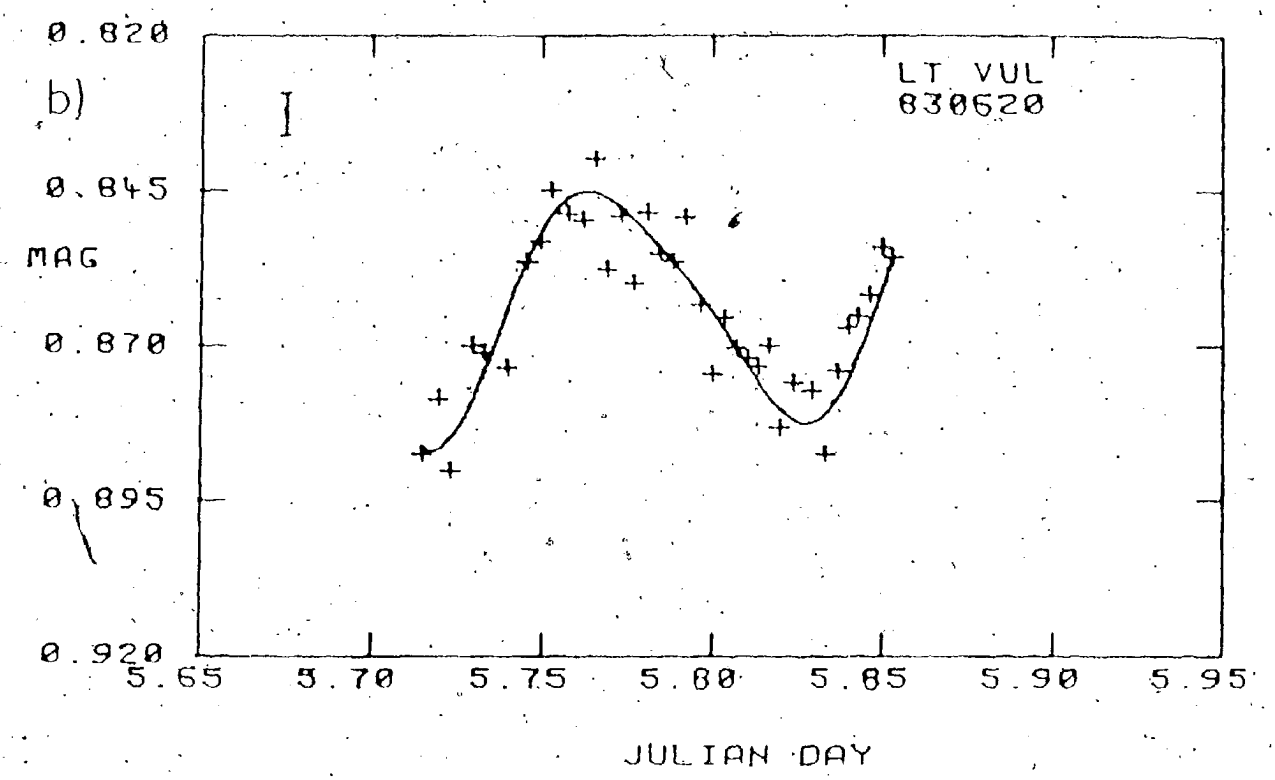
b)
LT VUL
830620
0.820
0.845
MAG
0.870
0.895
0.920
5.65
5.70
5.75
5.80
5.85
5.90
5.95
JULIAN DAY

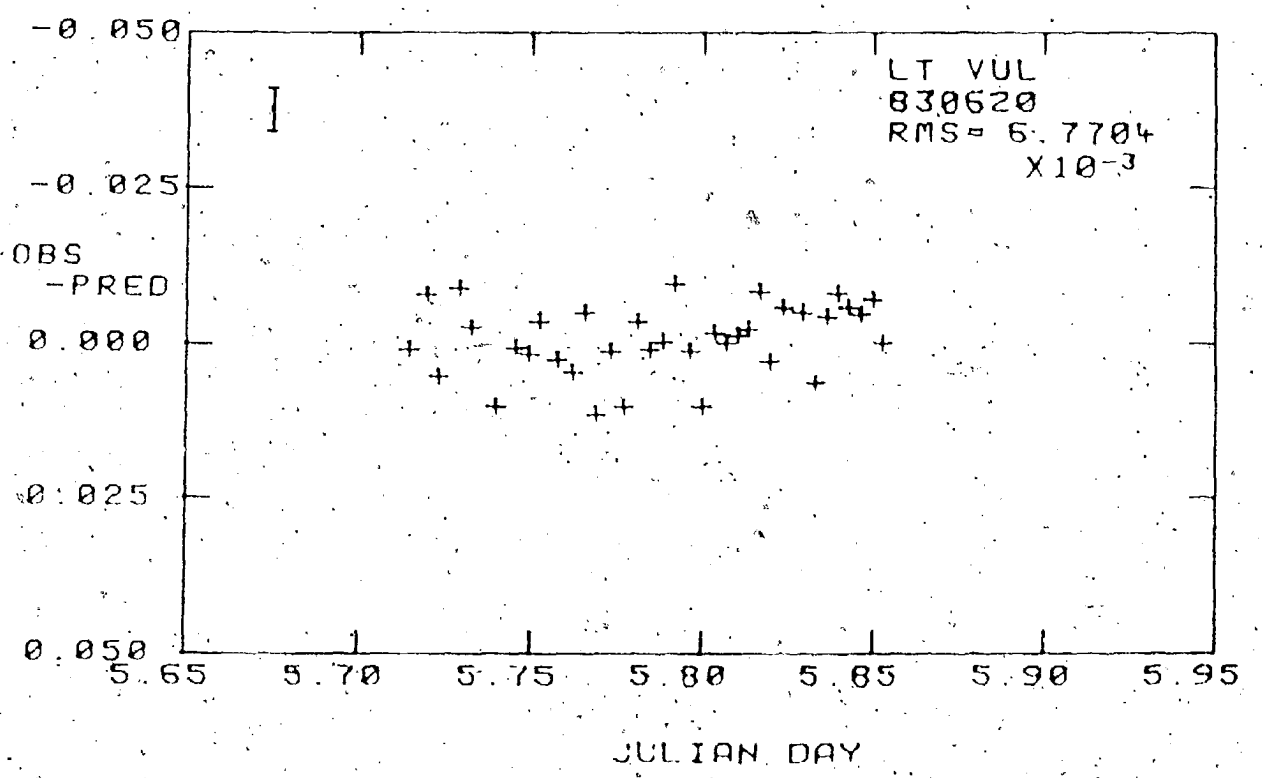
LT VUL
830620
RMS= 6.7704
X10-3
-0.050
-0.025
OBS
-PRED
0.000
0.025
0.050
5.65
5.70
5.75
5.80
5.85
5.90
5.95
JULIAN DAY

the light curves of LT Vul using only F_A and F_B. As shown in both the diagrams themselves and the RMS values, the two-sine fit is obviously not quite as good as the four-sine fit. But, is the four-sine fit real? We think perhaps not. More observations of LT Vul are needed before a firm decision either way can be made.

Previous work on LT Vul resulted in only one frequency (period) of 10.42 cy/d ($_d$0.096) being detected (Breger 1969), which is comparable to the value of F_A obtained here. The discussion of the periods of LT Vul continues in the next chapter.

Chapter V: Discussion of Results

As as aid to the discussion of the results for the three program stars, it is instructive to compare the location of these stars in the HR diagram with the location of other δ-Scuti variables. For this purpose it is necessary to estimate their luminosities and effective temperatures, parameters which can be determined as in Petersen and Jorgensen (1972) (hereinafter PJ) using Stromgren system and H photometry of the stars. Such estimates are necessarily rather crude due to the limitations imposed by photometric errors (typically $\sim 0^{m}.01$) and scatter in the transformations to M_{bol} and $\log T_{eff}$. However, they do provide a sound basis for understanding the cause of the light variations in our program stars.

Table V.1. summarizes the pulsation frequencies for the three program stars as obtained in Chapter IV. Corresponding periods have also been included, as it is now more convenient to speak of 'period' rather than 'frequency'. Included in the table are estimates of stellar mass M/M$\odot$, log surface gravity g, absolute bolometric magnitude M_{bol}, and log effective temperature T_{eff}, taken from PJ. These values have been used to determine pulsation constants Q_{n} for the stars, using the standard formula for the pulsation constant (equation (1), Chapter I) which has been transformed into the following equation (taken from PJ):

Table V.1.: Summary of Program Star Parameters

Star	$\frac{M}{M_\odot}$	M_{bol}	log g	log T_{eff}	n	P (d) (F (d^{-1}))	$\frac{P_n}{P_0}$	Q_n
63 Her	1.88	1.63	4.00	3.894	0	0.0884 (11.318)	----	0.0354
					2	0.0524 (19.070)	0.59	0.0210
					nr?	0.1295+ (7.723)	1.46	0.0519
V1208 Aql	2.25	0.63	3.67	3.893	0	0.1456 (6.870)	----	0.0313
					1	0.1063 (9.409)	0.73	0.0228
					nr?	0.1941+ (5.152)	1.33	0.0605
LT Vul	2.08	0.80	3.62	3.870	0	0.1449 (6.901)	----	0.0394
					1	0.1026 (9.747)	0.71	0.0208
					4?	0.0615+ (16.252)	0.42	0.0124
					7?	0.0314+ (31.827)	0.22	0.0085

* from Petersen and Jorgensen 1972

+ low-weight periodicity (see Chapter IV)

$$\log Q_n = -6.454 + \log P + 0.5 \log g + 0.1 M_{bol} + \log T_{eff}$$

Estimates for stellar mass needed to obtain values for the surface gravity can be made by comparing M_{bol} and $\log T_{eff}$ for these variables with the results predicted from stellar evolutionary models. Given the uncertainties in such models resulting from chemical composition differences and inaccuracies in the evolutionary codes, the resulting estimates of Q_n tend to be accurate only to about ten percent. However, this is accurate enough for our purposes.

Figure V.1. is an HR diagram for the three program stars and includes other selected single- and double-mode δ-Scuti variables taken from Andreasen (1983). The number accompanying each point indicates the fundamental period of pulsation in days for each star (P_0).

In a diagram of this type, lines of constant fundamental period run approximately perpendicular to the borders of the instability strip (Kraft 1963), and as Figure V.1. illustrates, δ-Scuti stars of similar period do seem to lie along lines which lie perpendicular to the instability strip's red edge (plotted as a dashed line in Figure V.1.). This characteristic of δ-Scuti stars (and pulsating stars in general) enables us to determine for each program star which period is likely to represent the fundamental period P_0 for radial pulsation.

63 Her appears to lie along a constant period line corresponding to about $P_0 \sim 0.09^d$, which leads us to conclude that its fundamental period is $P_0 = 0.0884^d$,

Figure V.1. HR diagram showing the positions and periods of the three program stars in comparison with the positions and periods of other known δ-Scuti stars (taken from Tables 2 and 4 of Andreason, 1983). Open squares and triangles indicate, respectively, single- and double-mode δ-Scuti variables. The dashed line approximately indicates the red edge of the instability strip.

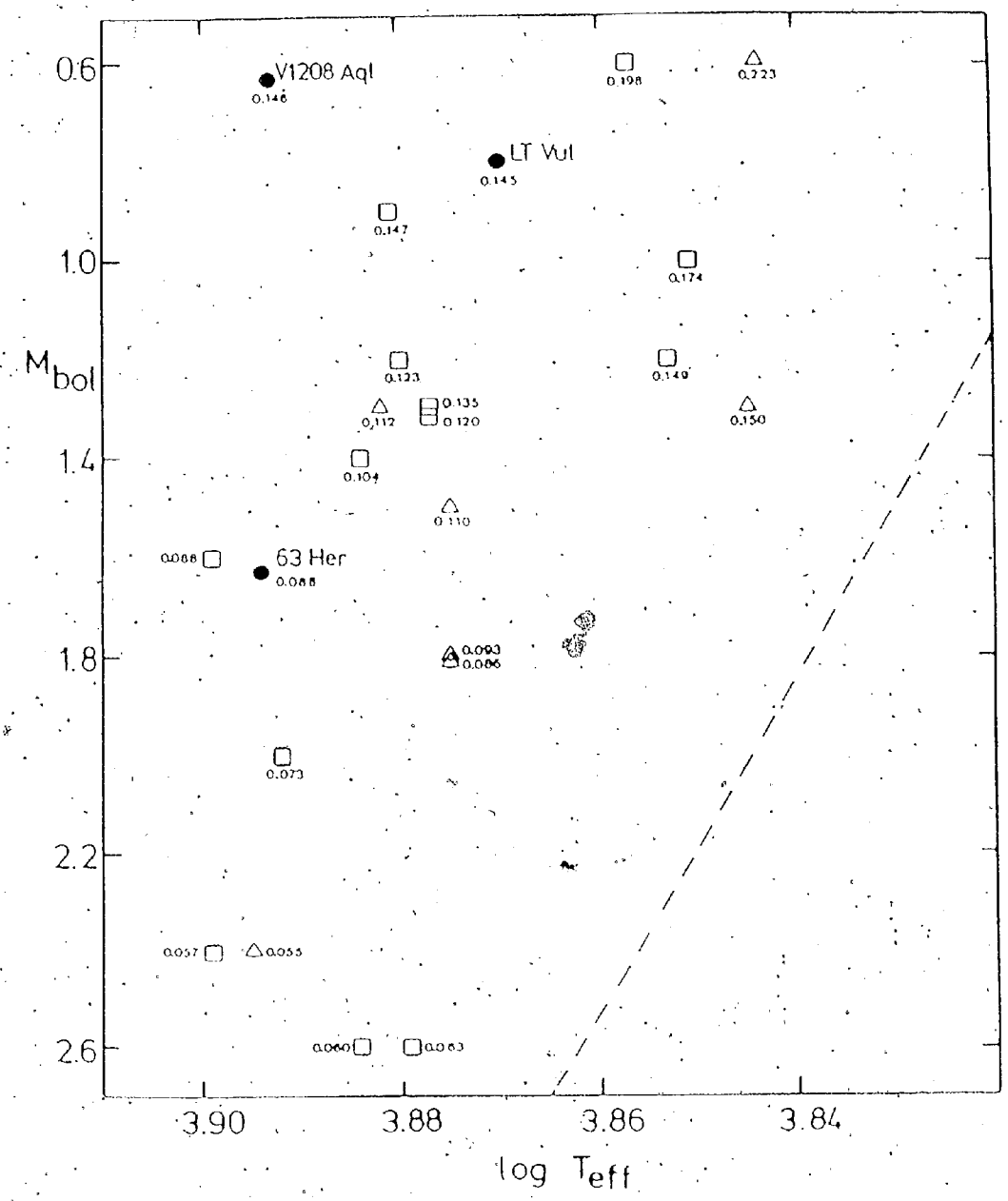
V1208 Aql
0.146
0.198
0.223
LT Vul
0.145
0.147
0.174
0.123
0.149
0.135
0.120
0.112
0.150
0.104
0.110
0.088
63 Her
0.088
0.093
0.086
0.073
0.057
0.055
0.060
0.063
0.6
1.0
1.4
1.8
2.2
2.6
M_{bol}
3.90
3.88
3.86
3.84
log T_{eff}

rather than $0^d.1295$, which is the longest period found here for this star. Previous authors (PJ; Petersen 1976; Breger 1979; etc.) have determined that a period ratio P_1/P_0 of 0.74 to 0.78 is typical of δ-Scuti radial pulsation in the fundamental and first overtone (P_1) modes, while a ratio of $P_2/P_0 = 0.60$ is expected for radial pulsation in the fundamental and second overtone (P_2) modes. For 63 Her, the ratio of the periods of its two largest amplitude variations $0^d.0524$ to $0^d.0884$ is 0.59, which appears to be indicative of radial pulsation in the fundamental and second overtone modes. The third period determined for this star, $0^d.1295$, does not combine with either of the other two periods to produce ratios which fit the predictions for radial pulsation. Quite possibly it represents some form of non-radial pulsation for the star, particularly since the amplitude associated with this variability is quite small.

Much the same type of argument can be constructed for V1208 Aql. Its location in the HR diagram suggests that its fundamental period should be $P_0 = 0^d.1456$, rather than $0^d.1941$. The period ratio of $0^d.1063$ to $0^d.1456$ gives 0.73, which suggests radial pulsation in the fundamental and first overtone modes. As with 63 Her, the third period, $0^d.1941$, conceivably represents a non-radial mode since it does not combine with other periods to produce ratios typical of radial pulsation models. An alternate possibility for the long period variations in both of

these stars is that they are simply spurious, as their amplitudes are no larger than the predicted observational scatter for the two stars.

LT Vul presents a slightly different case. Its position in the HR diagram indicates that its longest period of variability, $0^d.1449$, is probably also its fundamental period. However, the periodicity having the largest amplitude (i.e. the 'strongest' mode) is $P_1 = 0^d.1026$, which can be identified with pulsation in the first overtone mode. The low P_n/P_0 ratios for the remaining two periods indicate that they may be radial overtone modes of a higher order (possibly n = 4 and 7!), although their amplitudes are so small compared to the observational noise that they could simply be spurious.

Table V.I. summarizes the radial (n) and non-radial (nr?) pulsation mode identifications for the three program stars as discussed above. Low-weight identifications (i.e. those having amplitudes no larger than observational noise) are marked with a cross (+) in the table, and it should be noted that these light variations could in all cases be spurious.

Petersen (1976) and Andreasen et.al (1983) have calculated the following theoretical pulsation constants for radial pulsation based upon Population I, main sequence; δ-Scuti models:

$$Q_0 \text{ (theo)} = 0.0310 - 0.0340,$$
$$Q_1 \text{ (theo)} = 0.0240 - 0.0270,$$

$$Q_2 \text{ (theo)} = 0.0201,$$

$$Q_3 \text{ (theo)} = 0.0170.$$

For all three program stars, the values of Q_0 (all three stars), Q_1 (V1208 Aql and LT Vul) and Q_2 (63 Her) seem to correlate fairly well with these predictions. Although some scatter is present, especially in the case of LT Vul, these Q values tend to reinforce our conclusions regarding which radial modes of pulsation are present.

In summary, it appears that 63 Her, V1208 Aql and LT Vul are pulsating with the periods and modes discussed above and listed in Table V.1. Although progress has been made in identifying periodicities in the light variations for these three stars, further observations would greatly help to confirm all of the estimated periods discussed here. In the case of V1208 Aql and LT Vul especially, a larger data set will be necessary to determine whether or not the low-amplitude periods for each star are real.

We have also concluded that the Jurkevich-Swingler period search technique yields cleaner, clearer frequency diagrams which are much easier to interpret than those produced using the original Jurkevich routine. This improved method for generating such diagrams should be of great value in future δ-Scuti (or similar) period search work.

APPENDIX A

DIFFERENTIAL PHOTOMETRY FOR 63 HERCULIS
IN THE FORMAT (VARIABLE-CHECK STAR)

NUMBER OF POINTS = 327
COLUMNS ARE: JULIAN DAY (-2444 5580)
DIFFERENTIAL V MAGNITUDE

8.7116	0.8663
8.7179	0.8692
8.7219	0.8733
8.7258	0.8670
8.7294	0.8669
8.7334	0.8741
8.7373	0.8705
8.7412	0.8748
8.7450	0.8658
8.7489	0.8682
8.7530	0.8717
8.7569	0.8596
8.7607	0.8806
8.7653	0.8807
8.7692	0.8813
8.7731	0.8840
8.7783	0.8833
8.7823	0.8786
8.7862	0.8645
8.7902	0.8658
8.7939	0.8558
8.7975	0.8527
8.8009	0.8550
8.8046	0.8475
8.8087	0.8558
8.8122	0.8582
8.8160	0.8688
8.8196	0.8691
8.8231	0.8722
8.8267	0.8676
8.8312	0.8882
8.8348	0.8940
8.8385	0.8863
8.8445	0.8813
8.8481	0.8754
8.8515	0.8758
8.8553	0.8640
8.8593	0.8665
8.8625	0.8734
8.8722	0.8874
8.8758	0.8885
8.8793	0.8903
8.8826	0.8732
8.8862	0.8748
8.8896	0.8808
9.6769	0.8704
9.6810	0.8547
9.6846	0.8522
9.6889	0.8581
9.6927	0.8573
9.6964	0.8508

9.7002	0.8568
9.7036	0.8594
9.7071	0.8659
9.7112	0.8727
9.7147	0.8734
9.7180	0.8768
9.7251	0.8676
9.7289	0.8735
9.7328	0.8591
9.7371	0.8576
9.7405	0.8668
9.7445	0.8689
9.7487	0.8536
9.7526	0.8566
9.7615	0.8529
9.7657	0.8718
9.7696	0.8758
9.7742	0.8790
9.7780	0.8647
9.7820	0.8717
9.7858	0.8562
9.7914	0.8790
9.7952	0.8707
9.7988	0.8719
9.8030	0.8767
9.8066	0.8738
9.8100	0.8798
9.8135	0.8839
9.8167	0.8769
9.8204	0.8859
9.8238	0.8794
9.8281	0.8807
9.8326	0.8614
9.8364	0.8774
9.8403	0.8660
9.8446	0.8696
9.8484	0.8514
9.8539	0.8611
9.8579	0.8713
9.8620	0.8587
9.8658	0.8521
9.8695	0.8604
9.8742	0.8673
9.8843	0.8734
9.8880	0.8736
10.6740	0.8843
10.6803	0.8709
10.6849	0.8713
10.6891	0.8825
10.6936	0.8834
10.7077	0.8734
10.7121	0.8895
10.7158	0.8857
10.7201	0.8836
10.7241	0.8814
10.7286	0.8734

10.7359	0.8592
10.7400	0.8641
10.7442	0.8596
10.7479	0.8568
10.7522	0.8632
10.7562	0.8650
10.7594	0.8595
10.7639	0.8744
10.7679	0.8699
10.7716	0.8793
10.7749	0.8776
10.7797	0.8879
10.7840	0.8738
10.7881	0.8841
10.7922	0.8868
10.7955	0.8693
10.7999	0.8815
10.8033	0.8730
10.8068	0.8861
10.8102	0.8869
10.8136	0.8767
10.8170	0.8766
10.8201	0.8730
10.8230	0.8784
10.8267	0.8837
10.8304	0.8670
10.8347	0.8615
10.8383	0.8647
10.8423	0.8705
10.8454	0.8562
10.8484	0.8737
10.8518	0.8622
10.8548	0.8641
10.8584	0.8788
16.6757	0.8653
16.6798	0.8715
16.6845	0.8785
16.6882	0.8694
16.6920	0.8701
16.6957	0.8790
16.6988	0.8797
16.7029	0.8826
16.7066	0.8767
16.7103	0.8737
16.7139	0.8698
16.7171	0.8650
16.7206	0.8642
16.7244	0.8694
16.7276	0.8739
16.7311	0.8814
16.7345	0.8754
16.7375	0.8770
16.7409	0.8769
16.7439	0.8745
16.7472	0.8747
16.7503	0.8734

16.7530	0.8629
16.7559	0.8701
16.7593	0.8702
16.7622	0.8704
16.7654	0.8663
16.7687	0.8658
16.7717	0.8672
16.7747	0.8650
16.7780	0.8746
16.7812	0.8731
16.7841	0.8730
16.7876	0.8867
16.7907	0.8851
16.7937	0.8911
16.7980	0.8864
16.8012	0.8933
16.8050	0.8780
16.8082	0.8875
16.8113	0.8891
16.8146	0.8721
16.8191	0.8618
16.8224	0.8568
16.8253	0.8598
16.8286	0.8654
16.8324	0.8504
16.8357	0.8507
16.8390	0.8590
16.8421	0.8666
16.8454	0.8671
18.7293	0.8695
18.7323	0.8778
18.7355	0.8853
18.7394	0.8827
18.7427	0.8851
18.7462	0.8823
18.7492	0.8870
18.7527	0.8800
18.7563	0.8815
18.7608	0.8741
18.7641	0.8672
18.7673	0.8612
18.7712	0.8559
18.7748	0.8575
18.7782	0.8547
18.7819	0.8550
18.7852	0.8589
18.7889	0.8666
18.8033	0.8606
18.8062	0.8696
18.8093	0.8655
18.8132	0.8729
18.8168	0.8687
18.8198	0.8789
18.8229	0.8641
18.8259	0.8695
18.8292	0.8773

18.8323	0.8798
18.8359	0.8866
18.8391	0.8868
19.7028	0.8628
19.7054	0.8748
19.7093	0.8697
19.7125	0.8765
19.7156	0.8717
19.7185	0.8775
19.7226	0.8808
19.7259	0.8859
19.7290	0.8908
19.7322	0.8794
19.7349	0.8811
19.7377	0.8809
19.7405	0.8723
19.7438	0.8635
19.7469	0.8635
19.7500	0.8665
19.7529	0.8700
19.7560	0.8624
19.7589	0.8566
19.7619	0.8601
19.7651	0.8632
19.7686	0.8550
19.7718	0.8669
19.7754	0.8728
19.7786	0.8846
19.7821	0.8779
19.7853	0.8842
19.7887	0.8867
19.7918	0.8776
19.7953	0.8813
19.7986	0.8726
19.8020	0.8773
19.8048	0.8711
19.8078	0.8784
19.8108	0.8776
19.8145	0.8786
19.8268	0.8530
19.8295	0.8410
19.8342	0.8652
19.8379	0.8675
19.8419	0.8702
19.8464	0.8679
19.8493	0.8658
19.8523	0.8640
19.8553	0.8747
19.8583	0.8727
19.8613	0.8635
19.8644	0.8749
19.8673	0.8630
19.8703	0.8733
19.8734	0.8697
19.8763	0.8740
19.8797	0.8701

19.8828	0.8783
19.8861	0.8842
19.8890	0.8890
19.8921	0.8868
19.8951	0.8893
19.8985	0.8915
19.9017	0.8887
20.7057	0.8542
20.7189	0.8638
20.7219	0.8630
20.7347	0.8575
20.7376	0.8599
20.7407	0.8587
20.7439	0.8633
20.7469	0.8600
20.7498	0.8623
20.7534	0.8628
20.7572	0.8675
20.7604	0.8729
20.7637	0.8753
20.7671	0.8781
20.7703	0.8810
20.7739	0.8971
20.7770	0.8956
20.7807	0.9030
20.7840	0.8927
20.7874	0.8936
20.7909	0.8900
20.7943	0.8917
20.7975	0.8817
20.8006	0.8720
20.8037	0.8674
20.8086	0.8691
20.8119	0.8615
20.8151	0.8642
20.8180	0.8723
20.8209	0.8752
20.8249	0.8678
20.8290	0.8694
20.8318	0.8693
20.8347	0.8704
20.8380	0.8738
20.8411	0.8744
20.8443	0.8753
20.8479	0.8747
20.8510	0.8707
20.8541	0.8723
20.8570	0.8737
20.8601	0.8720
20.8634	0.8748
20.8660	0.8805
20.8690	0.8746

APPENDIX B

DIFFERENTIAL PHOTOMETRY FOR V1208 AQUILAE
IN THE FORMAT (VARIABLE-COMPARISON STAR)

NUMBER OF POINTS = 140
COLUMNS ARE: JULIAN DAY (-244 5610)
DIFFERENTIAL V MAGNITUDE

3.7079	0.5292
3.7118	0.5352
3.7169	0.5273
3.7215	0.5253
3.7249	0.5202
3.7287	0.5234
3.7324	0.5254
3.7368	0.5168
3.7402	0.5161
3.7438	0.5090
3.7506	0.5014
3.7538	0.5032
3.7569	0.4953
3.7602	0.5007
3.7761	0.4899
3.7798	0.4884
3.7827	0.4925
3.7860	0.4990
3.7899	0.4967
3.7933	0.4885
3.7997	0.4960
3.8032	0.5006
3.8073	0.5024
3.8105	0.5073
3.8135	0.5086
3.8166	0.5253
3.8197	0.5064
3.8226	0.5320
3.8260	0.5293
3.8290	0.5133
3.8351	0.5175
3.8386	0.5190
3.8417	0.5265
3.8446	0.5238
3.8480	0.5224
3.8509	0.5204
3.8539	0.5116
3.8569	0.5189
3.8604	0.5315
3.8635	0.5240
4.7014	0.5131
4.7052	0.5116
4.7091	0.5218
4.7135	0.5105
4.7178	0.5121
4.7218	0.5259
4.7257	0.5176
4.7300	0.5228
4.7337	0.5252
4.7373	0.5192
4.7440	0.5230

4.7478	0.4873
4.7511	0.5171
4.7544	0.5185
4.7577	0.5127
4.7609	0.5102
4.7645	0.5114
4.7676	0.5033
4.7709	0.4978
4.7741	0.5021
4.7808	0.4907
4.7840	0.4976
4.7872	0.4963
4.7914	0.4911
4.7948	0.4970
4.7980	0.4896
4.8011	0.4926
4.8042	0.5016
4.8091	0.4964
4.8126	0.4990
4.8189	0.4948
4.8244	0.4971
4.8275	0.5084
4.8312	0.5058
4.8460	0.5187
4.8491	0.5105
4.8535	0.5171
4.8578	0.5168
4.8609	0.5256
4.8660	0.5283
4.8720	0.5284
4.8749	0.5276
4.8778	0.5312
4.8814	0.5315
4.8850	0.5321
4.8893	0.5293
4.8925	0.5263
4.8958	0.5287
4.8985	0.5304
4.9014	0.5222
9.6990	0.5173
9.7028	0.5126
9.7080	0.5216
9.7113	0.5146
9.7147	0.5059
9.7185	0.5157
9.7215	0.5047
9.7259	0.5046
9.7290	0.5001
9.7328	0.5024
9.7528	0.4968
9.7560	0.5052
9.7589	0.4969
9.7624	0.5059
9.7658	0.5095
9.7689	0.4999
9.7724	0.5098

9.7753	0.5125
9.7784	0.5069
9.7811	0.5049
9.7878	0.5018
9.7907	0.5123
9.7962	0.5168
9.7990	0.5148
9.8026	0.5112
9.8057	0.5244
9.8087	0.5274
9.8127	0.5209
9.8160	0.5221
9.8190	0.5119
9.8256	0.5217
9.8286	0.5185
9.8317	0.5177
9.8350	0.5207
9.8390	0.5167
9.8422	0.5152
9.8467	0.5195
9.8499	0.5123
9.8541	0.5058
9.8572	0.5104
9.8645	0.5092
9.8678	0.5190
9.8706	0.5043
9.8737	0.4990
9.8769	0.5047
9.8798	0.5091
9.8833	0.5099
9.8860	0.5047
9.8891	0.5030
9.8924	0.5062

APPENDIX C

DIFFERENTIAL PHOTOMETRY FOR II VULPECULAE
IN THE FORMAT (VARIABLE-COMPARISON STAR)

NUMBER OF POINTS = 66
COLUMNS ARE: JULIAN DAY (-244 5600)
DIFFERENTIAL V MAGNITUDE

2.7188	0.8786
2.7233	0.8646
2.7274	0.8678
2.7317	0.8744
2.7362	0.8798
2.7401	0.8732
2.7436	0.8842
2.7471	0.8889
2.7505	0.8711
2.7550	0.8947
2.7586	0.8914
2.7624	0.8764
2.7655	0.8620
2.7690	0.8568
2.7729	0.8636
2.7769	0.8602
2.7806	0.8514
2.7841	0.8465
2.7875	0.8347
2.7966	0.8359
2.8007	0.8335
2.8042	0.8327
2.8075	0.8434
2.8112	0.8500
2.8149	0.8766
2.8188	0.8594
2.8221	0.8700
2.8258	0.8689
2.8291	0.8846
2.8327	0.8723
5.7151	0.8873
5.7201	0.8785
5.7236	0.8902
5.7297	0.8698
5.7333	0.8712
5.7403	0.8737
5.7459	0.8564
5.7497	0.8532
5.7530	0.8449
5.7577	0.8486
5.7621	0.8497
5.7655	0.8400
5.7690	0.8575
5.7732	0.8489
5.7774	0.8599
5.7811	0.8483
5.7848	0.8550
5.7888	0.8563
5.7923	0.8492
5.7968	0.8633
5.8009	0.8747

5.8035	0.8653
5.8073	0.8703
5.8106	0.8718
5.8139	0.8734
5.8173	0.8699
5.8205	0.8832
5.8241	0.8760
5.8297	0.8771
5.8336	0.8873
5.8372	0.8740
5.8403	0.8670
5.8434	0.8652
5.8466	0.8616
5.8502	0.8538
5.8533	0.8556

$

APPENDIX D-1

```
      PROGRAM REDUCE
C
C     THIS PROGRAM REDUCES PHOTOMETRIC DATA TO INSTRUMENTAL
C     MAGNITUDES, TAKING INTO CONSIDERATION EXTINCTION (DE-
C     RIVED FROM THE COMPARISON STAR), BUT LEAVING THE MAG-
C     NITUDES UNTRANSFORMED TO THE UBV SYSTEM.
C
C     ALAT AND ALONG - LATITUDE AND LONGITUDE OF LOWELL OBSERVATORY
C     XV AND XVERR - EXTINCTION COEFFICIENT IN V AND ITS ERROR
C     NOBS - NUMBER OF OBSERVATIONS
C     RAV AND DECV - RA AND DEC OF VARIABLE STAR
C     RAC AND DECC - RA AND DEC OF COMPARISON STAR
C     RAH AND DECH - RA AND DEC OF CHECK STAR
C     VINST - INSTRUMENTAL V MAGNITUDE
C     STAR - STAR COUNTS
C     SKY - SKY COUNTS
C     GMST - GREENWICH MEAN SIDEREAL TIME AT 0 HOURS UT
C     SIDTIM - LOCAL SIDEREAL TIME
C     HA - HOUR ANGLE
C     SECZ - SECANT OF ZENITH ANGLE
C     AIRMAS - AIRMASS
C     V0 - EXTINCTION-CORRECTED INSTRUMENTAL V MAGNITUDE
C
      REAL*8 XV,XVERR,INTCPT,INTERR
      DIMENSION UT(180),STAR(180),SKY(180),HA(180),V0(180)
      DIMENSION VINST(180),CONST(50),SIDTIM(180),AIRMAS(180)
      DIMENSION X(180),Y(180),RA(180),DEC(180)
      COMMON XX(100),YY(100)
      LOGICAL*1 FILNAM(15)
      CHARACTER*9 VARBLE,NAME(180)
      INTEGER DATE
      FILNAM(15)=0
      FACTOR=0.0174533
      ALAT=35.203333
      ALONG=7.4444
      N=0
      TYPE 24
      ACCEPT 25,FILNAM
      OPEN(UNIT=3,TYPE='OLD',NAME=FILNAM)
      READ(3,15) VARBLE,DATE,NOBS,GMST
      TYPE*, VARBLE,DATE,NOBS,GMST
      READ(3,17) RAV,DECV
      READ(3,17) RAC,DECC
      READ(3,17) RAH,DECH
      DO 10 I=1,NOBS
      READ(3,1) NAME(I),UT(I),STAR(I),SKY(I)
 10   CONTINUE
      CLOSE(UNIT=3)
C
C-------CALCULATE INSTRUMENTAL MAGNITUDES, SIDEREAL TIME AND AIRMASS
C
      DO 20 I=1,NOBS
      IF(NAME(I).EQ.'V') THEN
      RA(I)=RAV
      DEC(I)=DECV
      ELSE IF (NAME(I).EQ.'C') THEN
```

```
          RA(I)=RAC
          DEC(I)=DECC
          ELSE
          RA(I)=RAH
          DEC(I)=DECH
          END IF
   20     CONTINUE
          DO 38 I=1,NOBS
          STAR(I)=DEADTM(STAR(I))
          SKY(I)=DEADTM(SKY(I))
          VINST(I)=-2.5*ALOG10((STAR(I)-SKY(I))/1000000.0)
          SIDTIM(I)=GMST+(1.002737*UT(I))-ALONG
          HA(I)=ABS(SIDTIM(I)-RA(I))
          PART1=(SIN(ALAT*FACTOR)*SIN(DEC(I)*FACTOR))
          PART2=COS(ALAT*FACTOR)*COS(DEC(I)*FACTOR)*COS(HA(I)*FACTOR*15)
          SECZ=1.0/(PART1+PART2)
          AIRMAS(I)=SECZ-0.0018167*(SECZ-1.0)
   38     CONTINUE
          DO 30 I=1,NOBS
          IF(NAME(I).NE.'C') GO TO 30
          M=M+1
          XX(M)=AIRMAS(I)
          YY(M)=VINST(I)
   30     CONTINUE
          CALL LLS(KV,KVERR,INTCPT,CRTERR)
          DO 60 I=1,NOBS
          V0(I)=VINST(I)-(KV*AIRMAS(I))
   60     CONTINUE
C
C--------WRITE RESULTS INTO THE OUTPUT FILE
C
          OPEN(UNIT=4,STATUS='NEW',NAME='REDUCE.OUT')
          WRITE(4,2) VARBLE,DATE
          WRITE(4,3)
          WRITE(4,4)
          WRITE(4,32)
          WRITE(4,5) (NAME(I),UT(I),HA(I),AIRMAS(I),VINST(I),I=1,NOBS)
          WRITE(4,6)
          WRITE(4,7)
          WRITE(4,9)
          WRITE(4,33)
          WRITE(4,19) (NAME(I),SIDTIM(I),V0(I),I=1,NOBS)
          WRITE(4,29)
          WRITE(4,28)
          WRITE(4,8) KV,KVERR
          WRITE(4,16) INTCPT,CRTERR
          CLOSE(UNIT=4)
C
C--------FORMAT STATEMENTS
C
    1     FORMAT(A2,2X,F7.4,2X,F6.0,2X,F4.0)
    2     FORMAT(1X,A7,2X,I6,/)
    3     FORMAT(1X,'TABLE I',/)
    4     FORMAT(1X,'STAR',3X,'UT',6X,'HA',7X,'X',5X,'VINST')
```

```
 42     FORMAT('-----------------------------------------')
 33     FORMAT('-------------------------')
  5     FORMAT(2X,A2,2X,F6.4,2X,F6.4,2X,F7.5,2X,F5.3)
  6     FORMAT(' ')
  7     FORMAT(1X,'TABLE I('/)
 28     FORMAT(1X,'FROM THE LLS ROUTINE)'/)
  8     FORMAT(1X,'KV = ',F7.5,'+/-',F7.5)
 29     FORMAT(1X,'    ')
 16     FORMAT(1X,'INTERCEPT = ',F7.5,'+/-',F7.5)
  9     FORMAT(1X,'STAR',4X,'SY',7X,'V0')
 19     FORMAT(1X,A2,3X,F7.4,2X,F7.4)
 18     FORMAT(F7.4,F8.4)
 15     FORMAT(A9,I6,1X,I3,1X,F9.6)
 17     FORMAT(5X,F6.3,4X,F6.3)
 24     FORMAT(1X,'WHAT DATA FILE?')
 25     FORMAT(I5/)
C
C-------END
C
       CALL EXIT
       END
C
C      THE FOLLOWING FUNCTION CALCULATES DEAD-TIME CORRECTION.
C      STAR AND SKY-COUNTS IN THE DATA FILE ARE ASSUMED TO BE
C      COUNTS PER SECOND.
C
       FUNCTION DEADTM(CNTS)
       DEADTM=CNTS*(1.0D0-2.0E-7*CNTS)
       RETURN
       END
C
C      THE FOLLOWING SUBROUTINE IS A LINEAR LEAST SQUARES PROGRAM
C      THAT CALCULATES SLOPE AND Y-INTERCEPT AND THEIR PROBABLE
C      ERRORS.
C
       SUBROUTINE LLS(KV,KVERR,INTCPT,INTERR)
       COMMON XXX(100),YYY(100)
       REAL*8 INTCPT,INTERR,KV,KVERR
C
C------INITIALIZE EVERYTHING
C
       SUMX=0.0
       SUMY=0.0
       SUMXS=0.0
       SUMXY=0.0
       OME=A=0.0
C
C------FIND SUMS
C
       DO 21 I=1,24
       SUMX=SUMX+XXX(I)
       SUMY=SUMY+YYY(I)
       SUMXY=SUMXY+XXX(I)*YYY(I)
       SUMXS=SUMXS+XXX(I)**2
```

```
 21     CONTINUE
C
C--------CALCULATE SLOPE AND INTERCEPT
C
       D=24*SUMXS-(SUMX)**2
       KV=((24*SUMXY)-(SUMX*SUMY))/D
       INTCPT=((SUMXS*SUMY)-(SUMX*SUMXY))/D
       DO 30 I=1,24
       OMEGA=OMEGA+(YYY(I)-INTCPT-(KV*XXX(I)))**2
 30    CONTINUE
C
C--------CALCULATE PROBABLE ERRORS IN SLOPE AND INTERCEPT
C
       OMEGA=OMEGA/FLOAT(24-2)
       KVERR=SQRT(OMEGA*SUMXS/D)
       INTERR=SQRT(OMEGA*24/D)
C
C--------END
C
       RETURN
       END
```

APPENDIX B-2

```
      PROGRAM SYNCUV
C     GENERATES SYNTHETIC SINUSOIDAL CURVES OF THE FORM:
C     Y = A1*SIN(2*PI*T/P1)+A2*SIN(2*PI*T/P2+PHI2)+SIG*RANDOM
      DIMENSION X(500),Y(500),T(500)
      REAL MBAR
      LOGICAL*1 FILNAM(15)
      OPEN(UNIT=3,NAME='B3:[0,0]JK1',TYPE='OLD',READONLY)
      READ(3,3) NP
      READ(3,4) (X(I),I=1,NP)
    3 FORMAT(I3)
    4 FORMAT(F10.4)
      TYPE*,'INPUT: A1,P1,PHI1,MBAR'
      ACCEPT*,A1,P1,PHI1,MBAR
      TYPE*,'INPUT: RANDOM SPREAD IN MAGNITUDES'
      ACCEPT*,SIGMA
      TP=6.2831853
      J=0
      I=0
      DO 20 K=1,NP
      B1=(TP*X(K)/P1)+PHI1
      Y(K)=A1*SIN(B1)+MBAR
C     NOTE: UNIFORM RANDOM DISTRIBUTION, NOT RANDOM
20    Y(K)=Y(K)+SIGMA*RAN(J)-SIGMA/2.
      TYPE*,'NAME OF NEW FILE?'
      ACCEPT 25,FILNAM
25    FORMAT(15A1)
      FILNAM(15)=0.
      OPEN(UNIT=2,NAME=FILNAM,TYPE='NEW')
      WRITE(2,30) NP
30    FORMAT(I3)
      WRITE(2,31) (X(K),Y(K),K=1,NP)
31    FORMAT(F10.4,4X,F10.4)
      CLOSE(UNIT=2)
      CLOSE(UNIT=3)
      TYPE*,'DATA WRITTEN TO DISK'
      CALL EXIT
      END
```

```
      PROGRAM JURKMOD
C
C     SWINGLER'S MODIFICATION OF JURKEVICH PERIODOGRAM PROGRAM
C     THIS PROGRAM GIVES INDEX AS A FUNCTION OF FREQUENCY
C
C     NPNTS - NUMBER OF DATA POINTS
C     X - ARRAY OF VALUES OF X
C     Y - ARRAY OF VALUES OF Y
C     PHI - PHASE OF EACH DATA POINT
C     FSTART - INITIAL FREQUENCY
C     FDELTA - SPACING BETWEEN TRIAL FREQUENCIES
C     NPRD - NUMBER OF FREQUENCIES TO BE SEARCHED
C     RESULT - ARRAY OF JURKEVICH INDEX FOR EACH TRIAL PERIOD
C     GAMMA -
C     SUMRL =   Y COS(GAMMA )
C     SUMIM =   Y SIN(GAMMA )
C
      REAL PHI(470)
      DIMENSION TCOUNT(20),BINDEX(20),X(470),Y(470)
      DIMENSION RESULT(1000)
      COMMON XVALUE(20),YVALUE(20)
      LOGICAL*1 FILNAM(15),DATE(8),XNAME(10)
      TYPE*,'NAME OF FILE TO BE READ?'
      ACCEPT 15,FILNAM
 15   FORMAT(15A1)
      FILNAM(15)=0
      OPEN(UNIT=2,NAME=FILNAM,TYPE='OLD',READONLY)
      READ(2,29) NPNTS
      READ(2,22) (X(K),Y(K),K=1,NPNTS)
 29   FORMAT(I3)
 22   FORMAT(F10.4,4X,F10.4)
C
C-------THE FOLLOWING IS A TEST TO SEE IF THE DATA FILE
C-------IS BEING READ PROPERLY
C
D     TYPE 22,(X(K),Y(K),K=1,10)
C
      CLOSE(UNIT=2)
      PI=3.14159265
      TYPE*,'NAME OF STAR?'
      ACCEPT 17,XNAME
 17   FORMAT(10A1)
      TYPE*,'YOUR FILE CONTAINS ',NPNTS,' DATA POINTS'
      NPRD=1000
C
C-------FOR EACH PERIOD, CALCULATE THE INDEX
C
      TYPE*,'INPUT FSTART, FEND, AND FDELTA'
      ACCEPT*,FSTART,FEND,FDELTA
      DO 8 IA=1,NPRD
      FREQ=FSTART+FDELTA*FLOAT(IA-1)
      SUMRL=0.
      SUMIM=0.
```

```
      DO 5 IB=1,NPNTS
      PHI(IB)=AMOD(X(IB)*FREQ,1.0)
      IF(PHI(IB).LT.0.0) PHI(IB)=PHI(IB)+1.0
      GAMMA=PHI(IB)*2.*PI
      TEMPR=Y(IB)*COS(GAMMA)
      TEMPI=Y(IB)*SIN(GAMMA)
      SUMRL=SUMRL+TEMPR
      SUMIM=SUMIM+TEMPI
    5 CONTINUE
      RESULT(IA)=SUMRL**2+SUMIM**2
      RESULT(IA)=(2./NPNTS)**2*(RESULT(IA))
    8 CONTINUE
      CALL EXIT
      END
```

References

Andreasen,G.K. 1983, Astron.Astrophys. 121, 250.

Andreasen,G.K.,Hejlesen,P.M., and Petersen,J.D. 1983, Astron. Astrophys. 121, 241.

Breger,M. 1969, A.J. 74, 166.

Breger,M. 1979, Pub.A.S.P. 91, 5.

Breger,M. and Pregman,J.N. 1975, Ap.J. 200, 343.

Breger,M.,Hutchins,J. and Kuhl,L.V. 1976, Ap.J. 210, 163.

Cox,J.N. and Giuli,R.T. 1968, Principles of Stellar Structure, Vol. 2 (New York: Gordon and Breach).

Crawford,D.L.,Golson,J.C. and Landolt,A.U. 1971, Pub.A.S.P. 83, 652.

DuPuy,D.L. 1985 (private communication).

DuPuy,D.L. and Burgoyne,L.G. 1983, Pub.A.S.P. 95, 61.

DuPuy,D.L.,Collins,G. and Swingler,D.N. 1982, Pub.A.S.P. 94, 177.

Hardie,R.H. in 1962, Stars and Stellar Systems, Vol.2 (Chicago: University of Chicago Press).

Hoffleit,D. 1964, Catalogue of Bright Stars, 3rd. ed., (Saint Paul: H.M. Smith).

Irlarte,B.,Johnson,H.L.,Mitchell,R.I. and Wisniewski,W.K. 1965, Sky and Telescope 30, 21.

Jurkevich,I. 1971, Ap. and Space Sci. 13, 154.

Kholopov,P.N. 1984, Sov.Sci.Rev.E Astrophys.Space Phys., vol.3, 97.

Kraft, R.P. in 1963, Basic Astronomical Data, (Chicago: University of Chicago Press).

Kukarkin,B.V.,Kholopov,P.N.,Fedorovich,V.P.Frolov,M.S.,
Kukarkina,N.P.Kurochrin,N.E.,Medvedeva,G.L.,Perova,N.B.
Pskovsky,Yu.P. 1976, The Third Supplement to the Third
Edition of the General Catalogue of Variable Stars,
(Moscow: Academy of Sciences of the U.S.S.R.).

Millis,R.L. 1983 (private communication).

Morris,S. 1979, M.Sc. Thesis, Saint Mary's University.

Morris,S. and DuPuy,D.L. 1980, Pub.A.S.P. 92, 303.

Osborn,W. 1983 (private communication).

Pena,J.H. and Warman,J. 1979, A.J. 84, 1046.

Petersen,J.O. 1976 in Multiple Periodic Variable Stars
I.A.U. Coll. 29, W.S. Fitch, ed. (Budapest: Akademia i
Kiado), 195.

Petersen,J.O. and Jorgensen,H.E. 1972, Astron.Astrophys. 17,
367.

Swingler,D.N. 1985a, A.J. 90, 575.

Swingler,D.N. 1985b (private communication).

Turner,D.G. 1985 (private communication).

Valtier,J-C.,Baglin,A. and Auvergne,M. 19. Astron.
Astrophys. 73, 329.

Curriculum Vita

Name:	Laureen Gaye Reed (nee Burgoyne)
Date of Birth:	May 5, 1961
Place of Birth:	Red Deer, Alberta
Post-Secondary Education:	B.Sc. (Physics), 1983 Saint Mary's University Halifax, N.S., Canada
	M.Sc. (Astronomy), 1986 Saint Mary's University Halifax, N.S., Canada
Awards:	Saint Mary's University Entrance Scholarship 1979-80
	Burke-Gaffney Scholarship, Saint Mary's Univ. 1983-84 and 1984-85
Experience:	Astronomy Research/Teaching Assistantships Saint Mary's University 1981-85
	Physics Laboratory Instructor 1982-83 and 1983-84, Saint Mary's University 1985-86, Mount Saint Vincent University
	Various observing runs on 24-inch and 31-inch telescopes at Lowell Observatory, Flagstaff, Arizona 1983-85

Publications in Referreed Journals:

DuPuy, D.L. and Burgoyne, L.G., "HR5960: New Observations and Period Search" in 1983 Pub. A.S.P. 95, 61.